2017

IMPACT OF CLIMATE CHANGE ON EXTREME HYDROLOGICAL EVENTS IN THE KENTUCKY RIVER BASIN

Somsubhra Chattopadhyay
University of Kentucky, schattop14@uky.edu
Digital Object Identifier: https://doi.org/10.13023/ETD.2017.245

STUDENT AGREEMENT:

I represent that my thesis or dissertation and abstract are my original work. Proper attribution has been given to all outside sources. I understand that I am solely responsible for obtaining any needed copyright permissions. I have obtained needed written permission statement(s) from the owner(s) of each third-party copyrighted matter to be included in my work, allowing electronic distribution (if such use is not permitted by the fair use doctrine) which will be submitted to UKnowledge as Additional File.

I hereby grant to The University of Kentucky and its agents the irrevocable, non-exclusive, and royalty-free license to archive and make accessible my work in whole or in part in all forms of media, now or hereafter known. I agree that the document mentioned above may be made available immediately for worldwide access unless an embargo applies.

I retain all other ownership rights to the copyright of my work. I also retain the right to use in future works (such as articles or books) all or part of my work. I understand that I am free to register the copyright to my work.

REVIEW, APPROVAL AND ACCEPTANCE

The document mentioned above has been reviewed and accepted by the student's advisor, on behalf of the advisory committee, and by the Director of Graduate Studies (DGS), on behalf of the program; we verify that this is the final, approved version of the student's thesis including all changes required by the advisory committee. The undersigned agree to abide by the statements above.

Somsubhra Chattopadhyay, Student

Dr. Dwayne R. Edwards, Major Professor

Dr. Donald Colliver, Director of Graduate Studies

IMPACT OF CLIMATE CHANGE ON EXTREME HYDROLOGICAL EVENTS IN THE KENTUCKY RIVER BASIN

DISSERTATION

A dissertation submitted in partial fulfillment of the requirements for the degree of Doctor of Philosophy in the College of Engineering at the University of Kentucky

By

Somsubhra Chattopadhyay

Lexington, Kentucky

Director: Dr. Dwayne R. Edwards

Professor of Biosystems and Agricultural Engineering

Lexington, Kentucky

2017

ABSTRACT OF DISSERTATION

IMPACT OF CLIMATE CHANGE ON EXTREME HYDROLOGICAL EVENTS IN THE KENTUCKY RIVER BASIN

Anthropogenic activities including urbanization, rapid industrialization, deforestation and burning of fossil fuels are broadly agreed on as primary causes for ongoing climate change. Scientists agree that climate change over the next century will continue to impact water resources with serious implications including storm surge flooding and a sea level rise projected for North America. To date, the majority of climate change studies conducted across the globe have been for large-sized watersheds; more attention is required to assess the impact of climate change on smaller watersheds, which can help to better frame sustainable water management strategies.

In the first of three studies described in this dissertation, trends in annual precipitation and air-temperature across the Commonwealth of Kentucky were evaluated using the non-parametric Mann-Kendall test considering meteorological time series data from 84 weather stations. Results indicated that while annual precipitation and mean annual temperature have been stable for most of Kentucky over the period 1950-2010, there is evidence of increases (averages of 4.1 mm/year increase in annual precipitation and 0.01 °C/year in mean annual temperature) along the borders of the Kentucky. Considered in its totality, available information indicates that climate change will occur – indeed, it is occurring – and while much of the state might not clearly indicate it at present, Kentucky will almost certainly not be exempt from its effects. Spatial analysis of the trend results indicated that eastern part of the state, which is characterized by relatively high elevations, has been experiencing decreasing trends in precipitation.

In the second study, trends and variability of seven extreme precipitation indices (total precipitation on wet days, PRCPTOT; maximum length of dry and wet periods, CDD and CWD, respectively; number of days with precipitation depth ≥20 mm, R20mm; maximum five-day precipitation depth, RX5day; simple daily precipitation intensity, SDII; and standardized precipitation index, SPI were analyzed for the Kentucky River Basin for both baseline period of 1986-2015 and the late-century time frame of 2070-2099. For the baseline period, the majority of the indices demonstrated increasing trends; however, statistically significant trends were found for only ~11% of station-index

combinations of the 16 weather stations considered. Projected magnitudes for PRCPTOT, CDD, CWD, RX5day and SPI, indices associated with the macroweather regime, demonstrated general consistency with trends previously identified and indicated modest increases in PRCPTOT and CWD, slight decreases in CDD, mixed results for RX5day, and increased non-drought years in the late century relative to the baseline period. The study's findings indicate that future conditions might be characterized by more rainy days but fewer large rainfall events; this might lead to a scenario of increased average annual rainfall but, at the same time, increased water scarcity during times of maximum demand.

In the third and final study, the potential impact of climate change on hydrologic processes and droughts over the Kentucky River basin was studied using the watershed model Soil and Water Assessment Tool (SWAT). The SWAT model was successfully calibrated and validated and then forced with forecasted precipitation and temperature outputs from a suite of CMIP5 global climate model (GCMs) corresponding to two different representative concentration pathways (RCP 4.5 and 8.5) for two time periods: 2036-2065 and 2070-2099, referred to as mid-century and late-century, respectively. Climate projections indicate that there will be modest increases in average annual precipitation and temperature in the future compared to the baseline (1976-2005) period. Monthly variations of water yield and surface runoff demonstrated an increasing trend in spring and autumn, while winter months are projected as having decreasing trends. In general, maximum drought length is expected to increase, while drought intensity might decrease under future climatic conditions. Hydrological droughts (reflective of water availability), however, are predicted to be less intense but more persistent than meteorological droughts (which are more reflective of only meteorological variables). Results of this study could be helpful for preparing any climate change adaptation plan to ensure sustainable water resources in the Kentucky River Basin.

KEYWORDS: Climate Change, Trend Analysis, Kentucky River Basin, Extreme Precipitation Indices, Soil and Water Assessment Tool, Drought Indices

Somsubhra Chattopadhyay

May 31, 2017

IMPACT OF CLIMATE CHANGE ON EXTREME HYDROLOGICAL EVENTS IN THE KENTUCKY RIVER BASIN

BY

Somsubhra Chattopadhyay

Dr. Dwayne R. Edwards

Director of Dissertation

Dr. Donald Colliver

Director of Graduate Studies

May 31, 2017

DEDICATION

"Matri devo bhava, Pitri devo bhava"

("Revere your Mother as God; Revere your Father as God")

Derived from the Hindu Scripture - The Upanishads

I dedicate this dissertation to my parents for their blessings, unconditional love and support.

ACKNOWLEDGMENTS

Firstly, I would like to thank my major advisor and mentor Dr. Dwayne Edwards for his guidance, motivation and support during the past three years. During this period, I had the opportunity to learn a lot of valuable technical skills from him. His scientific and expert advice helped me to build strong foundation in watershed hydrology. Dr. Edwards was a wonderful teacher and a friend who always lifted my spirits. I also appreciate my committee members for their support and critical insights in my research.

I am grateful to Darren Ficklin, Assistant Professor, Indiana University and Ed Maurer at Santa Clara University for their help during climate model data acquisition. I appreciate Jose Guijarro at Spanish State Meteorological Agency for his support during various stages of this research. Thanks to my friend Yao Yu for his help with data analysis. I am also grateful to my colleague Ali Hamidisepehr for his assistance. A warm note of appreciation to my friends: Arindam, Kanishka, Arpan da, Madan da and Moumita for their moral support.

Last but not the least, my deepest gratitude for my parents, brother and all my family members for their continuous blessings and support throughout my career and life.

Table of Contents

List of Tables

List of Figures

CHAPTER 1: INTRODUCTION

1.1 Background

Water resources management in the 21st century is challenged by climate change-related impacts on the hydrologic cycle. Although climate change is a global phenomenon, regional scale variations can be significant, such as within the United States (Portman et al., 2009). Trends in meteorological variables, often considered as important tools in climate change detection (Gocic and Tracjovik, 2013), demonstrate this regional variation. While many regions within the United States, have demonstrated increasing trends in precipitation frequency and/or intensity (Donat et al., 2013; Guilbert et al., 2015), this is by no means a spatially uniform finding. This being the case, it is prudent to investigate climate variability on a more local scale, especially in regions that exhibit complex weather patterns such as Kentucky.

Impacts of extreme precipitation, particularly in the form of flooding, have caused more loss and property damage in the United States than any other natural disaster during the 20th century (Easterling et al., 2000). Establishing a direct linkage between changes in extreme precipitation with flooding can be difficult, however, as records are often confounded by changes in land use and increasing settlement in floodplains (Kunkel, 2003). However, great floods (defined as floods with discharges exceeding 100-year levels from basins larger than 190,000 km^2) have increased in the 20th century and are only exacerbated by increasing rainfall rates (Milly et al., 2002). Historical analysis and projection of climate extremes involving outputs from coordinated modelling experiments such as Climate Model Intercomparison Phase 5 (CMIP5) with Expert Team on Climate Change Detection and Indices (ETCCDI) indices or other measures have been

performed for many regions in the United States (Sillman et al., 2013; Wuebbles et al., 2013). However, direct comparison of one study with other is complicated by differences in watershed characteristics, climatic conditions, resolution of data and analyses, climate models, emission scenarios, downscaling methods, and other factors. To our knowledge, there exists no study that exclusively focuses on trends and variability of climatological variables (both means and extremes) in the Commonwealth of Kentucky.

Similar to flooding, drought is a commonplace occurrence that has caused both economic losses and conflicts over rights of water usage in the United States (Mitra and Srivastava, 2016). Kentucky has been affected by recent droughts; the drought of 2012, for example, caused more than $275M in economic loss to the region, and the EPA (2016) projects longer drought durations in the future. Understanding spatiotemporal characteristics of droughts can help in evaluating future drought risk and selecting appropriate drought mitigation strategies.

1.2 Objectives

The objectives of this research were to:

1. Analyze the historical long term-trends and variability in precipitation and air temperature for the Commonwealth of Kentucky.
2. Evaluate the spatio-temporal characteristics of contemporary and future extreme precipitation indices in the Kentucky River Basin.
3. Assess the implications of climate change on water resources availability and droughts in the Kentucky River Basin.

1.3 Dissertation outline

This dissertation is organized as six chapters. Chapter 1 presents broad background information and the research objectives. Chapter 2 provides relevant reviews regarding trend analysis studies of hydroclimatic variables and extreme precipitation events. The chapter also presents reviews of studies describing climate change impacts on droughts using various drought indices. Chapter 3 describes the results from a long-term trend analysis of precipitation and air-temperature across the Commonwealth of Kentucky in which trends in annual average time series were computed for 84 weather stations using non-parametric methods. Chapter 4 provides the comparison of trends and variability of seven extreme precipitation indices for the historical and future time periods for the Kentucky River Basin. Chapter 5 presents the results from an investigation of climate change impacts on hydrologic processes and droughts in the Kentucky River Basin. Chapter 6 integrates and summarizes the major findings from the three studies and provides recommendations for future research.

The bulk of the material in this dissertation is either published or accepted for publication in a peer-reviewed scientific journal. The material of Chapter 3 is identical to final version of the manuscript subsequently published in *Climate*:

> Chattopadhyay, S., Edwards D.R. (2016) Long term trend analysis of precipitation and air temperature for Kentucky, United States. *Climate,* 4, 10, doi: 10.3390/cli4010010

The material of Chapter 4 is identical to the final version of the manuscript subsequently published in *Water*:

Chattopadhyay, S., Edwards, D. R., Yu, Y. (2017) Contemporary and future characteristics of precipitation indices in the Kentucky River Basin. *Water*, 9, 109, doi: 10.3390/w9020109

The original text of Chapter 5 was submitted for publication in *Environmental Processes* and was accepted for publication. The current text of Chapter 5 represents the original text as modified on the basis of Advisory Committee member comments; it is anticipated that the current text will be highly similar to the manuscript version that is ultimately published, but the revision and follow-up review process is currently ongoing. The citation for the upcoming article is:

Chattopadhyay, S., Edwards, D. R., Yu, Y., Hamidisepehr, A. (2017) An assessment of climate change impacts on future water availability and droughts in the Kentucky River Basin. *Environmental Processes* (accepted).

CHAPTER 2: LITERATURE REVIEW

2.1 Introduction

The Intergovernmental Panel on Climate Change (IPCC) (2013) have estimated that near-surface global mean temperatures have increased by 0.72° C between 1951 and 2012, while global mean annual land precipitation has displayed a slightly increasing trend of approximately 1.1 ± 1.5 mm per decade between 1901 and 2005. In other words, global climate has been changing over a relatively short duration. These changes, considered as due primarily to anthropogenic activities (fossil fuel consumption in connection with growing industrialization and urbanization) have the potential to influence almost every aspect of life on the planet with noteworthy examples that include agriculture, aquatic and terrestrial ecosystems and water resources. Indeed, some impacts of a changing climate may already be occurring in the form of increasingly frequent extreme weather events (intense floods and droughts) (IPCC, 2013).

At smaller scales of space and time, historical trends in precipitation and temperature are less uniform; magnitudes, directions and statistical significance of trends can vary appreciably in space on a management/decision-making scale, with these variations demonstrating additional dependence on season. Similar findings have been reported with respect to extreme precipitation, streamflow and drought, all of which strengthen the case for relatively high-resolution studies in situations for which a relatively practical application of the results is envisioned.

Projections of future climate and its impacts rely necessarily on highly complex mathematical simulation models to (a) forecast basic climate variables and (b) translate

those forecasted variables into the associated hydrological impacts. Such studies typically involve the outputs of one or more global climate model (GCM) simulation for a given period of time, with the outputs then cast as inputs to a hydrological simulation model. This approach has been reported for a variety of locations worldwide, with results that can be helpful in anticipating future water availability and demands. It is not, however, without challenges. Apart from the conceptual challenges of compounding uncertainties in climate modelling with uncertainties in hydrological modelling, it is acknowledged that data from GCM simulations are subject to scale-based (both time and space) limitations. Methods for accommodating the typically coarse scale of outputs have been well-reported and are in widespread use; techniques for improving GCM performance on smaller time scales (hours and days; i.e., in the weather regime) are a topic of active research interest.

2.1.1 Precipitation variability

Precipitation is the primary element of the hydrological cycle, and changes in precipitation depths are often considered as one of the primary signals of climate change (McVicar et al., 2007; Irannezhad et al., 2014). Global precipitation patterns are changing as a result of global warming; these changes can have dramatic effects on the hydrological cycle and, consequently, both ground and surface water resources availability (Arnell, 2001). Hulme et al. (1998) have reported that global average precipitation has increased by approximately 2% during the 1900-1998 time period, although considerable variation is possible at the regional scale (Dai et al., 1997). Both regional and local variations in precipitation were evident in the increasing trends across regions north of 30°N for the period 1900-2005 along with decreasing trends in the

tropical region since the 1970s (IPCC, 2013). Scaling down the results for northern Europe, annual precipitation exhibited an 8-14% increase in Norway during last century (Hanssen-Bauer and Forland, 2000), while a slightly smaller increase for northern and southern Sweden was reported by Raisannen and Alexandersson (2003). An increase of 0.92 ± 0.50 mm/year for annual precipitation in Finland was noted by Irannezhad et al. (2014). Liuzzo et al. (2016) studied the spatial and temporal variation of rainfall trends in Sicily during 1921-2012. These researchers reported a generally decreasing trend in precipitation during 1921-2012; when only the last 30 years (1981-2012) were analyzed, however, the trend direction was positive. Spatiotemporal variations in rainfall over the period of 1940-2012 in Greece were quantified by Markonis et al. (2016). Findings of this study highlighted that while most of the regions demonstrated a decline since 1950, an increase since 1980 (stable since last 15 years) is also present.

Similar precipitation trend analysis studies have been conducted in India for the eastern state of Jharkhand by Chandniha et al. (2016) and for the Sindh River Basin by Gajbhiye et al. (2016). Monthly rainfall data from 18 weather stations for the time period of 1901-2011 were analyzed to determine spatiotemporal trends in the state of Jharkhand. Results showed that five stations out of 18 experienced decreasing trends in annual rainfall. Though the authors did not propose a physical explanation, the year 1949 was identified as a change point in the time series; trends from 1901-1949 were found to be positive, whereas the trend was negative for 1950-2011 time frame. Contrasting results were found for precipitation trends in Sindh River Basin, where significant increasing trends prevailed for both annual and seasonal time series during 1901-2002. In the desertification prone region (DPR) of China, the majority of the stations in the western

region exhibited increasing precipitation trends, while negative trends prevailed over the eastern region for the time period of 1960-2013 (Shi et al., 2016). The authors' analysis suggested that while climate is becoming wetter in the western regions of DPR, the likely condition for the eastern region is drier. Similar studies in China were performed by Huang et al. (2013) and Wang et al. (2012). Huang et al. (2013) investigated precipitation trends during 1960-2008 in Jiangxi province of southeast China. They found that significant differences existed among the stations with positive and negative precipitation trends present at monthly, annual and seasonal scales. Another prominent feature of the analysis was that significant increasing trends were mostly occurring in January, August, winter and summer in contrast to significant decreasing trends mostly in October and autumn.

Recent studies in North America include spatiotemporal trend analysis and change point detection in Kansas by Rahmani et al. (2015) and in Florida by Martinez et al. (2012). The average rate of increase in precipitation for Kansas was found to be 0.68 mm/year over the time period 1890-2011. These studies and others on trends in United States precipitation are summarized in Table 2.1. Similar to the earlier-discussed studies of precipitation trends on other continents, the results can be considered as having a very mixed nature, with trend directions, magnitudes and statistical significance dependent on factors such as season, location, and the time frame under investigation. Considered in the aggregate, therefore, even the studies specific to the United States suggest that finer spatial resolution is necessary to develop results that are meaningful to policy makers and water resources managers/planners. To our knowledge, no peer-reviewed studies have been performed on quantifying the historical trends in precipitation in Kentucky to date.

Table 2.1. Summarized studies on precipitation trends in the United States.

Study area	Time frame	Major findings	Reference
Upper Tennessee River Valley	1950-2009	Average trend: -0.50 mm/year Range: (-14.27 – 5.04 mm/year)	Jones et al. (2015)
North Carolina	1950-2009	Range of trend: -5.5 – 9 mm/year	Sayemuzzaman and Jha (2014)
Kansas	1890-2011	Increasing trend of 0.68 mm/year	Rahmani et al. (2015)
12 Midwestern states (Illinois, Indiana, Iowa, Kansas, Michigan, Minnesota, Missouri, Nebraska, Ohio, South Dakota, North Dakota and Wisconsin)	1980-2013	Majority of locations with increasing trend (few significant) in growing season precipitation, but declining in late growing season	Dai et al. (2016)
Florida	1895-2009 and 1970-2009	Significant decreasing trends in October and May for the time periods of 1895-2009 and 1970-2009, respectively	Martinez et al. (2012)
Great Plains	1900-2000	Increasing precipitation varied by 15-30% during July from easternmost part of the Ogallala Aquifer to Indiana.	DeAngelis et al. (2010)

2.1.2 Air temperature variability

Surface air temperature is a crucial climatic parameter that can play a prominent role in many hydrological processes and particularly with respect to evapotranspiration. An increase of 0.65 – 1.06 °C in global mean annual temperature has been reported in the 5th assessment report of IPCC over the time period 1880-2012 (IPCC, 2013). Although temperature is usually more spatially homogenous than precipitation, predicting spatiotemporal variability of temperature across local and global scales can still be a challenging task (Shi and Xu, 2008; Moral, 2010). Muslih and Blazejczyk (2016) used linear regression and the Mann-Kendall test as parametric and non-parametric methods, respectively, to analyze inter-annual and long-term variations in monthly air-temperature

in Iraq. The study period consisted of the years 1941-2013, which was later divided into two separate periods (1941-1980 and 1995-2013) to ensure homogeneity in the datasets. Results indicated that, consistent with the global warming pattern, increasing trends were experienced in Iraq beginning in the mid-1970s.

Islam et al. (2015) analyzed temporal changes in seasonal temperature extremes over Saudi Arabia for the time period of 1981-2010, finding warming trends in extreme indices for a majority of the 27 stations with statistically significant trends in spring and summer seasons. In contrast, the autumn and winter seasons evidenced mixed results with both increasing and decreasing trends present in the data. Temperature trends along with diurnal temperature range and sunshine duration in northeast India were evaluated by Jhajharia and Singh (2011). These researchers found increasing trends in temperature in the monsoon and post-monsoon seasons, but temperatures remained stable during winter and pre-monsoon seasons. Mikkonen et al. (2015) employed a dynamic linear model to investigate trends in average temperature across Finland for the period 1847-2013. Mean temperature over Finland was found to have risen over 2°C during the 166-year period, corresponding to an increase of to 0.14°C per decade. The warming rate was found to have accelerated after the 1960s, indicating an amplifying effect of global warming. Supportive results have been documented by Shi et al. (2016) for a 54-year period (1960-2013) in China and by Kenawy et al. (2012) for the period 1920-2006 in northeastern Spain. By-season analyses showed that spring months were associated with higher warming rates than the annual average, while summer months did not experience significant warming. Saboohi et al. (2012) showed that, on an annual scale, most stations in the western and southern parts of Iran had significant positive trends. Most of the

significant trends occurred in the summer season, which implied that climate in Iran has been growing warmer, particularly in summer.

Sayemuzzaman and Jha (2014) reported that the majority of the 249 stations considered in North Carolina demonstrated increasing trends in mean temperature with decreasing differences between minimum and maximum temperatures. Change point analysis using the sequential Mann-Kendall test further indicated that significant increasing trends in minimum temperature data and decreasing trends in maximum temperature data began roughly after 1970 and after 1960, respectively, for most of the stations. In a similar investigation by Martinez et al. (2012), increasing trends (particularly in summer and autumn) were reported for temperatures in Florida.

The Sayemuzzaman and Jha (2014), Martinez et al. (2012), and related studies on temperature trends in the United States are summarized in Table 2.2. Considered collectively, it is evident that similar to other parts of the world, climate change is in progress in the United States; more specifically, the studies generally indicate that the change is in the direction of increasing temperature. Similar to precipitation, though, the studies are not unanimous in terms of magnitude or direction of trend, and the results are suggestive of variation with location, study time frame, season, proximity to urban environment, and other factors. These differences among studies reinforce the earlier conclusion that relatively high-resolution studies may be most helpful in the context of water resources policy and management decisions

Table 2.2. Summarized studies on temperature trends in the United States.

Study area	Time frame	Major Findings	Reference
North Carolina	1950-2009	Highest warming trend: 0.073°C/year (autumn) Highest cooling trend: 0.12°C/year (summer) Change point: 1970	Sayemuzzaman et al. (2014)
Florida	1895-2009 and 1970-2009	Trends in mean, minimum maximum temperature generally positive, higher percentage in 1970-2009	Martinez et al. (2012)
Urban and rural temperature trends near large cities in the United States	1951-2000	Mean decadal rate of change in the heat island intensity: 0.05°C	Stone, 2007
California	1950-2000	Average warming of 0.99°C	Ladochy et al. (2007)
North Carolina	1949-1998	Temperatures warmest during 1950's but last 10 years warmer than average	Boyles and Raman (2003)
Southeastern United States (Florida, Alabama, Georgia, South Carolina and North Carolina)	1948-2010	Majority of the stations with higher warming rates in urban areas	Misra et al. (2012)
Prairie Pothole Region (Dakotas, Minnesota, Iowa)	1906-2000	Minimum daily temperature warmed by 1°C, maximum daily temperature cooled by 0.15°C	Millett et al. (2009)

2.2 Extreme precipitation events

Extreme climatic events pose significant risks to human society in general, which makes it prudent investigate the potential future behavior of these events. The broad scientific community take the view that, on a global scale, climate change due to anthropogenic activities has intensified extreme precipitation (IPCC 2007, 2012). Tank and Konnen (2003) found increases in all Europe-wide average indices of precipitation extremes including maximum rainfall in 10 consecutive days (RX10) and number of days with more than 20 mm rainfall (R20mm) over the 1946–99 period, even though the trends were not spatially consistent. Lupikasza (2010) analyzed spatial and temporal

variability of extreme precipitation in Poland for the period of 1951-2006. The five extreme precipitation indices selected for investigation in the study were highest five day precipitation total, precipitation total from events ≥90^{th} and 95^{th} percentiles of daily precipitation amount, and number of days with precipitation ≥ 90^{th} and 95^{th} percentiles of daily precipitation amount. Results indicated that decreasing trends dominated in both the summer and winter seasons. The summer season demonstrated the greatest number of statistically significant decreasing trends, while autumn exhibited highest number of positive trends. The southern parts of the country were associated with decreasing (though statistically insignificant) trends. Increasing trends, however, were found to have no distinct spatial pattern. Very similar conclusions about the seasonal trends of extreme precipitation indices in Portugal were drawn by Santos and Fargoso (2013). The authors found decreasing trends in selected extreme precipitation indices during annual, spring, winter and summer seasons, but increasing trends in autumn.

Increasing trends in maximum one- and five-day precipitation, precipitation on very wet days and the number of consecutive dry days were reported in Japan by Duan et al. (2015). Song et al. (2015) investigated changes in extreme precipitation and droughts over the Songhua River basin in China during 1960-2013. Regional average total precipitation on wet days (PRCPTOT) as well as precipitation total from events ≥90^{th} and 95^{th} percentiles of daily precipitation amount (R95 and R99) evidenced increasing trends. The simple daily precipitation intensity (SDII), however, exhibited a statistically significant negative trend with an average annual trend slope of -0.02 mm/day/year. All stations showed significant positive trends in consecutive dry days (CDD), while maximum five-day precipitation total (RX5) demonstrated significant positive trends in

April and October. Spatially complex trends in extreme precipitation in Yunnan Province, China for a similar time frame (1960-2012) were noted by Li et al. (2015). The majority of the 10 extreme precipitation indices exhibited increasing trends in western Yunnan and decreasing trends in eastern Yunnan. An increasing trend in CDD and decrease in consecutive wet days (CWD) (although most of the trends were insignificant) were noted for the western, southern and central regions. Precipitation intensity demonstrated a consistent increasing (only 10% of the stations were significant) trend over Yunnan. Total annual precipitation experienced a slight decrease on a region-average basis which was correlated with the increase in precipitation intensity. Perhaps Zhang et al. (2013) provide the most robust analysis of extreme precipitation behavior, analyzing daily precipitation data from 590 stations in China over the period of 1960-2005. The non-parametric Mann-Kendall test and parametric approach of linear regression were used to determine patterns of extreme precipitation events. Results indicated that 1) northwest China experienced a wetting trend, which was reflected in increasing consecutive rainy days and decreasing non-rainy days, 2) a drying tendency is exhibited mainly in regions within the Yellow River Basin, the Huaihe River Basin while relatively small variations in precipitation indices were found for northeast China, and 3) the highest intensity of extreme precipitation events was mainly associated with regions east of 100° E, particularly in the case of south China, and specifically the lower Yangtze River basin, the southeast rivers and the Pearl River basin. An increase in annual rainfall caused by increases in frequency and intensity of heavy precipitation in summer was reported for Korea (Jung et al., 2011).

Omondi et al. (2014) found a significant decrease in total precipitation on wet days for the Greater Horn of Africa region for the period 1961-2010. Very weak and insignificant trends in extreme precipitation indices were noted by Alp and Washington (2014) for 1986-2008 in the Arabian Peninsula with the only exception being the number of days with precipitation more than 10 mm (R10), which showed significant negative trends. Oliveira et al. (2016) investigated trends in extreme precipitation for northeastern Brazil. These authors used daily rainfall data from 148 rain gauges for the period 1972 - 2002. Heavy, normal and weak rainfall were defined as rainfall above 95^{th} percentile, between 45^{th} and 55^{th} percentile and under 5^{th} percentile, respectively. Based on Mann-Kendall trend results and cluster analysis, the authors concluded that the region was not substantially influenced by El Niño and La Niña, and that dry areas have greater variability and the highest number of intense events. Aguilar et al. (2005) reported that although no significant increases in the total amount were found, rainfall events were intensifying, and the contributions of wet and very wet days were increasing in Central America and northern South America for the period of 1961-2003.

The frequency of extreme precipitation events at the sub-daily time scale, which is often responsible for flash flooding in the United States, was investigated by Lejiang et al. (2016). Observed hourly precipitation data from the North American Land Data Assimilation System Phase 2 were used to determine trends in the frequency of extreme precipitation events of short (1, 3, 6, 12 and 24 h) duration for the time period 1979-2013. Results varied for different parts of the country. While an increasing trend was noticed for the central and eastern parts of the country, most of the western United States (particularly the Southwest and the Intermountain West) exhibited negative trends.

Mallakpour and Villarini (2016) noted a striking similarity regarding the increasing trend in frequency of heavy precipitation over large areas of the contiguous United States (with the exception of northwest). Powell and Keim (2015) reported an overall increasing trend in magnitude and intensity of extreme precipitation events in the southeastern United States for 1948-2012 except for the more easterly locations (specifically South Carolina). Extreme wet spell and dry spell durations are projected to be longer in the future for many locations in the eastern United States (Schoof, 2015). Jiang et al. (2016) studied the spatiotemporal characteristics of extreme precipitation events in the Western United States. The authors' analysis included spatial characterization of the El Nino Southern Oscillation (ENSO) and identification of multiscale temporal variability in precipitation extremes. Based on the results of indices such as R10, RX5, CDD and R95, a dipolar pattern was observed with a transition zone that separates the west into two main dipolar centers referred to as the Pacific Northwest and the Desert Southwest.

To summarize the major findings from all the above-reported studies, it can be concluded that changes in extreme precipitation occur according to mixed patterns and with regionally-dependent variation, arguing again in favor of regional- and local-scale studies if the results are to be used in a practical setting.

2.3 Drought events

Growing populations, increasing industrial activities, and many other factors have led to increasing demand for freshwater resources (Zarch et al., 2015). This demand becomes much more acute during periods of drought. Many countries have suffered devastating losses in the economy, infrastructure as well as direct loss of human life due to extreme weather events such as droughts, particularly during the last several decades (Rosenzweig

et al., 2001; Coumou and Rahmstorf, 2012). Drought is a natural feature of climate that occurs frequently across different climatic regimes. According to Gocic and Trajkovic (2014), drought is an extended period of water deficit and typically occurs when an area receives below-normal precipitation for several months. Mishra and Singh (2010) presented a comprehensive review of drought concepts and modelling. Three different types of drought events can be defined depending on the hydrological variable and perspectives: a) meteorological or climatological drought, b) hydrological drought and c) agricultural drought (Tallaksen and van Lanen, 2004). Meteorological droughts result from a deficit of precipitation, while a shortage in water supply leads to hydrological drought (closely related to meteorological drought). A lack of sufficient soil moisture for crop growth that results in decreased crop production is termed an agricultural drought.

Several drought indices have been proposed in the scientific literature to quantify different types of drought, including the Palmer Drought Severity Index (PDSI) (Palmer, 1965); the Standardized Precipitation Index (SPI) (McKee et al., 1993); the Surface Water Supply Index (SWSI) (Shafer and Dezman, 1982); the Standardized Precipitation Evapotranspiration Index (SPEI) (Vicente-Serrano et al., 2010); the Reconnaissance Drought Index (RDI) (Tsakaris and Vangelis, 2005) and the copula-based joint deficit index (JDI) (Kao and Govindaraju, 2010). Each of these indices usually depends on some function or combination of precipitation, temperature, evaporation or potential evapotranspiration (PET), soil moisture and/or streamflow, and is used to describe a particular type of drought as summarized in Table 2.3. A fuller discussion of these indices appears in following sections, with particular attention given to those most important in the context of this study.

Table 2.3. Summarized drought indices.

Index	Type of drought	Data used	Reference
Standardized Precipitation Index (SPI)	Meteorological	Rainfall	Mckee et al. (1993)
Reconnaissance Drought Index (RDI)	Meteorological	Rainfall, potential evapotranspiration (PET)	Tsakaris and Vangelis, 2005
Standardized Precipitation Evapotranspiration Index (SPEI)	Meteorological	Rainfall, PET	Vicente-Serrano et al., 2010
Surface Runoff Index (SRI)	Hydrological	Surface runoff	Shukla and Wood, 2008
Streamflow Drought Index (SDI)	Hydrological	Streamflow	Nalbantis and Tsakiris, 2009
Surface Water Supply Index (SWSI)	Hydrological	Reservoir storage and streamflow	Shafer and Dezman, 1982
Joint Deficit Index (JDI)	Hydrological	Rainfall, streamflow	Kao and Govindaraju, 2010
Palmer Drought Severity Index (PDSI)	Agricultural	Soil moisture	Palmer, 1965

2.3.1 Meteorological drought

The index most commonly used by researchers in describing meteorological drought is perhaps the SPI (Bonsal et al., 2013; Spinoni et al., 2014; Jenkins and Warren, 2015; Svoboda et al., 2015; Zhou and Liu, 2016), which has been recommended by the World Meteorological Organization (WMO) as the standard index for characterizing meteorological droughts (Hayes et al., 2011). Zhai et al. (2010) analyzed frequencies of dry and wet years and their trends for seven basins representing three regions in China using the time series of averaged annual SPI. Raziei et al. (2013) used SPI to analyze regional drought patterns in Iran with a focus on the effects of time scale and spatial resolution. The results showed that both spatial resolution of precipitation data and time

scale may affect drought frequency as well as their spatial homogeneity. Edossa et al. (2010) reported more frequent extreme droughts in the upper and middle portions of the Awash River basin in Ethiopia using SPI at a 12-month scale. Mild and moderate droughts, however, were more common in the middle and lower parts of the Awash River basin. Applying the SPI drought index method using rainfall data from 12 weather stations, Shahid (2008) investigated spatial and temporal drought characteristics in Western Bangladesh. The findings suggested that the north and northwestern parts of Bangladesh are most vulnerable to droughts.

Lee and Kim (2013) analyzed climate change effects on drought severity-duration-frequency relationships in Korea. For the historical assessment, observed data from the Seoul weather station were used; for assessment of future behavior, data from four different global climate models (GCMs) were considered. Results indicated a decrease in the future frequency of mild droughts and an increase in the future frequency of severe and extreme droughts. Additionally, the average duration of droughts is expected to increase.

The Reconnaissance Drought Index (RDI) uses both precipitation and evapotranspiration data in the calculations and is thus more sensitive to climatic variability than the SPI (Khalili et al., 2011). Kousari et al. (2014) used the RDI to detect trends in drought for the arid and semi-arid regions of Iran for the time period of 1975-2005. Increasing drought intensity was noted, which could be a threat to sustainable water resource management in the area. Xu et al. (2015) compared three drought indices (namely SPI, RDI and SPEI) to quantify spatiotemporal variations of drought in China

during 1961-2012. Although the three indices performed equally in the humid climatic regions, SPI and RDI were found more applicable in the arid regions than SPEI.

Zarch et al. (2015) assessed global drought conditions for both the historical time frame of 1960-2009 and future climatic conditions using the SPI and RDI. Results indicated the presence in arid zones of insignificant trends in both the downward and upward directions. Even so, however, agreement between the SPI and RDI in arid zones is higher than in the humid zones. In the semi-arid, sub-humid, and humid zones, where there are prominent inconsistencies in drought trends as assessed using the two indices, RDI showed more trends toward dryness than SPI. The SPI identified more years as drought-prone before 1998, while RDI computations resulted in more drought prone years after 1998. For future climatic conditions, agreement between SPI and RDI diminished considerably with time, which suggests the importance of the ET component of the hydrologic cycle in the context of global warming and indicates that it should not be neglected in drought modeling.

In conclusion, it can be noted that SPI is the most widely used index to quantify meteorological drought. The SPI has the distinct advantage of having a direct and exclusive relation to precipitation; however, the drawback of using the SPI is that it does not directly account for the impacts of evaporation or transpiration on soil moisture. Additionally, meteorological drought can be indirectly related to hydrological or agricultural drought as a precursor.

2.3.2 Hydrological drought

Some of the commonly-used indices to quantify hydrological drought include the Surface Runoff Index (SRI), the Surface Water Supply Index (SWSI) and the Streamflow Drought Index (SDI). Shukla and Wood (2008) developed the concept of the SRI based on SPI to include human water use practices, which are direct indications of hydrologic conditions. Comparing the behavior of SPI and SRI during drought events in a snowmelt region revealed similar patterns based on long accumulation patterns, but the authors found that the SRI was more reflective of the seasonal lags induced by the hydrologic processes. Faraj et al. (2014) investigated the sensitivity of surface runoff to drought and climate change in the Diyala watershed, shared between Iraq and Iran, using both SDI and RDI. Talaee et al. (2014) reported negative anomalies in river discharge during the warm phase of ENSO (El Nino) responsible for severe and extreme droughts in West Iran using standardized streamflow index (SSFI).

Nalbantis and Tsakiris (2009) introduced the concept of Streamflow Drought Index (SDI) and established a linear relationship between SDI and SPI. Since streamflow data can be difficult to obtain in real time, a direct comparison with an existing meteorological drought index is very helpful. Drought states were defined, which form a non-stationary Markov chain. The researchers validated the proposed methodology using the data from a basin in the West Sterea Hellas Water District in Greece.

2.4 Global climate models

Projections of future climate variables (precipitation and temperature) as well as dependent phenomena and processes (droughts, floods, water yield, etc.) are normally derived from climate models. Modern climate modeling emerged in the 1950s meteorology literature to predict atmospheric events through explicit solutions to the

equations describing conservation of energy, conservation of momentum, mass balance, and the behavior of gases. These efforts represented the first ever attempt at a "global circulation model" (Phillips, 1956; Manabe & Wetherald, 1975), or GCM. Thus, climate modeling was based on the fundamental equations known as the first law of thermodynamics, Newton's second law of motion, the continuity equation, and the ideal gas law. Diversification and increasing complexity of climate models have resulted in four broad categories of climate models (Shine & Henderson-Sellers 1983): (1) energy balance (EBM), (2) one-dimensional radiative-convective (RC), (3) two-dimensional zonally average dynamical models, often grouped with Earth system models with intermediate complexity (EMIC) and (4) three-dimensional general or global circulation.

Following the advent of high-performance computing, the three-dimensional GCMs largely replaced the other classes of models. As originally formulated, GCMs considered only the atmosphere, identical to a computational fluid dynamics simulation on large temporal and spatial scales. Given the prospect and implications of climate change, however, many GCMs evolved into fully coupled ocean-atmospheric circulation models with some including the biosphere and its carbon cycling (Sellers et al., 1986).

Parameterizations of current GCMs include equations intended to reflect small scale processes/phenomena and to approximate bulk effects of physical processes that are too complex to be represented (e.g., clouds, cumulus convection and surface albedo). Although the functional form of parameterization is physically-based, choices of parameter values are dependent on empirical studies. In broad terms, the input data required by GCMs typically describes Earth properties, CO_2 emissions, solar energy, volcanic activity, ozone concentrations, and other initial/boundary conditions. While

GCM computations are sensitive to projected atmospheric CO_2 concentrations, there is considerable uncertainty regarding their future values. The uncertainty is accommodated by specifying multiple emissions scenarios, referred to as Representative Concentration Pathways (RCPs). The four currently-recognized RCPs, which are derived on the basis of differing assumptions regarding global economic development, mitigation strategies and other factors, are summarized below in Table 2.4.

Table 2.4. Representative concentration pathways (RCPs) (van Vuuren et al., 2011)

RCP	Description	Global mean temperature anomaly (°C)	Global mean CO_2 concentration (ppmv)
RCP 8.5	Rising radiative forcing pathway leading to 8.5 W/m^2 in 2100	4.9	1370
RCP 6.0	Stabilization without overshoot pathway to 6 W/m^2 at stabilizing after 2100	3.0	850
RCP 4.5	Stabilization without overshoot pathway to 4.5 W/m^2 at stabilization before 2100	2.4	650
RCP 2.6	Peak in radiative forcing at 3 W/m^2 before 2100 and reaching 2.6 W/m^2 by 2100	1.5	490 then declines

The outputs of GCM simulations can be of a relatively comprehensive nature, including not only surface temperatures and precipitation, but detailed information on atmospheric and ocean circulation, aerosol concentrations, carbon cycling, sea and land ice coverage, ocean biogeochemistry and other processes. Since no single GCM is widely acknowledged as superior for all locations and applications, outputs are very often obtained from an ensemble of models whose results are averaged preparatory to inference and follow-on analysis.

The coarse spatial resolution of GCM outputs (typically hundreds of km horizontally) is often incompatible with regional- and smaller-scale analysis (Xu et al., 2013). Some

climate extremes, especially precipitation extremes, are mainly controlled by sub-grid processes. As a result, the coarse resolution of projected GCM outputs cannot meet the typical requirements of end users in research areas such as hydrology, conservation, and climate risk assessment (Diaz-Nieto and Wilby 2005). Therefore, appropriate downscaling is necessary to improve the coarse resolution and poor representation of precipitation and temperature in GCMs (Xu et al., 2013; Xu and Luo, 2015). Future chapters will provide expanded treatment of issues such as downscaling, resolution, use of ensembles, and GCM limitations.

2.5 Climate change impact assessment

Global warming has been identified as the driving factor of climatic change in the coming century, and global climate change has the potential to directly affect hydrological processes (Chattopadhyay and Jha, 2016; Zhang et al., 2016). Examples of hydrological processes that are susceptible to climate change include evapotranspiration (ET), water yield, soil moisture, streamflow and extreme events such as floods and droughts (Jha and Gassman, 2014; Neupane and Kumar, 2015; Li et al., 2016). Observed and projected behavior of streamflow and evapotranspiration are discussed more fully in subsequent paragraphs due to their relatively prominent role in the context of this research.

2.5.1 Streamflow

Several studies have noted that climate change is anticipated to accelerate hydrological response, which will directly affect streamflow (Ficklin et al., 2014; Dahal et al., 2016; Brianna et al., 2016; Mishra and Lilhare, 2016). For instance, Mishra and

Lilhare (2016) reported that streamflow could increase by more than 40% in eight basins during the monsoon season under the RCP 4.5 scenarios in India. The authors further observed that water availability in the sub-continental river basins is more sensitive to changes in the monsoon season precipitation rather than air-temperature. Streamflow sensitivity to future rainfall and temperature fluctuations in the Dinder River basin, Sudan was observed by Basheer et al. (2016). Shrestha and Htut (2016) investigated climate change impacts on the hydrology of the Bago River basin, Myanmar. The results of the study indicated that annual and rainy season stream flows are projected to increase by approximately 40% and 29% over the entire basin, respectively, while summer seasonal flows will decrease by 21%. Similarly, for the Lower Missouri River in the United States, most of the water fluxes are expected to increase consistent with future precipitation trends except during the summer season (Qiao et al., 2014). Thomson et al. (2003) found a wide range of variation in water yield (-210% to 77%) relative to the baseline levels within the entire United States. Brianna et al. (2016) reported that for Southern California, earlier snow melt and significantly stronger winter precipitation events in the future will pose increased flood risks and require water releases from the controlling reservoirs, which can result in less available water outside the wet season.

Novotny and Stefan (2007) linked increasing trends in streamflow to increasing mean annual precipitation and intense rainfall events in Minnesota. Chien et al. (2013) applied the SWAT model to assess potential impacts of climate change on streamflow in the agricultural watersheds of the Midwestern United States. The results of the study suggested that future streamflow will increase in winter but decrease in summer. Furthermore, increasing temperatures could influence both evapotranspiration and the

form of precipitation, both of which can impact streamflow patterns. Jha and Gassman (2014) used meteorological inputs from an ensemble of 10 GCMs to study changes in hydrology and streamflow in the Raccoon River Watershed in Iowa. Mid-century (2046-2065) projections indicated a modest 0.7% increase in annual average precipitation and a 2.7°C increase in annual average temperature. These changes in climate were assessed as reducing total water yield by 17%, while streamflow at the watershed outlet decreased by 17% on an average annual basis.

Decreasing trends in water balance components such as groundwater recharge and storage have been reported for Turkey (Erturk et al., 2014), with analogous changes in surface runoff and sediment yield reported for Spain (Zabaleta et al., 2014). Potential climatic variability can increase flood risks due to significant increases in streamflow at locations around the world. Relevant examples are found in studies by Middelkoop et al. (2001) for Germany, Jung et al. (2013) for Korea, Burn and Whitefield (2016) for Canada, Brath et al. (2006) for Italy and Viallrini et al. (2011) for the midwestern United States. Heim et al. (2013) reported that while flood magnitudes in the southwestern United States have been decreasing, the northeast and north-central United States have been experiencing increases in flood magnitudes.

Major findings from United States climate change impact studies are summarized in Table 2.5. These studies indicate that streamflow will demonstrate the expected sensitivity to future changes in climate. In keeping with the previously-developed theme, however, the impacts very often demonstrate significant regional and small-scale variations.

Table 2.5. Summarized findings of climate change impacts on streamflow.

Study area	Hydrologic Model	Major findings	Reference
Agricultural watersheds in Midwestern US	SWAT	Future streamflow will increase in winter but decrease in summer	Chien et al. (2013)
Raccoon River Watershed, Iowa	SWAT	Reducing total water yield and streamflow in mid-century (2046-2065) by 17%	Jha and Gassman (2014)
Western United States (Upper Colorado River Basin, Columbia River Basin and Sierra Nevada Basin)	SWAT	Significant decline in snowmelt and shift in streamflow timing because of warmer and wetter projections	Ficklin et al. (2015)
Arid central Arizona	SWAT	Stream discharge is projected to decrease by 31 % in the 2020s, 47 % in the 2050s, and 56 % in the 2080s compared to the mean discharge for the base period	Ye and Grimm (2013)
Contiguous US	VIC	Most regions with significant increase in future spring and winter runoff	Naz et al. (2016)
New York City water supply watershed	SWAT	Earlier snowmelt and reduced snowpack will advance the timing and increase the magnitude of discharge in the winter and early spring and corresponding decrease in late spring	Pradhanang et al. (2013)

2.5.2 Evapotranspiration (ET)

Given that the ET process is dependent on precipitation and air-temperature, increases in these variables normally result in increased actual ET (Zhang et al., 2016). Increasing temperature and decreasing precipitation could result in increasing ET during the 2080s in

California, as reported by Ficklin et al. (2013). In a very recently concluded study by Mehan et al. (2016), increasing temperatures (between 2.2°C to 3.3°C) combined with a decrease in precipitation (1.8 - 4.5%) will result in an increase in projected actual ET by 2 - 3% during the mid-21st century (2046-2065) in an agricultural watershed in South

Dakota. Chattopadhyay and Jha (2016) reported the higher sensitivity of ET to temperature than to precipitation changes in the Haw River Watershed, North Carolina for the future time frame of 2040-2069. While fewer studies devoted exclusively or primarily to future ET are available, published accounts suggest that its future behavior will react to temperature and precipitation changes in the expected manner and, by extension, with analogous variation.

CHAPTER 3: LONG-TERM TREND ANALYSIS OF PRECIPITATION AND AIR TEMPERATURE FOR KENTUCKY, UNITED STATES

Abstract

Variation in quantities such as precipitation and temperature is often assessed by detecting and characterizing trends in available meteorological data. The objective of this study was to determine the long-term trends in annual precipitation and mean annual air temperature for the state of Kentucky. Non-parametric statistical tests were applied to homogenized and (as needed) pre-whitened annual series of precipitation and mean air temperature during 1950–2010. Significant trends in annual precipitation were detected (both positive, averaging 4.1 mm/year) for only two of the 60 precipitation-homogenous weather stations (Calloway and Carlisle counties in rural western Kentucky). Only three of the 42 temperature-homogenous stations demonstrated trends (all positive, averaging 0.01 °C/year) in mean annual temperature: Calloway County, Allen County in southern-central Kentucky, and urbanized Jefferson County in northern-central Kentucky. In view of the locations of the stations demonstrating positive trends, similar work in adjacent states will be required to better understand the processes responsible for those trends and to properly place them in their larger context, if any.

Keywords: climate variability; trend analysis; Kentucky; non-parametric

3.1 Introduction

Precipitation and air temperature are two of the most important variables in the fields of climate sciences and hydrology. Precipitation is a critical component in rainfall–runoff relationships, and influences flood/drought assessment as well as mitigation measures. Temperature plays a prominent and well-known role in evaporation, transpiration, and water demand (both animal and human), and thus significantly affects both water requirements and strategies to assure its availability. The implications of changes in precipitation and temperature make it crucial for water resource planners to accurately assess their behavior and impacts on related hydrologic variables.

3.1.1 Relationship between climate data and hydrologic studies

Modeling studies, with hydrologic simulation models operated with data projections from climate models, have recently been undertaken to assess the potential hydrologic impacts of changing climate (Fickilin et al., 2013; Chatttopadhyay and Jha, 2016; Jin and Sridhar, 2012; Chattopadhyay and Jha, 2014; Modala, 2014; Abdo et al., 2009). Ficklin et al. (2013) applied a hydrologic model to the Upper Colorado River Basin and combined it with forecast data from 16 Global Climate Models (GCMs), finding a temporal shift in most hydrologic outputs with a significant decline in snowmelt projected by the end of the 21st century. Additionally, projected temperature increases translated to increased (23%) estimates of average annual evapotranspiration. In a similar study focusing on the Haw River Watershed in North Carolina, Chattopadhyay and Jha (2016) linked the Soil and Water Assessment Tool (SWAT) model (Neitsch et al., 2005) with climate projections from four Regional Climate Models (RCMs). The study indicated that an

overall average 14% increase in precipitation would increase water yield by a disproportionately high 38% on an annual basis. Jin and Sridhar (2012) used the same basic approach for hydrologic cycle impact assessment in the Boise and Spokane River Basins but used a different suite of climate models. For the Spokane River watershed, the projected precipitation changes ranged from 3.8 to 36%, and projected temperature changes ranged from 0.0 to 3.9 °C over the study period (2010–2060), corresponding to estimated changes in annual peak flows ranging from −58 to 106 m^3/s. The results for the Boise River watershed were similar; precipitation changes of −6.7–17.9% and temperature changes of 0.1–3.5 °C were projected to change annual peak flows by −198–88 m^3/s. The general findings of modeling studies such as these are strengthened by observations of hydrologic cycle changes on regional to global scales, attributable to greenhouse gas emissions (Brutsaert and Parlange 1998; Solomon et al., 2007; Prudhomme et al., 2003; Minville et al., 2008). The hydrologic cycle, then, responds in predictable ways to variation in influential variables, sometimes in a more-than-proportional manner. This outcome magnifies the importance of characterizing future climate in the context of hydrology.

3.1.2 Trends in air temperature

Many studies, representing a wide range of locations and scales, have investigated trends in climatic variables (New et al., 2001; Boyles and Raman, 2003; Small et al., 2006; Mohsin and Gough, 2010; Prat and Nelson, 2013; Sayemuzzaman et al., 2014; Sayemuzzaman et al., 2015). The overall trend with respect to temperature seems clear at the global scale. According to IPCC 5^{th} Assessment report, global mean annual temperature, for both surface and ocean air in combination, has increased by 0.65–1.06

°C over the period 1880–2012. At smaller spatial and temporal scales, there is less uniformity of findings. Zhao et al. (2014) reported that mean surface air temperature in Eastern China increased by 1.52 °C over the last 100 years. In a similar study, Ceppi et al. (2012) analyzed seasonal air temperatures in Sweden for the period 1959–2008, finding increasing trends that were greatest in summer (0.34–0.62 °C/decade) and least in autumn (0.02–0.38 °C/decade). Supportive results have been reported by Rio et al. (2011) for a 40-year period of records in Spain and by Degaetano and Allen (2002) for the period 1950–1996 in the US. At still smaller scales, increasing trends have been reported for Florida (2012) and several northeastern states (Karmeshu, 2012). Two of the nine states investigated by Karmeshu (2012), however, demonstrated no significant trend in temperature. Variation in long-term behavior of temperature thus appears to be present, especially at relatively small spatial and temporal scales.

3.1.3 Trends in precipitation

Recent reports on the long-term behavior of precipitation suggest similar, if not larger, variation on spatial and temporal scales. Toward the upper end of the spatial scale, (Xu et al., 2005; IPCC, 2001) reported that mean annual land-surface precipitation over the 20th century increased by 7%–12% in the middle and high latitudes (30°–85°) of the Northern hemisphere, but only by 2% for latitudes ranging from 0° to 55°S, whereas Karl and Knight (1998) reported a 10% increase in annual precipitation across United States between 1910 and 1996. On a smaller scale, Philandras et al. (2011) studied long-term precipitation within the Mediterranean region over the period 1901–2009, finding that the trends were generally negative. Slightly positive trends were detected, however, in the sub-regions of northern Africa, southern Italy and the western Iberian Peninsula.

Abbaspour et al. (2009) reported a similarly mixed result for Iran, noting that the wet regions of Iran are expected to receive more rainfall in future, while dry regions would receive less; i.e., an amplifying effect. In an investigation of extreme precipitation events in Bulgaria over the years 1961–2005, Bocheva et al. (2008) found that total precipitation was stable over this period. However, extreme events occurred more frequently, and weak/moderate events occurred less frequently during the last 15 years of the study period, again suggesting a relatively recent process of amplification.

Mixed findings are reported at still smaller scales. In a study involving 211 weather stations in the Campania region of southern Italy over the period 1918–1999, Longobardi et al. (2009) detected negative trends in annual precipitation for 27% of the stations and positive trends for 9% of the stations. When only the last 30 years were considered, however, negative trends were detected for 97% of the stations. In the northeastern US, on the other hand, Karmeshu (2012) found increasing trends in precipitation for seven of the nine states studied, with no trend detected for either Maine or New Hampshire. Jones et al. (2015) analyzed the temporal variability of precipitation in Upper Tennessee Valley for the period 1950–2009. Over this period, only 11% of the 78 sub-basins experienced either significant increasing or decreasing trends. The average trend for precipitation was −0.50 mm/year with the range being –14.27 mm/year to 5.04 mm/year.

The studies cited earlier suggest that, relative to temperature, the long-term behavior of precipitation is characterized by greater spatial variability, indicating a proportionately higher dependence on regional and local variables. In this case, relatively small-scale analyses (tens or hundreds of thousands of km^2) might be required in practical applications.

3.2 Objective

The potential magnitude and range of impacts of climate change makes it prudent to translate trends in hydrologic variables into effects experienced by ecosystems, populations and infrastructure. Reliably detecting and characterizing these trends is a necessary first step in such an analysis, whether at a relatively small scale (watershed) or at the larger scale of a political decision-making entity (state). The objective of this study was to evaluate trends in precipitation and air temperature for the state of Kentucky. The results can indicate whether additional analysis is required and, if so, serve as a necessary input to forecasting, decision-making and planning processes to mitigate any adverse consequences of changing climate.

3.3 Materials and methods

3.3.1 Study area description

Kentucky is situated roughly from 36º30’N to 39º09´N latitude and 81º58’W to 89º34´W longitude. Kentucky is the smallest of the eight states comprising the south-central region, encompassing a total area of roughly 105,000 km^2 (Figure 3.1). It is located approximately midway between the Gulf of Mexico to the south and the Great Lakes to the north, with the Atlantic Ocean and the Great Plains located to its distant east and west, respectively. The state is characterized by a broad range of elevations varying from 122 m above mean sea level (MSL) along the Mississippi River in the west to more than 1220 m MSL in the southeast, averaging 229 m MSL. Most of the river networks and streams in Kentucky drain to the Ohio River. Major land uses in the state include

forest and grassland in the eastern portions and cultivated cropland in the western portions. Major urban areas include Louisville and Lexington in the central part of the state; their metropolitan statistical areas contain populations of approximately 1.3 and 0.5 million residents, respectively, of the state's 4.4 million total residents. Annual average precipitation over the state varies from 1060 mm in the north to 1502 mm in the southwest with average annual temperature ranging from 10.8 °C in the northeast to 14.1°C in the southwest (Kentucky Climate Center). There are no distinct "wet" or "dry" seasons as observed in some other parts of the US, though summer often experiences more rainfall than the other seasons.

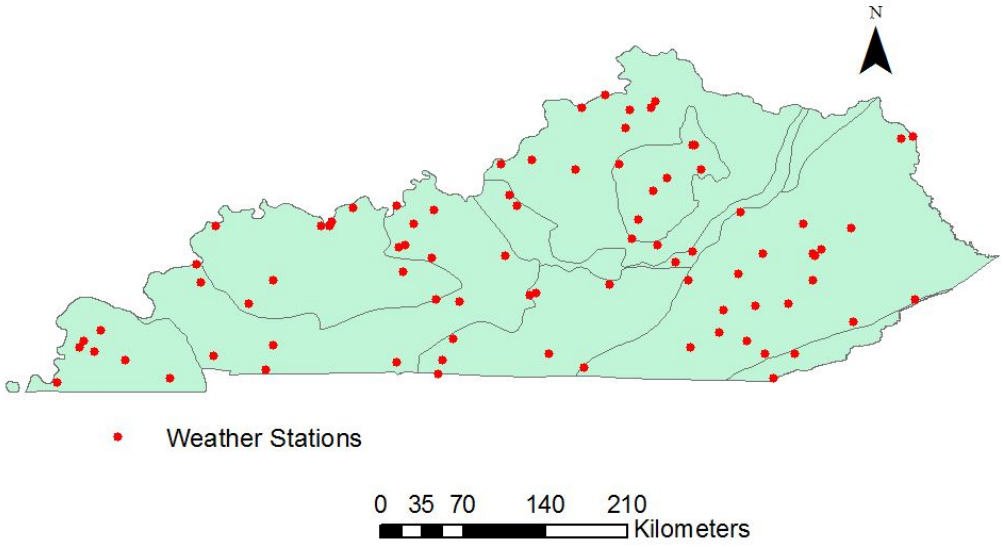

Figure 3.1 Locations of weather stations in the initial dataset. Lines are physiographic region boundaries.

3.3.2 Dataset description

Time series of daily precipitation, maximum air temperature and minimum air temperature, collectively covering each of Kentucky's 120 counties, were obtained from the US Department of Agriculture, Agricultural Research Service's (USDA ARS) online data retrieval tool. These data were derived from National Oceanic and Atmospheric Administration data sets as described by the USDA ARS (2014). The 61-year period from 1950 to 2010, inclusive, was selected as the study duration to ensure standardization among stations and an adequate record length. Stations not meeting this requirement were discarded from further analysis. Inspection of the remaining time series indicated that still others had a minimum of one instance of missing data for at least 30 consecutive daily days; these series were also discarded, leaving a total of 84 weather stations' data to be used in the study (Figure 3.1).

Subsequent processing was performed for individual stations' data series, rather than averaged series. While there is the potential for inferences to differ between averaged and individual series due to the relatively low variance of averaged data, individual series were preferred from the standpoint of achieving maximum spatial resolution of results. This, in turn, would ideally permit the data itself to point to any regions of consistent temperature and/or rainfall behavior rather than using an *a priori* definition of regions over which to average the stations' data.

3.3.3 Pre-processing of data

The 61 years of daily data were reduced to annual series of total precipitation and average temperature. Consistent with WMO guidance, these series were subsequently tested for homogeneity (i.e., to detect changes in station location, instruments and/or protocols) and to determine whether pre-whitening was appropriate. As reviewed and

critiqued by Costa and Suares (2009), methods for both absolute homogenization (in which series are tested separately) and relative homogenization (in which discontinuities are detected by comparison to applicable reference stations) are available, the categories differing in terms of assumptions, performance, applicability and available data. Homogeneity testing in this study followed an absolute method described by Longobardi et al. (2009), in which the time series must pass two separate tests (a *t*-test and modification of Ward's test) to be included for subsequent analysis. The *t*-test has also been applied in homogeneity testing by Panofsky and Brier (1968) and Alamgir et al. (2015) among others, whereas Ward's test has been additionally applied by Kalkstein et al. (1987) and Unal et al. (2003) for example. Absolute homogenization was preferred in this study on the basis of the minimal assumptions required and the lack of a requirement to identify optimal station groupings within the highly diverse study area.

The purpose of the t-test was to determine whether the mean μ_1 of the series subset consisting of the first n_1 values should be considered as different from the mean μ_2 of the remaining n_2 (= $n - n_1$) values of the series, in which case the overall series would be considered non-homogenous. The test statistic t_{n_1,n_2} was calculated as Longobardi et al. (2009):

$$t_{n_1,n_2} = \frac{\bar{X}_1 - \bar{X}_2}{S}\sqrt{n_1 n_2/(n_1 + n_2)} \quad (1)$$

where the weighted sample variance S is given by:

$$S = \sqrt{(n_1 {S_1}^2 + n_2 {S_2}^2)/(n_1 + n_2 - 2)} \quad (2)$$

t-statistics were calculated for all possible values of n_1 (and thus n_2) and compared to $t_{\nu,1-\alpha/2}$, where α was taken as 0.05 and the degrees of freedom ν were calculated from Longobardi et al. (2009):

$$v = \frac{\left[\frac{{S_1}^2}{n_1} + \frac{{S_2}^2}{n_2}\right]^2}{\frac{\left(\frac{{S_1}^2}{n_1}\right)^2}{n_1 - 1} + \frac{\left(\frac{{S_2}^2}{n_2}\right)^2}{n_2 - 1}} \tag{3}$$

If $t_{n_1,n_2} > t_{\nu,1-\alpha/2}$ for any value of n_1, then the null hypothesis H_o: $\mu_1 = \mu_2$ was rejected, and the alternate hypothesis H_a: $\mu_1 \neq \mu_2$ was accepted. The series was then considered non-homogenous, having failed the t-test for homogeneity, and excluded from subsequent analysis.

The data were also subjected to a modified and simplified version of Ward's test (Kalkstein et al., 1987) to assess whether the data should be considered as representing multiple clusters, which would be considered an indication of non-homogenous data. Following Longobardi et al. (2009), the Huygens decomposition of system deviance dev(x) of a process x with two subsets of sizes n_1 and $n_2 = n - n_1$ can be written as:

$$dev(x) = \sum_{i=1}^{2}\sum_{j=1}^{n_i}(x_{i,j} - \mu_{x_j})^2 + \sum_{i=1}^{2} n_i(\mu_{x_i} - \mu_x)^2 \tag{4}$$

As discussed by Longobardi et al. (2009), the goal is to identify the optimal value of n_1 (and thus n_2) that maximizes the second term of Equation (4) and, in so doing, provides the best definitions of the two clusters. Optimal values of n_1 other than the first five or last five values in the series were considered as evidence of distinct clusters within the series; *i.e.*, evidence of non-homogeneity. Series exhibiting non-homogeneity were

categorized as having failed Ward's test of homogeneity and excluded from subsequent analysis.

Several relevant studies (Douglas et al., 2000; Zhang et al., 2001; Yue et al., 2002; Matalas et al., 2003; Gocic and Trajkovic, 2013; Sayemuzzaman and Jha, 2014) have highlighted the need to test for serial correlation and, if present, correct for serial correlation in time series data prior to a trend analysis. Otherwise, trends might be incorrectly estimated, and the probability of a Type 1 error can increase. The precipitation and temperature series passing the homogeneity tests were next examined for the presence of significant serial correlation as described by (Gocic and Trajkovic, 2013; Sayemuzzaman and Jha, 2014) to determine whether pre-whitening was necessary. The serial correlation coefficient r_1 was calculated as

$$r_1 = \frac{\frac{1}{n-1}\sum_{i=1}^{n-1}(x_i - \overline{X})(x_{i+1} - \overline{X})}{\frac{1}{n}\sum_{i=1}^{n}(x_i - \overline{X})^2} \tag{5}$$

No significant serial correlation was judged present if the value of r_1 fell inside the bounds given by:

$$\frac{-1 - 1.645\sqrt{(n-2)}}{n-1} \leq r_1 \leq \frac{-1 + 1.645\sqrt{(n-2)}}{n-1} \tag{6}$$

If, however, significant serial correlation was detected, then a pre-whitened series x^* (with one fewer data point than the original) was created for subsequent analysis from:

$$x_i^* = x_{i+1} - r_1 x_i \tag{7}$$

3.3.4 Trend detection and characterization

A variety of statistical methods have been applied in studies such as those previously noted to detect trends and other changes in hydrologic and climatic variables (Modarres and Silva, 2007; Wang et al., 2009; Tabari et al., 2011; Jain et al., 2012; Sonali and Nagesh, 2013; Jha and Singh, 2013; Sayemuzzaman et al., 2014). These methods can be broadly categorized as parametric and non-parametric methods; parametric methods assume an underlying distribution (typically Normal) for the variables of interest, whereas non-parametric methods do not. Sonali and Nagesh (2013), among others, have advocated the use of non-parametric methods of trend detection, noting that untransformed hydrologic and climatic data are often distinctly non-normal with positive skewness.

The non-parametric Mann-Kendall test (Mann, 1945; Kendall, 1975) was used to assess the presence of significant trends in precipitation and temperature data, consistent with environmental applications reported by Modarres and Silva (2007) and Modarres and Sarhadi (2009). The Mann-Kendall statistic S_M of the series x is given by:

$$S_M = \sum_{i=1}^{n-1} \sum_{j=i+1}^{n} sgn\,(x_j - x_i) \tag{8}$$

where *sgn* is the signum function. The variance associated with S_M is calculated from (Mann, 1945; Kendall, 1975):

$$V(S_M) = \frac{n(n-1)(2n+5) - \sum_{k=1}^{m} t_k(t_k-1)(2t_k+5)}{18} \tag{9}$$

where m is the number of tied groups and t_k is the number of data points in group k. In cases where the sample size $n > 10$, the test statistic $Z(S_M)$ is calculated from (Mann, 1945; Kendall, 1975):

$$Z(S) = \begin{cases} \dfrac{S_M - 1}{\sqrt{V(S_M)}}, & if\ S_M > 0 \\ 0 & if\ S_M = 0 \\ \dfrac{S_M + 1}{\sqrt{V(S_M)}}, & if\ S_M < 0 \end{cases} \tag{10}$$

Positive values of $Z(S_M)$ indicate increasing trends, while negative $Z(S_M)$ values reflect decreasing trends. Trends are considered significant if $|Z(S_M)|$ are greater than the standard normal deviate $Z_{1-\alpha/2}$ for the desired value of α (taken as 0.05 in this study).

The Theil-Sen approach (TSA), a commonly-used method to quantify the significant linear trends in time series, was used in this study. The TSA is considered more robust than the least-squares method due to its relative insensitivity to extreme values and better performance even for normally distributed data (Hirsch et al., 1982) In general, the slope Q between any two values of a time series x can be estimated from

$$Q = \frac{x_k - x_j}{k - j}, k \neq j \tag{11}$$

For a time series x having n observations, there are a possible $N = n\ (n - 1)/2$ values of Q that can be calculated. According to Sen's method, the overall estimator of slope is the median of these N values of Q. The overall slope estimator Q^* is thus:

$$Q^* = \begin{cases} Q_{(N+1)/2}, N \text{ odd} \\ \dfrac{Q_{N/2} + Q_{(N+2)/2}}{2}, N \text{ even} \end{cases} \tag{12}$$

When significant trends in the data were detected, 95% confidence intervals were calculated using non-parametric techniques as described by Salmi et al. (2002). The quantity C_α is first calculated as

$$C_\alpha = Z_{1-\alpha/2}\sqrt{V(S)} \tag{13}$$

where Z is again the standard normal deviate, $V(S)$ is as defined earlier, and α is taken as 0.05. Indices M_1 and M_2 are determined from:

$$M_1 = \frac{N - C_\alpha}{2} \tag{14}$$

$$M_2 = \frac{N + C_\alpha}{2} \tag{15}$$

where N is as previously defined. Finally, the confidence limits are defined by the M_1^{th} and $(M_2+1)^{th}$ largest of the ordered estimates of Q, with interpolation as appropriate for non-integer values of M_1 and M_2.

3.4 Results and discussions

3.4.1 Precipitation

As indicated in Table 3.1, mean annual precipitation ranged from a low of 1080 mm for station Boyd (1) (Figure 3.2, station 6) to a high of 1352 mm for station Calloway (Figure 3.2, station 59) with a mean over all stations of 1224 ± 75 mm. Twenty-four stations' series failed either the *t*-test, Ward's test or both and were excluded from further analysis (Table 3.1) as non-homogeneous. Pre-whitening was necessary for only two of the remaining 60 stations (Boyd (2), Figure 3.2, station 7 with a serial correlation

coefficient of 0.28 and Garrard (2), Figure 3.2, station 31 with a serial correlation coefficient of 0.21) and did not affect the detection of a significant trend. For the great majority (58 of 60, or 97%) of the homogenous stations, no significant trends in annual precipitation were detected. In the two instances of significant trends, both trends were positive: Calloway, with a Sen slope of 3.51 mm/year (0.26% of the mean), and Carlisle (1) (Figure 3.2, station 60), with a Sen slope of 4.78 mm/year (0.37% of the mean). Figure 3.3 provides a more detailed depiction of the data for the Calloway County station, as an example, along with the calculated trend slope and 95% confidence limits on the slope. While it must be noted that the homogenization tests admit the possibility of a series with very low variability about a relatively large trend slope failing the tests, this appears not to have happened in this case. Only six of the 24 series assessed as non-homogenous would have had significant Sen slopes; however, the average of the six slope magnitudes was no greater than for the Calloway and Carlisle (1) stations.

Table 3.1 Summarized precipitation trend analysis results.

Station No.	Station	Elevation	Mean Annual Precipitation	Sen Slope
	County	(m)	(mm)	(mm/year)
1	Allen (2)	189	1280	1.29 (−2.07–4.24) [1]
2	Allen (3)	259	1324	0.57 (−2.33–3.83)
3	Ballard	113	1268	2.06 (−1.90–5.73)
4	Bell (1)	348	1274	−1.05 (−3.84–1.93)
5	Bell (2)	354	1297	−0.64 (−3.54–2.64)
6	Boyd (1)	171	1080	2.12 (−0.43–4.16)
7	Boyd (2)	226	1085	−1.01 (−4.29–2.45)
8	Boyle	274	1207	2.02 (−1.01–5.06)
9	Breckinridge (1)	116	1206	2.27 (−0.85–5.37)
10	Breckinridge (2)	180	1218	1.61 (−1.19–4.44)
11	Breckinridge (3)	218	1200	2.79 (−0.66–6.08)
12	Bullitt (1)	168	1238	1.36 (−1.66–4.16)

13	Carlisle (2)	125	1326	3.41 (−0.41–6.25)
14	Carlisle (3)	107	1291	2.99 (−0.41–5.88)
15	Casey	265	1336	0.29 (−3.11–2.93)
16	Christian (1)	171	1272	1.80 (−1.57–4.71)
17	Christian (2)	159	1276	1.68 (−1.70–4.70)
18	Clay (2)	265	1281	−0.25 (−3.65–3.21)
19	Clinton	284	1319	0.17 (−2.78–3.72)
20	Cumberland	183	1293	−0.42 (−3.92–2.53)
21	Daviess (1)	123	1162	0.98 (−1.82–4.10)
22	Daviess (2)	122	1156	1.52 (−1.21–4.59)
23	Daviess (3)	125	1153	1.62 (−1.28–4.46)
24	Edmonson (1)	125	1301	1.35 (−1.47–4.27)
25	Edmonson (2)	177	1321	0.85 (−2.32–4.18)
26	Edmonson (3)	241	1299	1.09 (−1.76–3.85)
27	Fayette (1)	294	1158	0.60 (−2.69–3.83)
28	Fayette (2)	284	1152	1.34 (−1.60–4.67)
29	Franklin	152	1111	1.33 (−0.85–5.07)
30	Garrard (1)	335	1225	−1.05 (−4.31–2.41)
31	Garrard (2)	311	1083	−0.34 (−2.8 –2.38)
32	Grant (1)	288	1108	1.09 (−1.58–3.34)
33	Grant (2)	287	1105	0.08 (−2.78–2.64)
34	Grant (3)	287	1309	1.64 (−1.93–4.59)
35	Graves	110	1301	0.68 (−2.75–3.80)
36	Grayson (2)	143	1234	2.60 (−0.24–5.75)
37	Green (1)	180	1314	0.06 (−3.27–3.44)
38	Green (2)	213	1267	1.04 (−2.32–3.44)
39	Hancock	128	1183	2.05 (−0.56–5.00)
40	Harrison (1)	213	1119	0.97 (−1.73–3.29)
41	Harrison (2)	220	1125	0.80 (−2.16–3.27)
42	Hopkins (2)	134	1217	2.70 (−0.26–5.44)
43	Jackson	381	1243	1.78 (−4.93–1.49)
44	Jefferson (1)	223	1193	1.60 (−1.49–4.64)
45	Jefferson (2)	141	1128	2.05 (−0.72–4.94)
46	Jessamine	165	1199	0.64 (−2.41–3.41)
47	Knox	302	1282	−0.39 (−3.60–2.64)
48	Larue	240	1260	0.37 (−2.88–3.74)
49	Laurel	384	1230	−0.81 (−3.90–2.79)
50	Madison	326	1189	−1.06 (−3.93–2.48)
51	Magoffin	277	1124	0.35 (−2.24–3.08)
52	Owen	293	1122	0.48 (−2.20–2.97)
53	Perry (2)	366	1236	−0.77 (−3.47–2.14)
54	Shelby	223	1187	2.68 (−0.28–5.98)
55	Simpson	220	1236	1.38 (−2.05–4.54)

56	Trigg	116	1290	2.29 (−1.40–5.29)
57	Whitley (1)	323	1254	−0.47 (−3.47–2.81)
58	Wolfe	308	1169	0.33 (−2.50–3.35)
59	Calloway	161	1352	**3.51 (0.10–7.06)** [2]
60	Carlisle (1)	110	1293	**4.78 (0.73–8.42)**

[1] Values in parentheses are 95% confidence limits on the Sen slope; [2] Bold values represent significant at $p = 0.05$.

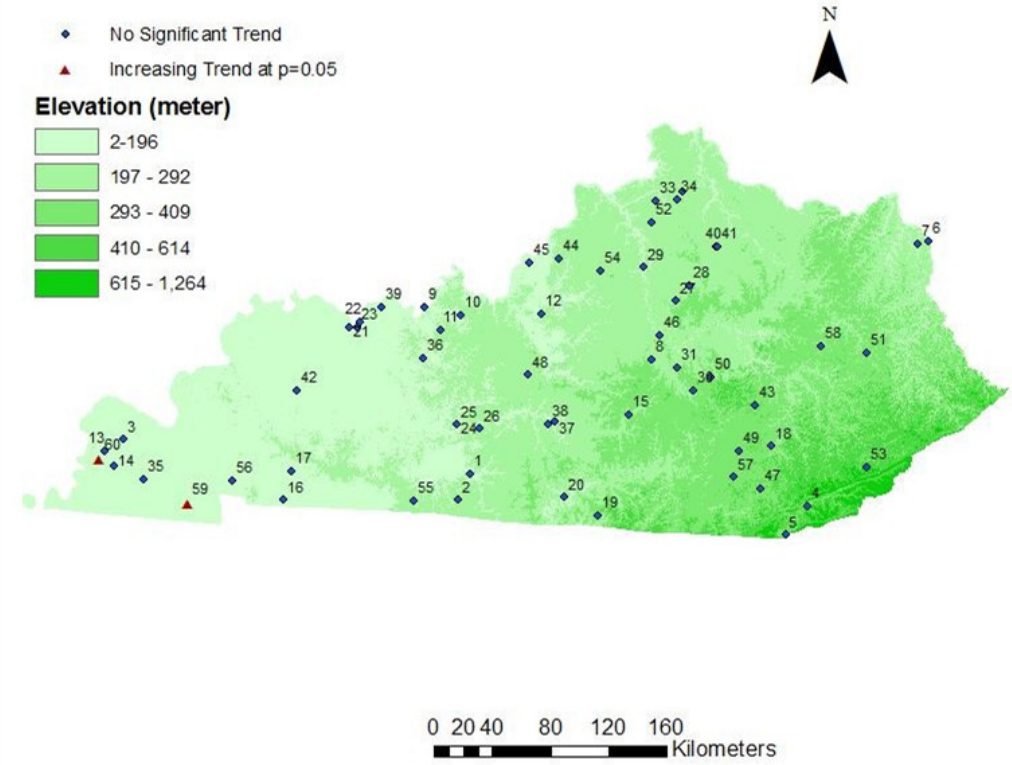

Figure 3.2 Spatial distribution of annual precipitation trend analysis results

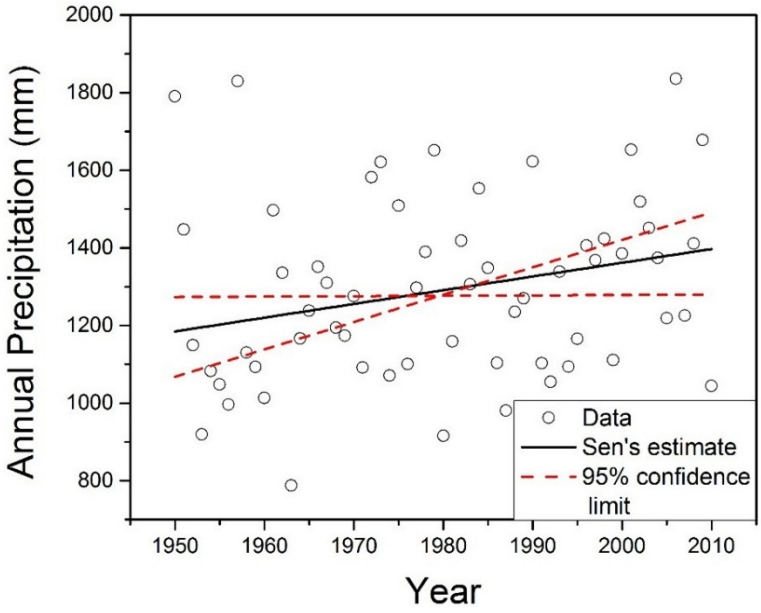

Figure 3.3 Annual precipitation with Sen slope estimate and 95% confidence intervals for the Calloway County, Kentucky, weather station.

The findings clearly indicate that, according to the dataset and methods used in this study, annual rainfall depths in Kentucky generally exhibit no statistically significant trends with respect to time. It is difficult to directly compare our findings to those from similar studies due to differences in data aggregation, trend detection methodology, and pre-processing technique (if any). Kentucky Climate Center reports overall increasing trends in annual precipitation for three of the state's four climate divisions (all except the easternmost), but an evaluation of the statistical significance of the trends is unavailable. In similar fashion, the online trend analysis tool available at NOAA indicates positive trends in annual precipitation ranging from 0.9 mm/year (eastern Kentucky) to 2.5 mm/year (western Kentucky) for Kentucky's four climate divisions when considering the same period of record as used in this study. This result is consistent with our findings in so far as the only stations identified in this study as having significant trends are in western Kentucky, the climate division having the highest trend as calculated by NOAA,

but little else can be said. Larger-scale studies provide perhaps the best context for our findings. As described in the IPCC AR5 report, the Global Historical Climatology Network (GHCN), Global Precipitation Climatology Center (GPCC) and Climatic Research Unit (CRU) datasets indicate positive—though not statistically significant—trends in annual precipitation for Kentucky. These data sets also indicate lower trend magnitudes in the eastern direction and higher magnitudes in the northern and (consistent with our findings) western directions, becoming statistically significant (p = 0.10) for grid points within 200–300 km north-northwest of Kentucky.

The two instances of significant trends in annual precipitation are noteworthy in the sense that (a) both are located in extreme southwestern Kentucky (the Mississippi Embayment physiographic region), (b) both have relatively high mean annual precipitation (the Calloway station has the highest among the stations studied, and Carlisle (1) has the 13th highest), (c) both stations are situated at relatively low elevations (Carlisle (1) is the second lowest and Calloway is the 13th lowest among the stations studied), and (d) the trend slopes are intermediate in comparison to what Sayemuzzaman and Jha (2014) reported for the Southern Coastal Plain region of North Carolina (a maximum of 9 mm/year), the findings published by Karmeshu (2012) for the northeastern US (up to 0.13 mm/year) and the results from the GHCN, GPCC and CRU datasets as reported by Hartmann et al., (2013); *i.e.*, within previously-reported bounds for the region. It thus seems possible that, instead of being anomalies or artifacts, the positively-trending stations might roughly mark the edge of a larger region of positively-trending annual precipitation. Analogous studies in the neighboring states, especially those to the north and west, would be required to explore this possibility more fully.

3.4.2 Temperature

As indicated in Table 3.2, 42 stations (50%) passed both the homogeneity tests. Mean annual temperature varied over these stations from 12.22 °C for the Shelby station (Figure 3.4, station 35) to 14.84 °C for the Calloway station (Figure 3.4, station 41), with an overall mean of 13.55 ± 0.66 °C. Pre-whitening was performed on eight of the 42 homogenous stations having serial correlation coefficients ranging from 0.32 to 0.42: Bell (1) (Figure 3.4, station 4), Clay (2) (Figure 3.4, station 15), Edmonson (3) (Figure 3.4, station 21), Garrard (1) (Figure 3.4, station 25), Grayson (3) (Figure 3.4, station 29), Simpson (Figure 3.4, station 36), Carlisle (2) (Figure 3.4, station 10) and Daviess (2) (Figure 3.4, station 20). Pre-whitening did not affect the statistical significance of subsequently-calculated trend slopes in any case. The general findings with regard to trends in the temperature series were similar to those reported earlier for precipitation: only a small proportion (3 of 42, or 7%) of the stations demonstrated a significant trend, though the trend in each case was in the increasing direction. Figure 3.5 provides an example of more detailed information for one of the stations having a positive trend in mean annual temperature (the Calloway station). As during the analysis precipitation data, trend slopes for series assessed as non-homogenous were examined to ensure that authentic non-homogeneities, rather than especially high trend slopes, were the reason for failing the homogeneity test(s). In all cases, the trend slopes of series assessed as non-homogenous were less than that for the homogenous Allen (2) station.

Table 3.2 Summarized temperature trend analysis results.

Station No.	Station	Elevation	Mean Annual Temperature	Sen Slope

	County	(m)	(°C)	(°C/year)
1	Allen (1)	213	14.24	0.001 (−0.010–0.012)[1]
2	Allen (3)	259	14.30	−0.001 (−0.140–0.010)
3	Ballard	113	14.26	0.004 (−0.006–0.015)
4	Bell (1)	348	12.84	−0.008 (−0.017–0.004)
5	Bourbon	247	12.57	−0.002 (−0.012–0.009)
6	Breckinridge (1)	116	13.18	0.009 (−0.006–0.019)
7	Breckinridge (2)	180	13.37	0.009 (−0.003–0.023)
8	Breckinridge (3)	218	13.33	−0.002 (−0.016–0.008)
9	Carlisle (1)	110	14.49	−0.001 (−0.010–0.009)
10	Carlisle (2)	125	14.44	−0.001 (−0.011–0.009)
11	Carlisle (3)	107	14.48	0.002 (−0.007–0.011)
12	Carroll	137	13.11	−0.001 (−0.009–0.011)
13	Casey	265	13.34	−0.008 (−0.018–0.003)
14	Christian (1)	171	14.29	0.008 (−0.009–0.009)
15	Clay (2)	265	13.06	−0.002 (−0.008–0.012)
16	Clinton	284	13.56	−0.005 (−0.003–0.019)
17	Crittenden (1)	110	14.07	−0.005 (−0.015–0.006)
18	Crittenden (2)	165	14.21	0.003 (−0.017–0.007)
19	Daviess (1)	123	14.06	0.000 (−0.008–0.011)
20	Daviess (2)	122	13.81	0.001 (−0.009–0.010)
21	Edmonson (3)	241	13.28	−0.001 (−0.015–0.011)
22	Fayette (1)	294	12.93	0.007 (−0.004–0.018)
23	Fayette (2)	284	12.69	0.009 (−0.002–0.020)
24	Fulton	116	14.54	−0.000 (−0.005–0.020)
25	Garrard (1)	335	13.25	0.004 (−0.009–0.015)
26	Garrard (2)	311	13.20	0.003 (−0.008–0.014)
27	Graves	110	14.60	0.006 (−0.005–0.025)
28	Grayson (2)	143	13.14	−0.003 (−0.016–0.009)
29	Grayson (3)	183	13.41	0.005 (−0.006–0.014)
30	Jessamine	165	13.01	0.004 (−0.009–0.015)
31	Laurel	384	13.07	0.001 (−0.007–0.013)
32	Madison	326	13.84	0.002 (−0.007–0.012)
33	Perry (1)	285	12.80	0.007 (−0.003–0.019)
34	Powell	366	13.13	0.000 (−0.010–0.011)
35	Shelby	223	12.22	−0.011 (−0.025–0.006)
36	Simpson	220	14.12	0.003 (−0.008–0.013)
37	Whitley (1)	323	13.23	−0.002 (−0.010–0.011)
38	Whitley (2)	326	13.09	−0.010 (−0.020–0.000)

39	Wolfe	308	12.80	−0.002 (−0.009–0.011)
40	Allen (2)	189	13.97	**0.021 (0.010–0.030)** [2]
41	Calloway	161	14.84	**0.012 (0.001–0.020)**
42	Jefferson (1)	223	13.06	**0.010 (0.001–0.019)**

[1] Values in parentheses are 95% confidence limits on the Sen slope; [2] Bold values represent significant at $p = 0.05$.

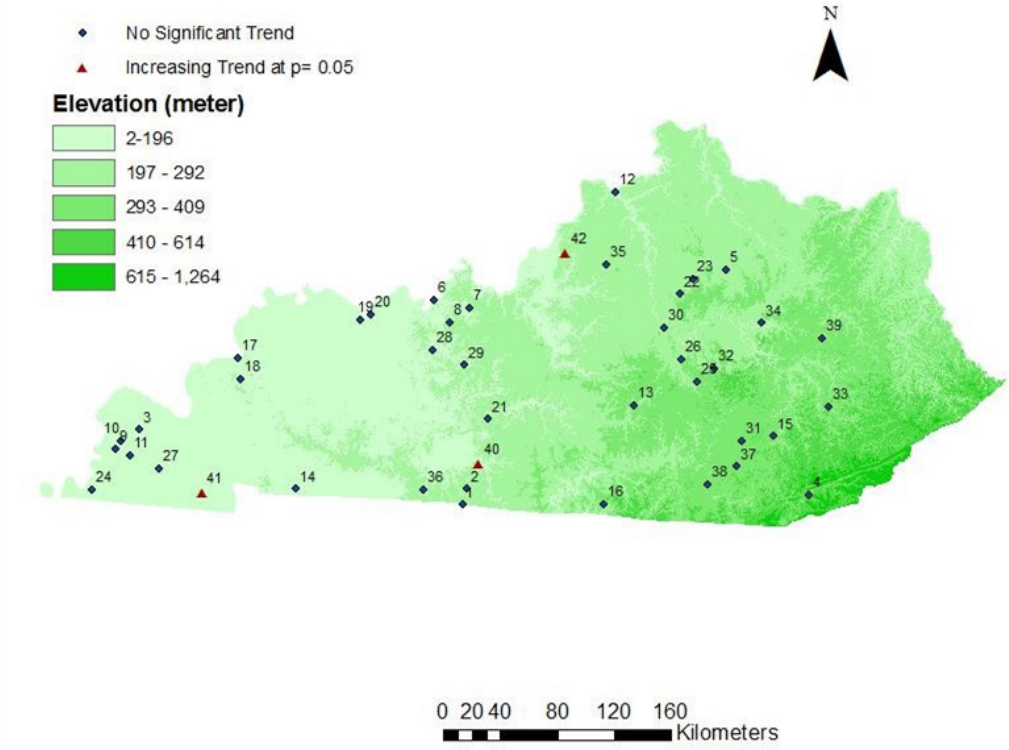

Figure 3.4 Spatial distribution of annual temperature trend analysis results

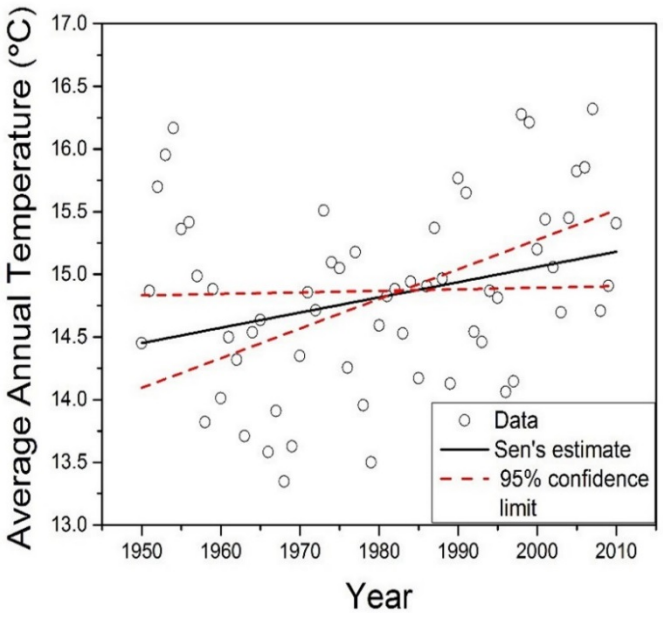

Figure 3.5 Annual temperature with Sen slope estimate and 95% confidence intervals for the Calloway County, Kentucky, weather station.

The data and analysis in the present study indicate that, broadly speaking, mean annual temperatures in Kentucky have not demonstrated a statistically significant trend with regard to time. The exceptions to this rule are the data from the Calloway, Allen (2) (Figure 3.4, station 40) and Jefferson (1) (Figure 3.4, station 42) stations. The Jefferson (1) station's results (with an estimated trend slope of 0.01 °C/year) are difficult to interpret; the included city of Louisville could have been exerting an urban heat island effect on temperatures, but as a hypothesized explanation, this seems unsatisfactory given Louisville's steadily declining population over the period 1960–2000. The other two stations having significant trends in mean annual temperature (Calloway at 0.01 °C/year and Allen (2) at 0.02 °C/year) seem not to have many relevant factors in common other than a non-urban dominant land-use and their location on or along Kentucky's southern border.

The magnitudes of the positive trends in this study detected are consistent with results reported elsewhere in the world by Zhao et al. (2014) for China (1.52 °C over the last century) and by Ceppi et al. (2012) for Sweden, to cite two examples. The existence of spatially-varied results over the scale investigated in this study is also consistent with findings published by Karmeshu, (2012), who found that comparably-sized regions with positive temperature trends and with no significant trends could exist within relatively short distances of one another. In closer proximity to our study area, Portmann et al. (2009) reported an overall cooling trend for the southeastern region of the United States for 1950–2006, but, at finer resolution, an increasing trend in daily maximum and minimum temperature along the western parts of Kentucky (consistent with the locations of the trends identified in this study as significant).

State-wide positive trends in temperature are identified by both Kentucky Climate Center and NOAA though, as discussed previously for these sources, the statistical significance of these trends is not assessed. A study reported by Tebaldi (2012) using data from the period 1912–2011 indicates a slight (0.04 °C/century; statistically insignificant) increasing trend in state-wide temperatures. Comparable findings of positive, though statistically insignificant, trends are reported by Hartmann et al., (2013) based on three datasets: the CRU's HadCRUT4, the National Climatic Data Center (NCDC) Merged Land-Ocean Surface Temperature (MLOST), and the Goddard Institute for Space Studies (GISS) datasets. Results differ, however, when considering shorter, more recent periods of record. When considering only the period 1970–2012, Tebaldi (2012) found a statistically significant trend of 0.02 °C/year state-wide, comparable to our findings for the Calloway, Allen (2) and Jefferson (1) stations. A very similar result is

reported by Hartmann et al. (2013) for the MLOST dataset over the period 1981–2012. Overall, the findings of the present study are consistent in many respects with others, including larger scale studies, but indicate an influence of data handling, selected period of record, and other factors on the results and inferences.

3.5 Conclusions

This study of annual precipitation and mean annual temperature in the state of Kentucky indicates that, over the period 1950–2010, both of these variables generally (97% of the precipitation stations and 93% of the temperature stations) did not exhibit any statistically significant trends with respect to time. Should it hold true with the accumulation of more data, this finding can serve to simplify (or at least not to complicate) larger analyses that depend on this type of data as inputs, especially for the interior and eastern portions of the state. The relatively small number of significant trends detected, however, were all in the positive direction, and all were associated with weather stations very close to the borders of the state; these findings are comparable to those from larger-scale studies employing differing methods of analysis and periods of record. Similar studies involving weather stations from surrounding states will be required to more satisfactorily contextualize the occurrence of those positive trends in annual rainfall and mean annual temperature and to gain a broader understanding of how these variables are behaving on the larger regional scale.

CHAPTER 4: CONTEMPORARY AND FUTURE CHARACTERISTICS OF PRECIPITATION INDICES IN THE KENTUCKY RIVER BASIN

Abstract

Climatic variability can lead to large-scale alterations in the hydrologic cycle, some of which can be characterized in terms of indices involving precipitation depth, duration and frequency. This study evaluated the spatiotemporal behavior of precipitation indices over the Kentucky River watershed for both the baseline period of 1986-2015 and late-century time frame of 2070-2099. Historical precipitation data were collected from 16 weather stations in the watershed, while future rainfall time-series were obtained from an ensemble of 10 Coupled Model Intercomparison Project Phase 5 (CMIP5) global circulation models under two future emission pathways: Representative Concentration Pathways (RCP) 4.5 and 8.5. Annual trends in seven precipitation indices were analyzed: total precipitation on wet days (PRCPTOT), maximum length (in days) of dry and wet periods (CDD and CWD, respectively), number of days with precipitation depth ≥ 20 mm (R20mm), maximum five-day precipitation depth (RX5day), simple daily precipitation intensity (SDII) and standardized precipitation index (SPI, a measure of drought severity). Non-parametric Mann-Kendall test results indicated significant trends for only ≈ 11% of the station-index combinations, corresponding to generally increasing trends in PRCPTOT, CWD, R20mm and RX5day and negative trends for the others. Projected magnitudes for PRCPTOT, CDD, CWD, RX5day and SPI, indices associated with the macroweather regime, demonstrated general consistency with trends previously identified and indicated modest increases in PRCPTOT and CWD, slight decrease in CDD, mixed

results for RX5day, and increased non-drought years in the late century relative to the baseline period. Late-century projections for the remaining indices (SDII, R20mm) demonstrated behavior counter to trends in the trends identified in the baseline period data, suggesting that these indices - which are more closely linked with the weather regime and daily GCM outputs – were relatively less robust.

Keywords: climate change, drought, extreme precipitation; Kentucky River Basin

4.1 Introduction

The hydrologic cycle is recognized as subject to significant changes as a result of anthropogenic global warming (Narsimlu et al., 2013; Ashraf et al., 2014; Ficklin et al., 2014; Chattopadhyay et al., 2016; Mehan et al., 2016). As per IPCC AR5 estimates, the global average surface temperature will rise by 1.8 - 4.0° C ; precipitation is expected to increase by 5 - 20% over the period of 1990 - 2100, suggesting increasing floods on a widespread basis (Hirabayashi et al., 2013). Portmann et al. (2009) have linked spatial variations in the US temperature trends to variations the in hydrologic cycle with more pronounced effects anticipated in the southern US. The authors reported a statistically significant inverse relationship between trends in daily temperature and average daily precipitation across 30- 40° N latitudes during May-June and a weaker relationship between the variables in the northern (40 – 50°N) United States during July-August. Karl et al. (2009) highlighted a significant increase in extreme precipitation events and moderate to severe droughts for the Southeast US in the 20th century. Sayemuzzaman and Jha (2014) investigated spatial and temporal trends in precipitation for North Carolina and found mixed results for annual, Spring and Summer precipitation time series. Up to

100 mm more total extreme precipitation (95th percentile and greater) is expected in the eastern US by the end of 2050's according to Gao et al. (2012). Chattopadhyay and Edwards (2016) studied long-term climatic variability considering the annual trends in precipitation and temperature across the state of Kentucky (84 weather stations) for the time period of 1950-2010. The majority of the stations demonstrated an increasing trend for both precipitation and air-temperature; however, the relatively small number of statistically significant trends were mostly found along the western parts of the state. Considered collectively, these and similar studies indicate that climate change due to global warming is in progress to varying degrees in North America, at both the regional and smaller (state-wide) scales; the potential for disruptive consequences argues for increased scrutiny of both future changes and likely impacts.

Being less dependent on relatively specific variables such as topography and land use, precipitation is a common subject of investigations into the effects of climate change on the hydrologic cycle. While society is most sensitive to extremes (extreme magnitudes, intensities and frequencies) in precipitation (IPCC, 2012), their infrequent nature can raise challenges in accurately assessing them under stationary conditions, let alone non-stationary conditions. For such reasons, precipitation inputs to the hydrologic cycle are often characterized in the form of several statistics and indices, such as numbers of "wet" and "dry" days, number of days with precipitation greater than some threshold depth, and total annual precipitation. Use of such indices is widespread in climate research, with recent applications reported for China by Ren et al. (2015), mainland Portugal by Lima et al. (2015) and in India by Mondal and Majumdar (2015).

Historical trends in indices may be identified through simple linear regression or, due to its relative lack of required assumptions, through nonparametric regression (Roth et al., 2015; Kamruzzaman et al., 2016). However, regression can be an unsatisfactory technique for generating projections of climate data due to the lack of physical basis in the predictive model. Rather, the class of complex, physically-based, global-scale models (General Circulation Models, or GCMs) is typically used for this task. Relatively recent research has resulted in enhanced predictive capability through refined representation of the relevant physical processes and more robust coupling of sea, atmosphere and land-based processes (Yuan et al., 2011; Mearns et al., 2015).

Use of GCMs for climate data projections is associated with well-known and substantial challenges. Due to internal model differences, projections can vary significantly with regard to GCMs, output variables, and seasons as discussed by Fu et al. (2013). More relevant to the present study, GCM performance can vary among model outputs. Deser et al. (2012) found the internal variability of GCM outputs to be higher for precipitation than temperature, and Rocheta et al. (2014) note that precipitation simulations are typically of lower fidelity than others (e.g., temperature). As discussed by Emori et al. (2005), additional challenges occur as the result of evaluating outputs, especially precipitation, from climate models on the daily time scale. Lafon et al. (2013) have noted that GCMs often simulate daily precipitation to occur more often, but at lower intensities, than observed. Such behavior can introduce bias into daily precipitation statistics and indices. Ines and Hansen (2006), for example, reported GCM outputs tended to overestimate runs of dry days even after bias correction for precipitation depths. Mahoney et al. (2013) discuss the particular challenges involved in extreme precipitation

simulation. Downscaling the relatively course-resolution GCM outputs to regional or local scales is often desirable from the standpoint of decision-making and resource management. While the method of downscaling can have significant impact on the quality of the projections, there remains no consensus on a single best downscaling method (Sunyer et al., 2015). Finally, there is no uniform agreement on how to compare the performance of one model relative to another, with a variety of metrics such as skill scores (Johnson and Sharma, 2009) root mean square error (Radic and Clarke, 2011) and Nash-Sutcliffe model efficiency (Miao et al., 2012) in current use. Notwithstanding such challenges, GCM projections remain the state-of-the-art for spatially-consistent assessments of future climate and its impacts, with GCM outputs being directly available for application at both large and (through downscaling) relatively local scales.

The objectives of this study were to (a) evaluate spatio-temporal magnitudes and trends of historical extreme precipitation indices for a river basin in Kentucky and (b) compare these findings to projections from global circulation models (GCMs). The specific basin to be studied is the Kentucky River basin, a major tributary of the Ohio River that provides water for nearly 70 municipalities and roughly one-sixth of the Commonwealth's population. Given the relatively recent (2008 and 2012) droughts in Kentucky and the Kentucky River basin and the impacts of drought on ecosystems, agriculture and water management, the findings of this study can be beneficial to policy makers, planners and managers entrusted with ensuring appropriate protection and sustained supplies for the basin's residents.

4.2 Materials and methods

4.2.1 Study area

The Kentucky River watershed is centered at approximately 38°41´N 85°11´W and encompasses an area of roughly 18,000 km^2 in the north-central part of the state (Figure 4.1). Elevations range from 110 m in the northwest to 998 m in the southeast with a mean elevation of 554 m. The length of the main stream of the Kentucky River is 418 km. Mean annual rainfall varies from 1107 to 1308 mm, with the southern portion generally receiving more rainfall than the northern. The major land uses in the watershed are forest (55%) and hay production (25%) with smaller proportions in urban (8%), rangeland (6%), agricultural (2%) and other (4%) land uses. The Kentucky River provides 378,000 m^3/day water for drinking and other uses (Kentucky River Facts).

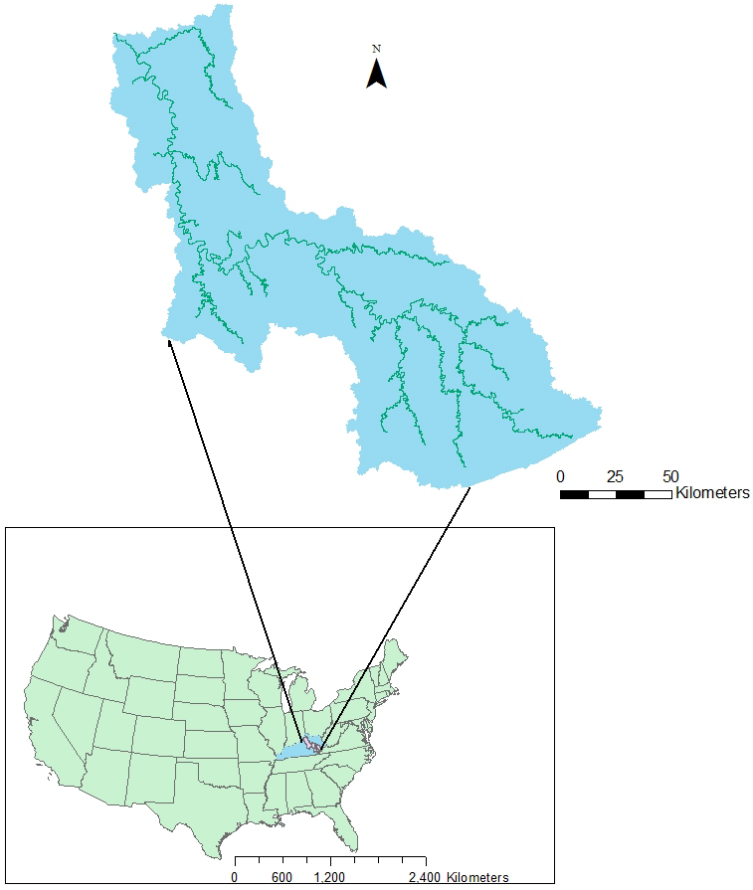

Figure 4.1 Location of Kentucky River basin inside the United States.

4.2.2 Data collection and quality assessment

Daily precipitation data were obtained from the Global Historical Climatology Network (GHCN) database (http://www.ncdc.noaa.gov/oa/climate/ghcn-daily/) maintained on the National Oceanic and Atmospheric Administration (NOAA) server (https://www.ncdc.noaa.gov/cdo-web/). Sixteen weather stations in the watershed were considered for the selected 30-year period of 1986–2015, subsequently referred to as the *baseline period*. The 30-year record length, which was near the limit of availability for consistent and near-complete stations in the basin, has a greater potential for bias than

longer record lengths but is consistent with historical record lengths used in similar analyses (Li et al., 2010; Pierce et al., 2015; Schoof and Robeson, 2016). Characteristics of the stations are summarized in Table 4.1, and their locations in relation to elevations, land uses and physiographic regions in the basin are given in Figure 4.2. The Climatol software package (Guijarro, 2013) was used to assess relative homogeneity of the data for each station and, had discontinuities been detected, to apply appropriate corrections. No discontinuities were detected in the data, and Climatol was further used to interpolate missing data on the basis of observations at neighboring stations.

Table 4.1 Weather stations used in the study.

Station Name	Latitude (° N)	Longitude (° W)	Elevation (m)	Mean Annual Rainfall (mm)	Missing Data
Whitesburg	37.1167	−82.8167	355.1	1308.0 ± 184.5	1%
Skyline	37.0667	−82.9667	366.1	1233.0 ± 197.3	<1%
Carr Fork	37.2333	−83.0333	309.1	1159.9 ± 226.1	<1%
Hazard	37.2500	−83.1833	267.9	1287.5 ± 219.1	<1%
Buckhorn	37.3500	−83.3833	285.3	1266.7 ± 214.7	<1%
Jackson	37.6000	−83.3167	416.1	1273.9 ± 213.1	<1%
Crab Orchard	37.4833	−84.4333	335.9	1238.0 ± 199.2	<1%
Berea	37.5666	−84.3333	309.1	1201.0 ± 192.8	<1%
Danville	37.6500	−84.7667	291.1	1228.4 ± 247.1	<1%
Dix Dam	37.8000	−84.7167	265.2	1116.4 ± 251.3	1%
Clay	37.8666	−83.9333	192.0	1172.0 ± 242.7	<1%
Lexington	38.0333	−84.6000	294.4	1220.6 ± 227.3	<1%
Frankfort Lock	38.2333	−84.8667	152.4	1176.2 ± 203.6	2%
Frankfort	38.1833	−84.9000	230.1	1249.0 ± 250.9	<1%
Georgetown	38.2000	−84.5500	271.0	1224.2 ± 233.8	<1%
Gest Lock	38.4167	−84.8833	149.4	1153.6 ± 201.0	1%

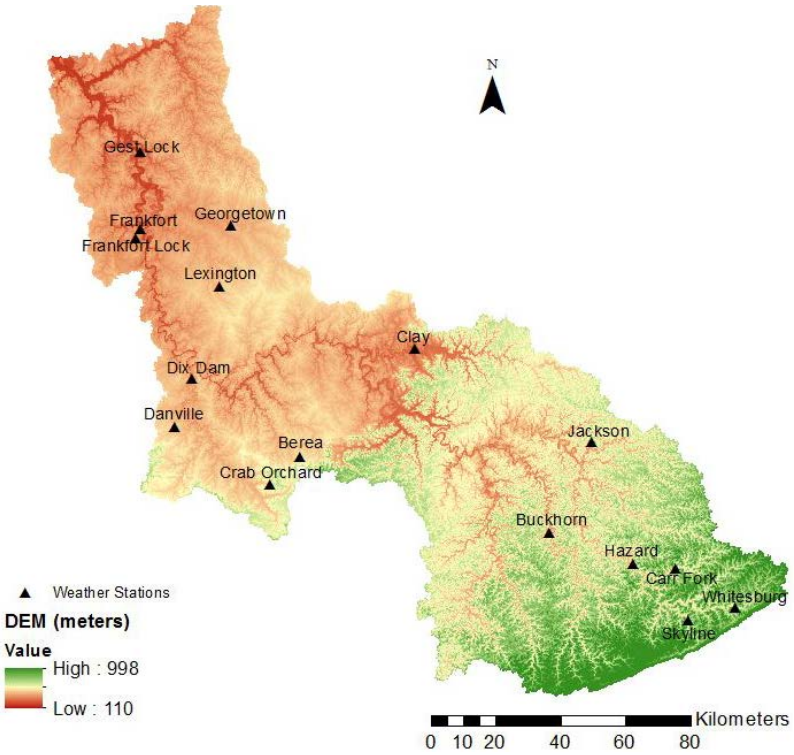
N
Gest Lock
Frankfort
Georgetown
Frankfort Lock
Lexington
Clay
Dix Dam
Danville
Berea
Crab Orchard
Jackson
Buckhorn
Hazard
Carr Fork
Whitesburg
Skyline
Weather Stations
DEM (meters)
Value
High : 998
Low : 110
Kilometers
0 10 20 40 60 80

(a)

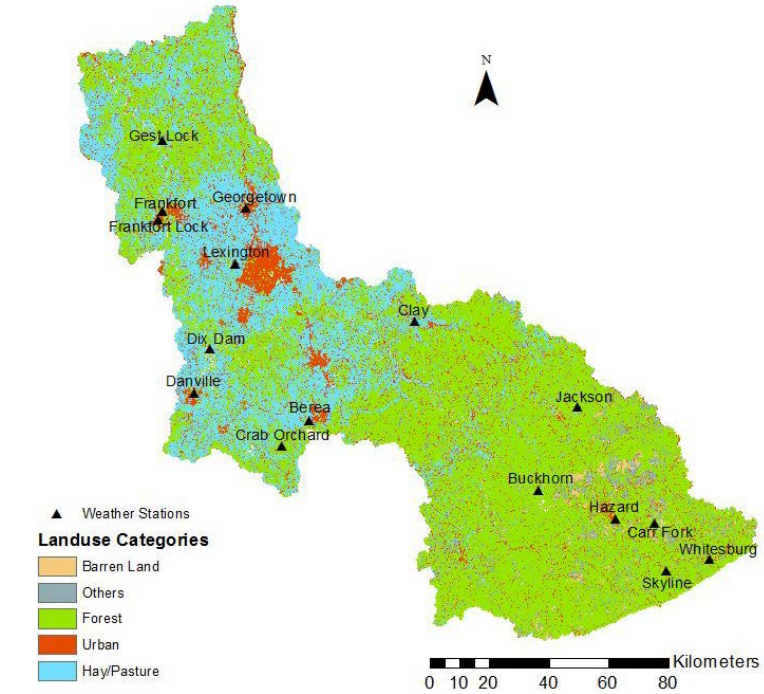
N
Gest Lock
Frankfort
Georgetown
Frankfort Lock
Lexington
Clay
Dix Dam
Danville
Berea
Crab Orchard
Jackson
Buckhorn
Hazard
Carr Fork
Whitesburg
Skyline
Weather Stations
Landuse Categories
Barren Land
Others
Forest
Urban
Hay/Pasture
Kilometers
0 10 20 40 60 80

(b)

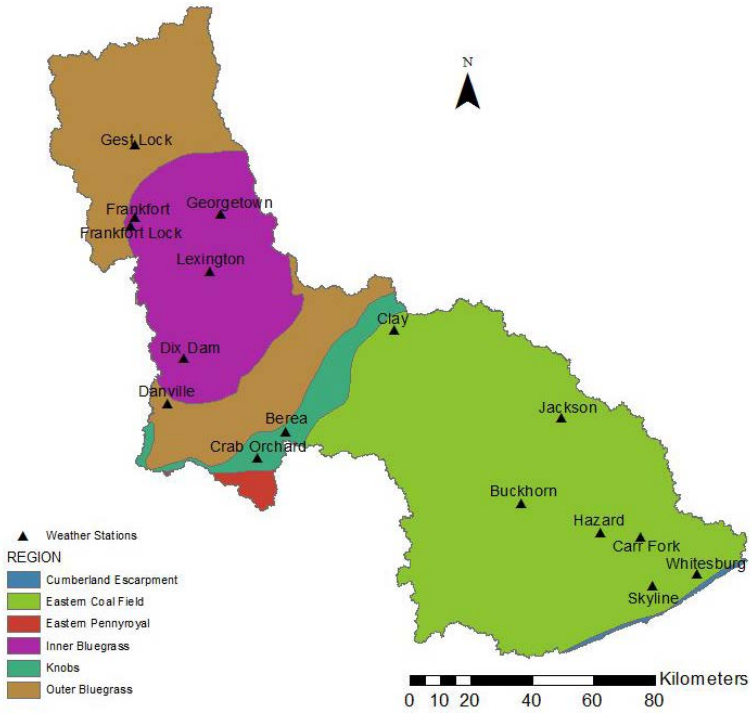

(c)

Figure 4.2 (a) Elevation; (b) land use; and (c) physiographic regions of the Kentucky River Basin.

4.2.3 Future climate data compilation

This study employed a suite of CMIP5 GCMs to generate daily precipitation data for the period 2070–2099 (subsequently referred to as the *late-century period*) at a resolution of 0.125°. A total of 10 GCMs (Table 4.2) were used to incorporate the models' output variability into the study and to reduce the uncertainty associated with choosing any particular model. Subsequent calculations of precipitation indices were based on the means of ensemble output of the GCMs as reported by, for example, Jha et al. (2014), Zhang et al. (2015) and Venkataraman et al. (2016). Since the focus of this paper is only

on extreme precipitation indices, only RCP 4.5 and 8.5 were chosen, as they represent the intermediate and upper range, respectively, of radiative forcings at the end of century. These two emission pathways are considered more realistic in comparison to RCP 2.6.

The bias-corrected and spatially-disaggregated (BCSD) method (Maurer et al., 2009; Bennett et al., 2012; Rana & Moradkhani, 2015) was adopted to downscale the GCM results. The BCSD method is a statistical downscaling algorithm that can be considered as consisting of two steps: a bias correction (BC) step and a spatial disaggregation (SD) step. The BC step broadly consists of a comparison of GCM outputs with corresponding observations over a common period. The results of the comparison are used to adjust projections to achieve greater agreement with the historical data and thus a more realistic representation of the spatial domain of interest (Wood et al., 2004; Thrasher et al., 2012). The SD step involves interpolating the bias-corrected GCM outputs to higher-resolution grids by utilizing the spatial detail provided by observationally-derived datasets. Ning et al. (2015) used the BCSD method to analyze projected changes in extreme climatic events over the northeastern United States and provided a detailed description of procedures used for bias correction and spatial disaggregation of GCM outputs. It is to be noted that, as reported by Ines et al. (2006), this type of downscaling method does not guarantee close correspondence between short-term (days or weeks) behavior in observations and GCM projections. Additionally, elevation differences are unaccounted for in the interpolation algorithm. Even so, the quantile mapping technique (Panofsky and Brier, 1968) used in BCSD to eliminate bias in daily precipitation data resulted in monthly and annual precipitation predictions that agreed very well with observations (Coats et al., 2013). In the present study, only the GCM grid points located nearest to the

ground-based weather stations were considered in comparing GCM outputs to historical data.

Table 4.2 Description of CMIP5 models used in this study.

Model Name	Institution	Spatial Resolution	Reference
ACCESS 1-0	Commonwealth Scientific and Industrial Research Organization, Australia	1.9° × 1.2°	Lewis and Karoly (2014)
BCC-CSM 1.1	Beijing Climate Center, China Meteorological Administration, China	2.8° × 2.8°	Xin et al. (2013)
CCSM4	National Center for Atmospheric Research, United States	1.25° × 0.94°	Gent et al. (2011)
CNRM-CM5	National Center for Meteorological Research, France	1.4° × 1.4°	Voldoire et al. (2013)
GFDL-ESM2G	NOAA/Geophysical Fluid Dynamics Laboratory, United States	2.5° × 2.0°	Donner et al. (2011)
HadGEM2-CC	Met Office Hadley Center, United Kingdom	1.9° × 1.2°	Jones et al. (2011)
IPSL-CM5A-MR	L'Institut Pierre-Simon Laplace, France	2.5° × 1.25°	Dufresne et al. (2013)
MIROC5	Japan Agency for Marine-Earth Sciences and Technology, Atmosphere and Ocean Research and National Institute for Environmental Studies, Japan	1.4° × 1.4°	Watanabe et al. (2010)
MIROC-ESM	Japan Agency for Marine-Earth Sciences and Technology, Atmosphere and Ocean Research and National Institute for Environmental Studies, Japan	2.8° × 2.8°	Watanabe et al. (2010)
NorESM1-M	Norwegian Climate Center, Norway	2.5° × 1.8°	Bentsen et al. (2013)

4.2.4 Extreme precipitation indices

Following the joint recommendation of World Metrological Organization Commission for Climatology (CCI), World Climate Research Programme project on Climate Variability and Predictability, several extreme precipitation indices have been used in recent studies to characterize precipitation (Santos and Fragoso, 2013; Trambalay et al., 2013). This study considered six of these indices as relevant to the basin and its potential

hydrologic issues in terms of describing depth, duration and intensity for precipitation events up to a moderately extreme nature:

1. The total precipitation in wet days (days with ≥1 mm precipitation) (PRCPTOT, mm)
2. The maximum length of dry periods (CDD, days)
3. The maximum length of wet periods (CWD days)
4. Number of days in a year with precipitation ≥20 mm (R20mm, days)
5. The annual maximum precipitation over five consecutive days (RX5day, mm)
6. The simple daily precipitation intensity (SDII, mm/day), calculated as PRCPTOT/(number of wet days)

The R package Climdex was used to calculate these indices from the daily time series data produced from each GCM, which were subsequently averaged over all GCMs. The final index used in the study was the Standardized Precipitation Index (SPI) (Mckee et al., 1993), which has recently been recommended as a standard drought index by the World Metrological Organization (WMO) (Chen et al., 2013). For a given duration, the SPI is calculated as the standard normal deviate of the distribution of cumulative rainfall for that duration; hence, negative values of SPI represent relative drought conditions with drought severity increasing with more negative SPI values (e.g., an SPI ≤ -2 can be considered an extreme drought; Table 4.3). Following Wang et al. (2014), a 12-month duration (ending in December) was used for SPI computations to reflect longer-term conditions using the SPI package in R statistical software.

Table 4.3 Drought classification using the SPI index (Mckee et al., 1993)

Level	Drought Category	SPI Values
0	Non-drought	$0 \leq SPI$
1	Mild drought	$-1.0 < SPI < 0$
2	Moderate drought	$-1.5 < SPI < -1.0$
3	Severe drought	$-2.0 < SPI < -1.5$
4	Extreme drought	$SPI \leq -2.0$

4.2.5 Trend detection

Prior to trend detection, total annual rainfall was examined for the presence of serial correlation, since serial correlation can adversely affect the quality of trend estimates of the indices such as PRCPTOT and SPI. However, none of stations was found as having significantly serially correlated data.

Trends were estimated at annual scale for the extreme precipitation indices using the nonparametric Mann–Kendall test (Kendall, 1976). The Mann–Kendall test has the advantage of being relatively unaffected by outliers and is not restricted to a particular sample distribution. Trends were spatially interpolated for graphical representation purposes from the point estimates using the surface inverse-distance-weighted (IDW) algorithm in the ArcGIS framework. Interpolation techniques that account for elevation variations have been shown (Xu et al., 2015) to reduce the mean absolute error of daily precipitation interpolations from 7% to 18% relative to inverse distance weighting. Maps derived from the two methods were very similar in major regards; however, the influence of individual stations on the maps was greater for IDW than when altitude was accounted for. While these results were obtained for daily precipitation rather than precipitation indices, the indices might exhibit a similarly high degree of station influence when mapped using the IDW technique.

4.3 Results and discussion

4.3.1 GCM performance evaluation

Performance of the GCMs and ensemble mean in terms of total annual precipitation is indicated in Table 4.4, in which the mean absolute error (MAE) and normalized standard deviation (NSD) are used as metrics (Taylor et al., 2001; Taye et al., 2011; Venkataraman et al., 2016). Near-unity values of MAE and NSD imply relatively high accuracy and similar variation, respectively, of projections relative to observations. On the basis of both MAE and NSD values, then, the GFDL-ESM2G model can be considered as demonstrating best overall performance (Table 4.4). While the performance of the ensemble mean was better than that of any individual model, the ensemble mean was also associated with the lowest NSD, reflecting the damping effect of averaging projections across models. This is indicated in Figure 4.3, in which the GCM ensemble mean is shown to be very comparable to observations in terms of average magnitude, even if not reflecting the same degree of yearly variation. This comparison argues in favor of the ensemble mean if the interest is primarily in magnitudes (as may apply to studies involving data projections), though the variation in projections might be substantially lower than observed.

Figure 4.4 indicates that, relative to observations, GCM outputs were relatively consistent across models and comparable to observations. Across all GCMs and months, Mean Absolute Error (MAE) (Taylor et al., 2001; Taye et al., 2011; Venkataraman et al., 2016) ranged from 0.22 to 14.16 mm. Across all months, MAE was lowest for the HadGEM2-CC (4.16 mm) and highest for the MIROC5 (7.40 mm) GCMs. Across all GCMs, overall performance was best for February (MAE = 1.74 mm) and worst for

October (MAE = 10.30 mm). Based on *t*-tests applied to monthly results, the ensemble mean was in no case significantly ($p < 0.05$) different from the observed mean, indicating that the ensemble mean successfully reflects observed total monthly precipitation.

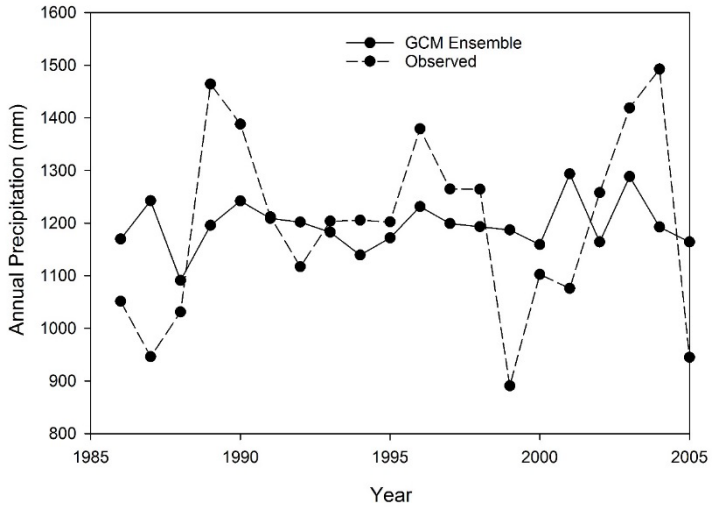

Figure 4.3 GCM ensemble and observed annual precipitation for the time frame of 1986–2005.

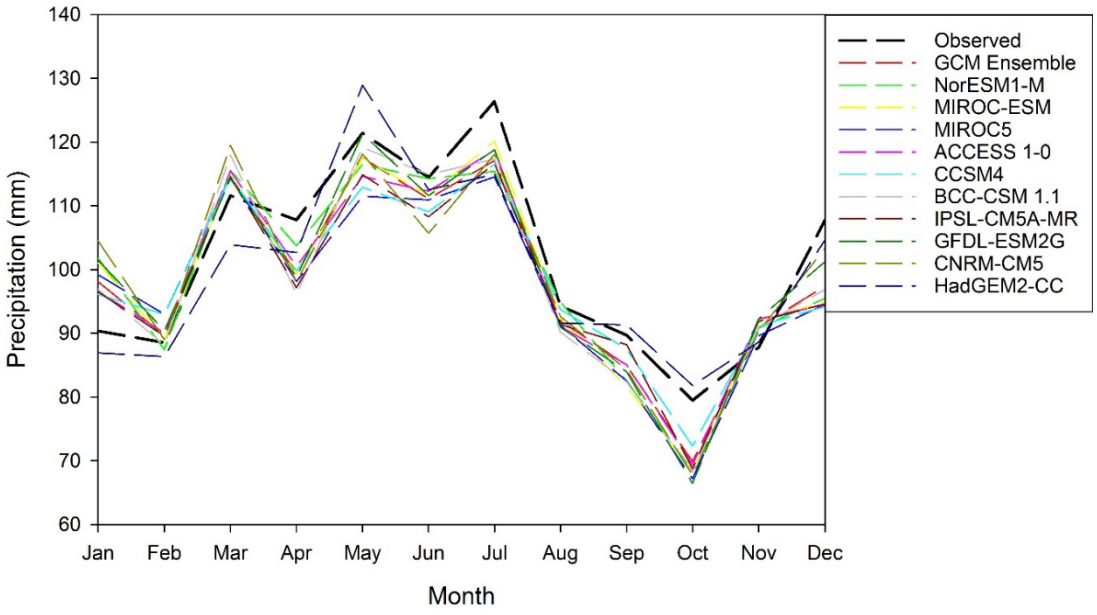

Figure 4.4 Observed and GCM simulated monthly precipitation in the Kentucky River Watershed (1986–2005).

Table 4.4 Mean Absolute Error (MAE) and Normalized Standard Deviation (NSD) of GCM simulated annual precipitation in the Kentucky River Watershed (1986–2005).

Model	MAE (mm)	NSD (mm)
ACCESS 1-0	206.65	0.97
BCC-CSM 1.1	164.51	0.84
CCSM4	202.35	0.92
CNRM-CM5	177.12	1.18
GFDL-ESM2G	136.21	1.02
HadGEM2-CC	140.58	0.78
IPSL-CM5A-MR	203.89	0.70
MIROC5	169.37	0.98
MIROC-ESM	206.87	0.92
NorESM1-M	164.67	0.69
Ensemble Mean	134.73	0.27

4.3.2 Trend analysis of extreme indices

Table 4.5 lists the annual mean values of the studied indices along with the trend slope estimates identified from baseline period data, each of which will be discussed individually in the coming subsections. Only a relatively small proportion (≈11%) of the trends were statistically significant ($p < 0.05$); all stations exhibiting a statistically significant trend for any of the indices were located in the central and northern portions of the basin (Clay station and north). The indices PRCPTOT, CWD and SDII demonstrated significant trends for the highest number of stations (three each), whereas trends in RX5day and SPI were not significant for any of the stations. Significant trends were identified for four of the seven indices for the Clay station, followed by three for the Lexington station.

Table 4.5 Mean annual index values with standard deviation and Sen slope estimates. Bold values indicate a significant ($p < 0.05$) trend.

Stations	PRCPTOT (mm)	CDD (days)	CWD (days)	R20mm (days)	RX5day (mm)	SDII (mm/day)	SPI
	Trend (mm/year)	Trend (days/year)	Trend (days/year)	Trend (days/year)	Trend (mm/year)	Trend (mm/day/year)	Trend (SPI value/year)
Whitesburg							
Mean	1284 ± 185	13.5 ± 3.3	9.6 ± 2.6	14.0 ± 4.3	101 ± 25	8.0 ± 1.2	0.0 ± 1.2
Trend	−0.97	−0.04	0.00	0.08	0.50	0.04	−0.01
Skyline							
Mean	1221 ± 197	15 ± 4	6.0 ± 1.5	16.6 ± 4.5	97 ± 24	9.8 ± 1.1	0.0 ± 1.1
Trend	4.50	−0.09	0.03	0.05	0.51	0.00	−0.02
Carr Fork							
Mean	1143 ± 225	17.1 ± 4.7	5.9 ± 2.1	14.8 ± 5.6	95 ± 29	9.6 ± 1.6	0.0 ± 1.2
Trend	0.22	0.00	0.00	−0.05	0.25	−0.02	−0.00
Hazard							
Mean	1278 ± 221	16.7 ± 3.9	5.9 ± 1.3	18.4 ± 5.1	111 ± 35	10.7 ± 1.3	0.0 ± 1
Trend	7.78	0.00	0.00	0.18	0.71	0.04	−0.02
Buckhorn							
Mean	1249 ± 217	16.4 ± 4.3	7.6 ± 2.6	15.6 ± 6.7	101 ± 23	9.2 ± 1.7	0.0 ± 1.1
Trend	7.92	−0.04	0.00	0.17	0.50	0.04	−0.01
Jackson							
Mean	1260 ± 213	16.3 ± 4.5	5.9 ± 2.0	18.9 ± 6.0	112 ± 27	10.7 ± 1.5	0.0 ± 1.1
Trend	2.30	0.00	0.00	0.00	−0.70	0.00	−0.01
Crab Orchard							
Mean	1230 ± 199	19.4 ± 5.4	6.0 ± 1.8	19.4 ± 4.8	72 ± 41	11.8 ± 1.8	0.0 ± 1.3
Trend	6.81	0.00	0.04	0.00	0.08	0.05	−0.00
Berea							
Mean	1182 ± 194	15.2 ± 3.0	8.4 ± 2.4	13.4 ± 6.3	105 ± 30	8.8 ± 2.2	0.0 ± 1.2
Trend	2.51	0.04	0.08	−0.21	−0.94	−0.06	−0.01
Danville							
Mean	1217 ± 246	19.0 ± 5.7	5.4 ± 1.6	18.4 ± 5.0	123 ± 42	11.8 ± 1.9	0.0 ± 1.2
Trend	2.08	0.13	0.00	0.00	0.10	−0.03	−0.02
Dix Dam							
Mean	1107 ± 250	20.6 ± 7.6	5.7 ± 1.6	16.2 ± 4.8	118 ± 39	11.05 ± 1.6	0.0 ± 1.2
Trend	−0.21	0.16	0.00	0.00	−0.35	−0.01	−0.02
Clay							
Mean	1169 ± 242	21.6 ± 8.0	5.1 ± 1.7	18.4 ± 5.3	122 ± 38	13.5 ± 2.9	0.0 ± 1.1
Trend	**15.68**	**−0.34**	**0.14**	0.14	−0.21	**−0.20**	−0.00
Lexington							
Mean	1208 ± 227	17.7 ± 4.3	5.1 ± 1.1	18.2 ± 5.2	122 ± 35	11.6 ± 1.4	0.0 ± 1.2
Trend	**10.63**	0.00	0.00	**0.25**	1.25	**0.07**	−0.07
Frankfort Lock							
Mean	1156 ± 202	16.7 ± 3.3	6.8 ± 2.5	14.4 ± 5.8	107 ± 29	9.9 ± 2.3	0.0 ± 1.2
Trend	7.54	−0.10	**0.15**	−0.20	0.03	**−0.16**	−0.01
Frankfort							
Mean	1239 ± 248	18.6 ± 5.3	6.0 ± 1.7	18.9 ± 5.0	120 ± 41	11.8 ± 1.4	0.0 ± 1.2
Trend	1.34	−0.10	0.00	0.00	0.25	−0.02	−0.00
Georgetown							
Mean	1212 ± 232	16.6 ± 4.4	6.3 ± 2.0	17.7 ± 5.6	116 ± 38	10.8 ± 1.7	0.0 ± 1.2
Trend	**12.51**	−0.09	0.00	**0.27**	0.74	0.07	−0.01
Gest Lock							
Mean	1139 ± 199	18.2 ± 7.0	6.9 ± 2.4	14.1 ± 5.7	109 ± 39	9.8 ± 2.5	0.0 ± 1.2
Trend	7.62	−0.05	**0.12**	−0.18	0.27	−0.12	−0.03
Overall							
Mean	1206 ± 52	17.4 ± 2.1	6.4 ± 1.2	16.7 ± 2.1	108 ± 13	10.6 ± 1.4	0.0 ± 0.92
Trend	5.51	−0.03	0.03	0.03	0.19	−0.02	−0.02

4.3.3 PRCPTOT

The majority of stations (87.5%) demonstrated an increasing trend in PRCPTOT, suggestive of an overall wetting trend over the baseline period. Trends in PRCPTOT were significant for three of the 16 stations (Clay, Georgetown and Lexington, Table 4.5) in the north-central portion of the watershed (Figure 4.5), ranging from 10.6 (Lexington) to 15.7 (Clay) mm/year.

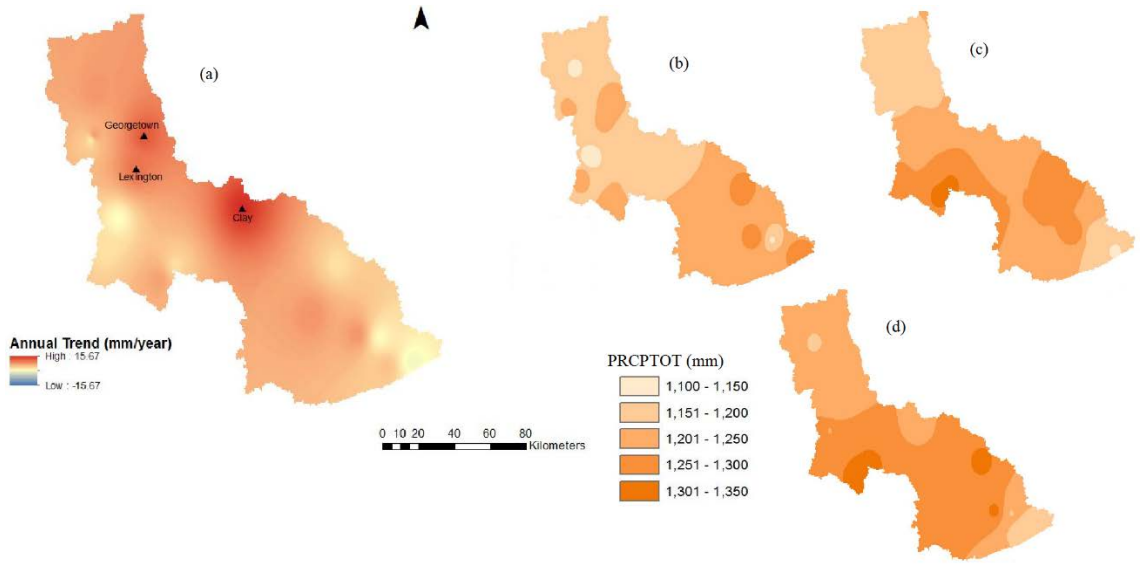

Figure 4.5 Spatial distribution of PRCPTOT (a) trend and mean values under: (b) baseline; (c) late-century RCP 4.5; and (d) late-century RCP 8.5, in the Kentucky River Basin. Filled triangles indicate a statistically significant ($p < 0.05$) trend.

The spatial distribution of PRCPTOT and its trends are given in Figure 4.5. Late-century projections for RCPs 4.5 and 8.5 are similar in the sense that both indicate modest basin-wide average increases in PRCPTOT (7 mm for RCP 4.5 and 29 mm for RCP 8.5), and except for the extreme southeastern portion (with decreases of 145–165 mm relative to the baseline period), most prominently in the southern portion of the watershed. In some cases, however, the projections are spatially inconsistent with baseline PRCPTOT values (Figure 4.5b) and trends (Figure 4.5a). The Lexington and Georgetown stations, for example, had significantly increasing trends over the baseline

period. Late-century projections, however, reflect a decrease (relative to the baseline period) of 8–36 mm for Georgetown and a net change of only −15–13 mm for Lexington. Similarly, the Clay station (which had the highest trend) is unremarkable in RCP 4.5 projections (Figure 4.5c) and has a lower PRCPTOT than the surrounding area in RCP 8.5 projections (Figure 4.5d).

4.3.4 CDD and CWD

Magnitudes of trends in CDD and CWD over the baseline period were generally low and significant in only four instances involving three stations (Clay, Frankfort Lock and Gest Lock). Figure 4.6a indicates generally negative trends in CDD in the northeastern portion of the basin, with (usually weakly) positive trends elsewhere. Figure 4.6b demonstrates that the northern portion of the basin had relatively higher CDD values than the southern for baseline conditions, a situation expected to persist according to late-century projections (Figure 4.6c, d). The late-century projections also indicate basin-wide decreases in CDD, with the areal average decreases ranging from two days (RCP 4.5) to three days (RCP 8.5). The projected decreases are generally consistent with trends identified in the baseline period with the possible exception of the west-central portion.

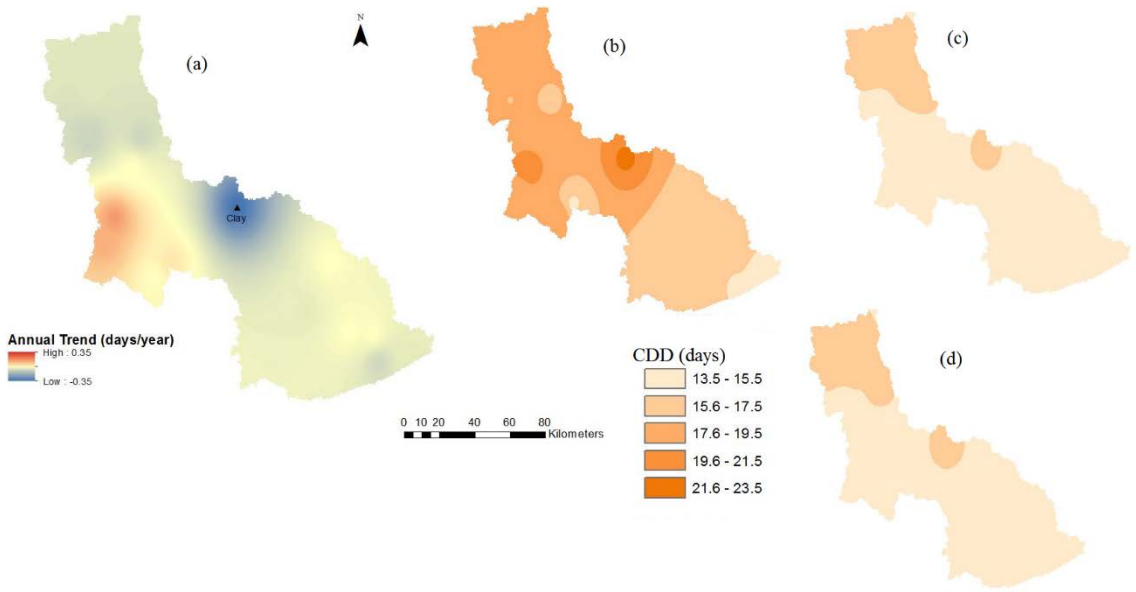

Figure 4.6 Spatial distribution of CDD (a) trend and mean values under: (b) baseline; (c) late-century RCP 4.5; and (d) late-century RCP 8.5, in the Kentucky River Basin. Filled triangles indicate a statistically significant ($p < 0.05$) trend.

Findings regarding CWD were generally complementary to those for CDD in that decreases in CDD were accompanied by increases in CWD. Trends in CWD were uniformly positive, strongest in the central and northern portions of the basin (Clay, Frankfort Lock and Gest Lock stations) and weaker elsewhere (Figure 4.7a). This general result is reflected in the late-century projections (Figure 4.7c, d) where, relative to baseline conditions, CWD is anticipated to increase (particularly in the southern portion) throughout the basin. Late-century projections indicate an increase in CWD averaging 3 days across the basin, concentrated primarily in the southern portion for RCP 4.5 and somewhat more uniformly-distributed for RCP 8.5. Similar to the situation of PRCPTOT, the relatively high baseline trend in CWD for the Clay is not reflected in CWD projections (Figure 4.5c, d). Taken together, the CDD and CWD results suggest basin-wide decreases in runs of dry days along with increases in runs of wet days in the late-century period. Schoof (2015) investigated changes in extreme precipitation indices for

contiguous US and reported very similar projected changes in CDD and CWD for the time frame of 2066–2095 around the study area.

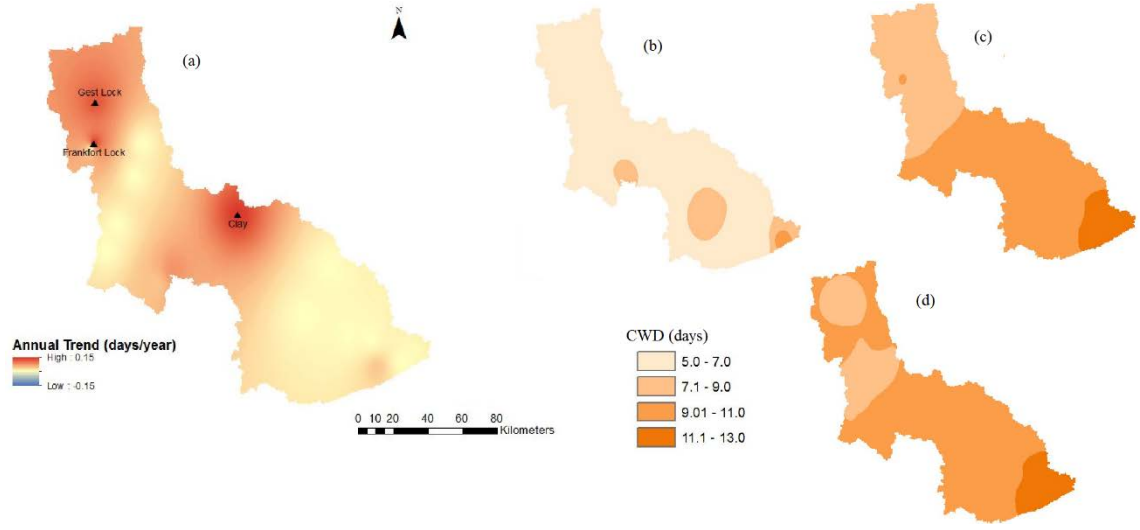

Figure 4.7 Spatial distribution of CWD (a) trend and mean values under: (b) baseline; (c) late-century RCP 4.5; and (d) late-century RCP 8.5, in the Kentucky River Basin. Filled triangles indicate a statistically significant ($p < 0.05$) trend.

4.3.5 R20mm

Two stations (Georgetown and Lexington) indicated significant trends in R20mm (0.27 and 0.25 days/year, respectively); the remainder of the basin was found to have an approximately equal distribution of weakly positive and negative trends (Figure 4.8a). It is noteworthy that the Georgetown and Lexington stations are nearest in proximity to the most heavily urbanized portion of the basin; Misra et al. (2011) suggested a linkage between urbanized areas in the US and increasing trends in indices such as daily maximum rainfall intensity and number of days with heavy precipitation, a finding more recently corroborated by Zilli et al. (2016).

Late-century projections reflect basin-wide decreases of 4–5 days in R20mm (Figure 4.8c, d). Although the Georgetown/Lexington area is, consistent with baseline period

trends, in the region of highest projected R20mm, late-century projections indicate decreases for these stations as well. The results in this case indicate spatial consistency with baseline period analysis, but not trend consistency. This finding is suggestive that, rather than indicating reversal of contemporarily-assessed trends, the GCM projections might be reflecting the issues discussed by Lafon et al. (2013); namely, underestimation of rainfall intensities.

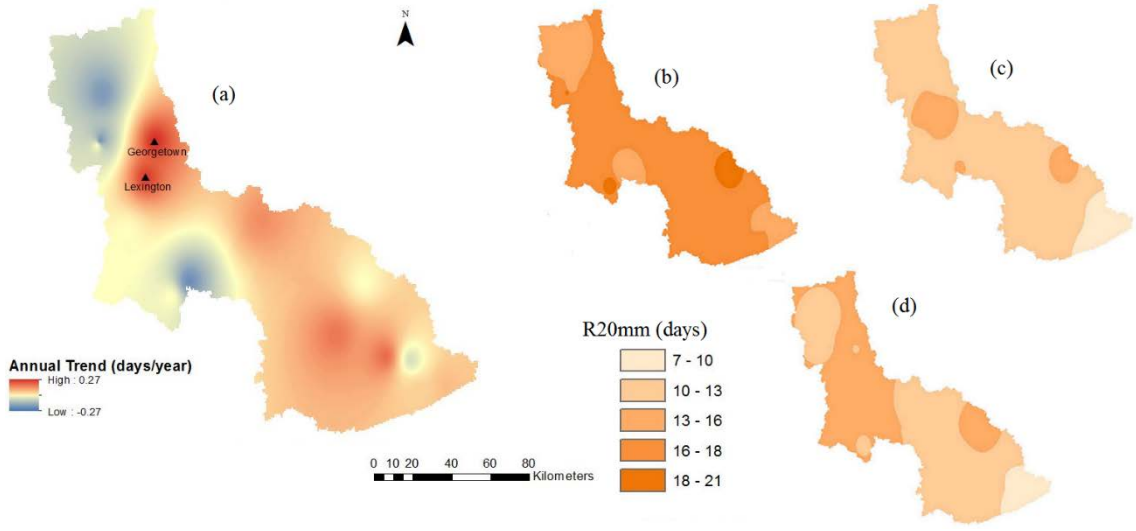

Figure 4.8 Spatial distribution of R20mm (a) trend and mean values under: (b) baseline; (c) late-century RCP 4.5; and (d) late-century RCP 8.5, in the Kentucky River Basin. Filled triangles indicate a statistically significant ($p < 0.05$) trend.

4.3.6 RX5day

Analysis of baseline period data indicated a tendency toward decreasing trends in RX5day in the central portion of the basin and increasing trends elsewhere (Figure 4.9a). However, no station demonstrated a statistically significant trend in annual maximum five-day rainfall. Consistent with this result, late-century projections indicated modest or very slight changes in RX5day (<7% decrease for RCP 4.5, <1% increase for RCP 8.5) relative to the baseline period (Figure 4.9b–d). Shifts in the spatial distribution of

RX5day across the basin are projected, however, with higher values in the north for the late-century.

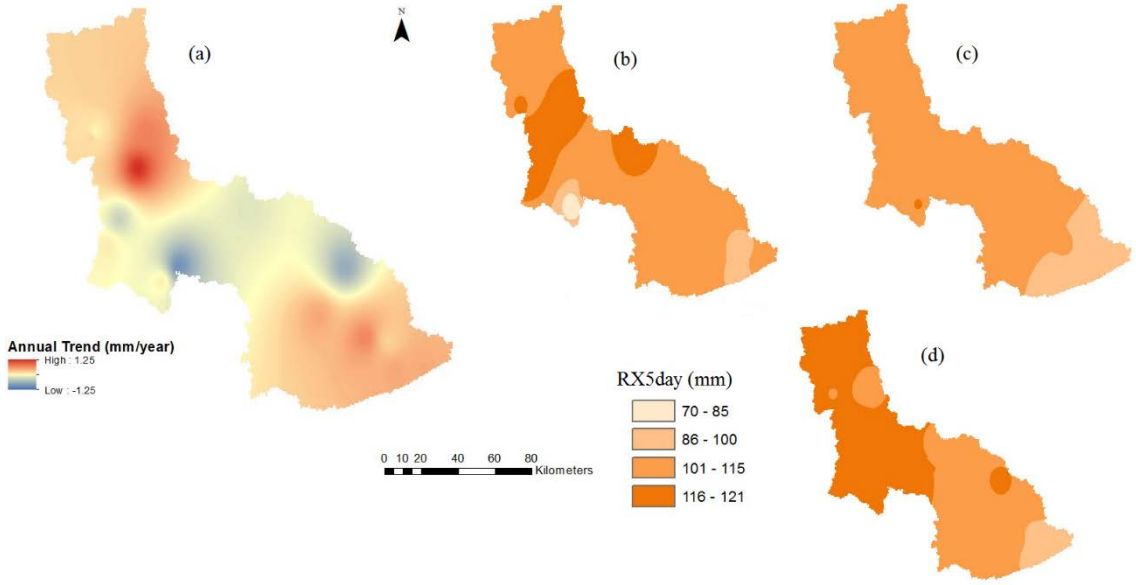

Figure 4.9 Spatial distribution of RX5day (a) trend and mean values under: (b) baseline; (c) late-century RCP 4.5; and (d) late-century RCP 8.5, in the Kentucky River Basin.

4.3.7 SDII

Baseline period trends in SDII were mixed; the statistically significant ($p < 0.05$) trends were negative for two stations (Clay and Frankfort Lock) and positive for the Lexington Station (Figure 4.10a), and inconsequential overall (Table 4.5). Projections for RCP 4.5 and 8.5 (Figure 4.10c, d), however, reflect decreases in SDII throughout the watershed for the late-century period (approximately 3 days for both RCP 4.5 and 8.5). As previously discussed, PRCPTOT was projected to increase (albeit modestly) by late century; this result must therefore necessarily reflect a projected change in annual numbers of wet days. Thus, this finding appears related to results related to CWD, collectively suggesting that either: (a) a currently-weak and mixed trends in SDII (or,

more precisely, numbers of wet days) will broadly shift toward the positive direction in the late-century; or (b) the GCM projections contain excessive numbers of wet days.

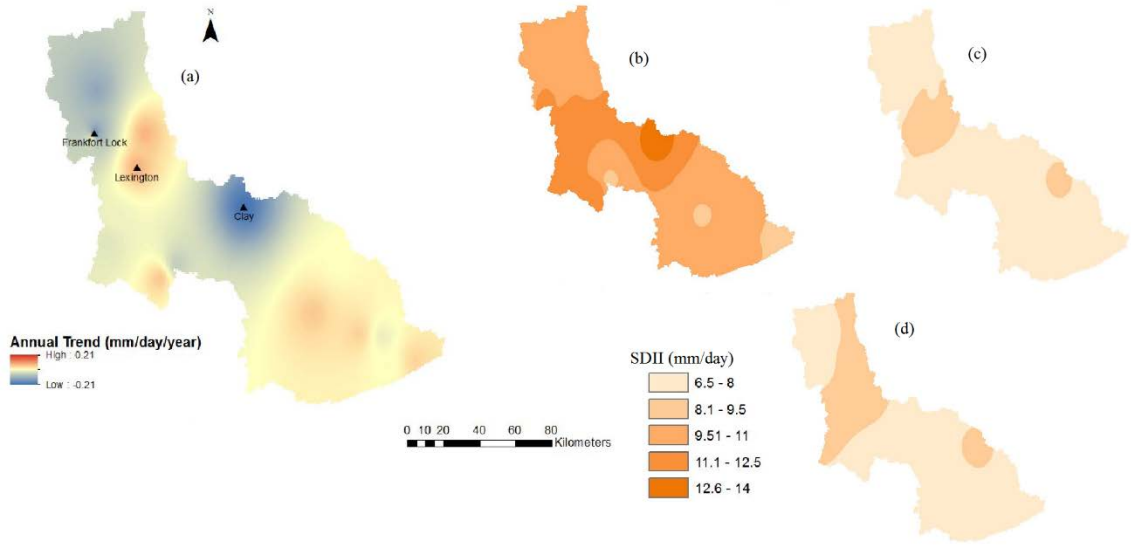

Figure 4.10 Spatial distribution of SDII (a) trend and mean values under: (b) baseline; (c) late-century RCP 4.5; and (d) late-century RCP 8.5, in the Kentucky River Basin. Filled triangles indicate a statistically significant ($p < 0.05$) trend.

4.3.8 SPI

While the direction of annual trend in year-ending SPI was in all cases negative, the trend in SPI was not significant ($p < 0.05$) for any of the 16 stations (Figure 4.11a). In terms of numerical magnitudes (Table 4.5), SPI values were quite small relative to drought category ranges (Table 4.3). Furthermore, as a result of the non-linear relationship between total annual rainfall and SPI, variation in annual rainfall (i.e., PRCPTOT) is amplified during SPI computations; this is evident in the relatively high standard deviations of year-ending SPI (Table 4.5).

Relative to baseline SPI values (Figure 4.11b; zero by definition), both scenarios project increasing average SPI values (i.e., less drought) that demonstrate spatial

variation across the watershed (Figure 4.11c,d). Projections from RCP 4.5 indicate a late-century basin-wide average SPI of 0.11, whereas RCP 8.5 indicates an average of 0.17. Both of these findings are consistent with the earlier-discussed results regarding PRCPTOT, which is also projected to increase modestly in the late-century.

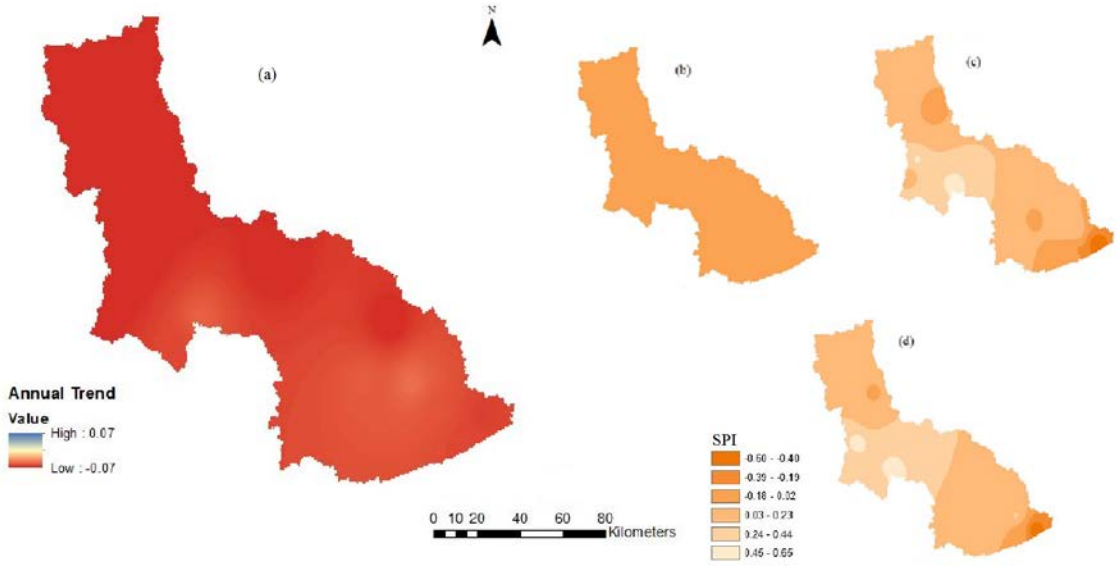

Figure 4.11 Spatial distribution of SPI (a) trend and mean values under: (b) baseline; (c) late-century RCP 4.5; and (d) late-century RCP 8.5, in the Kentucky River Basin.

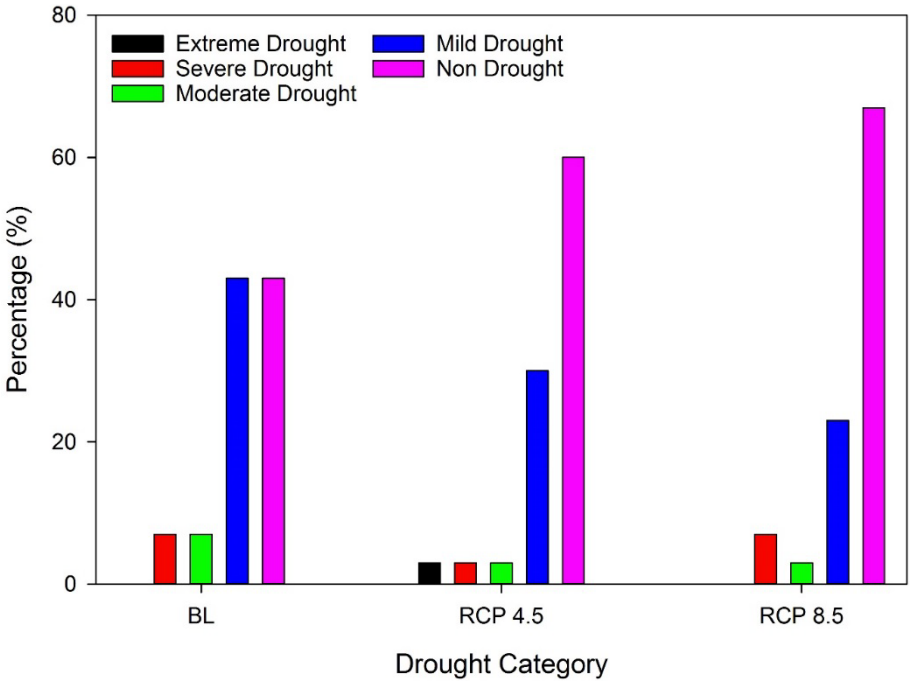

Figure 4.12 Percentage of time in each drought category under baseline and late-century conditions. (BL denotes baseline).

Figure 4.12 indicates a late-century reapportionment of time spent in non-drought and mild drought conditions. For baseline conditions, approximately 86% of year-ending SPI values were evenly divided between the non-drought and mild drought categories. Late-century projections indicate that the proportion of non-drought and mild drought years will remain similar, but with an increase in non-drought years (to 60%–67%, depending on RCP) and a corresponding decrease in mild drought years. The spatial distribution of average late-century SPI projections is similar for the two RCPs, indicating relatively high values in the central portion of the watershed and lower values in the extreme southeast.

4.4 Summary and conclusions

This study used data from 16 GHCN weather stations over the period 1986–2015 (the baseline period) to evaluate spatial variability and trends in precipitation indices for

the Kentucky River basin. These findings were then considered alongside projections from 10 CMIP5 GCMs for the period 2070–2099 (late-century period) to assess changes in index magnitudes and spatial distribution as well as consistency with trends identified during the baseline period.

Averaged baseline period findings indicated that the southern portion (with higher elevations and proportion of forest cover) of the basin experienced generally higher PRCPTOT with fewer days separating rainfall events (CDD) and, especially in the extreme southeastern portion, longer runs of days with rainfall ≥1 mm (CWD). The spatial distribution of other indices was generally more uniform; noteworthy variations are more suggestive of microclimate effects (e.g., the Lexington/Georgetown and Clay stations) than systematic spatial trends. Trends in the indices over the baseline period were significant for only about 11% of the station-index combinations, all in the central and (to a lesser degree) northern portions of the basin, which are generally dominated by pasture/hay and urban land uses. Trends in PRCPTOT were among the most consistent, demonstrating increasing values (up to 15.68 mm/year) for all but two of the 16 stations and significant for three stations in the north-central portion of the basin. The Lexington and Georgetown stations, both in close proximity to the most heavily urbanized portion of the basin and separated by only about 50 km, had significant trends in R20mm, indicative of an increasing number of heavy rainfall events over the baseline period. Trends for remaining indices were directionally and spatially mixed to a higher degree, demonstrating less apparent relation to elevation or land use. The Clay station, in particular, was associated with inconsistent (relative to neighboring stations) results, perhaps related to its location near a physiographic region boundary (in the transition

between Eastern Coal Fields and Outer Bluegrass, also transitional between dominant land uses), its relatively low elevation within the Kentucky River valley, or both.

Late-century projections for PRCPTOT, CDD, CWD, RX5day and SPI were, in the spatial aggregate, consistent with the trends identified on the basis of baseline data. These projections indicate modest (<2.5%) increases in total precipitation on wet (>1 mm) days with decreases (by 2–3 days) in maximum runs of dry days and increases (approximately three days) in maximum runs of wet days. Maximum five-day precipitation (RX5day) projections demonstrated more sensitivity to the RCP, ranging from a roughly 7% decrease for RCP 4.5 to a 1% increase for RCP 8.5. Both RCPs project that on the basis of watershed-wide average SPI values, non-drought years will be more-common in the late-century, with mild drought years becoming less common; the proportion of years with more intense drought conditions (moderate, severe or extreme) is projected to remain essentially unchanged from the baseline period. Additional analysis based on a higher level of temporal disaggregation of projections will be required to support water resource management planning and operations that are based on smaller time durations (e.g., semi-annually or seasonally).

It may be noted that the above indices are associated with the “macroweather” (Lovejoy, 2013) regime, considered as 5–10 days to 10–30 years. In other words, they are less vulnerable to the challenges of shorter-duration (i.e., the “weather” regime) GCM projections and could have been expected to be of relatively high fidelity. While this appears to have been the overall case, anomalous results occasionally surfaced in the spatial domain. The apparent microclimates in the vicinities of the Lexington/Georgetown and Clay stations, for example, were not evidenced as expected in

the projections. This phenomenon is likely an outcome of the GCM output downscaling algorithm and/or the mapping algorithm, especially given the distance and elevation difference between the Clay station and its neighbors.

In the cases of the remaining indices (R20mm and SDII), late-century projections sometimes stood in contrast to trends identified during the baseline period. The significant baseline period trends in R20mm, for example, were in the positive direction; projections from both RCPs, however, indicate basin-wide decreases in the late-century period. Similarly, an overall negligible trend was identified for SDII during the baseline period; however, basin-wide decreases were projected for the late-century, including stations for which the SDII trend was statistically significant ($p < 0.05$) and positive. Unlike the previous five indices, R20mm and SDII are highly associated with the "weather" regime with R20mm being a sum individual, not-necessarily-consecutive days and SDII being a function of a similar sum. To a relatively high degree, therefore, the robustness of these indices is dependent on that of daily GCM outputs. For this study, ensemble GCM projections appear to have more wet days, containing fewer instances of moderately severe rainfall, than anticipated on the strength of baseline data analysis. This, in turn, suggests opportunity in terms of improvements to appropriate internal model structure and/or supplementary output processing algorithms.

The inconsistencies between baseline period trends and late-century projections are cautionary; at a minimum, they suggest limitations in reconciling analyses on relatively small temporal and spatial scales to GCM projections, even when those projections are bias-corrected and spatially downscaled. It seems possible that this study's findings with regard to baseline period conditions and trends reflect relatively large influences of small-

scale variables such as elevation and land cover, whose relative importance diminishes in the context of relatively low-resolution GCM projections. While scale- and timeframe-related anomalies need not be irreconcilable, their occurrence can represent challenges to those charged with applying low-resolution projections to smaller scales of decision-making and effective management.

CHAPTER 5: AN ASSESMENT OF CLIMATE CHANGE IMPACTS ON FUTURE WATER AVAILABILITY AND DROUGHTS IN THE KENTUCKY RIVER BASIN

Abstract

Global climate change is anticipated to present a variety of challenges to water resources management due to shifts in water supplies, demands and their spatio-temporal distributions. This study evaluated the potential impacts of climate change on hydrologic processes in the Kentucky River basin using the Soil and Water Assessment Tool (SWAT). Following calibration and validation, the SWAT model was forced with forecasted precipitation and temperature outputs from a suite of CMIP5 GCMs, corresponding to two different representative concentration pathways (RCP 4.5 and 8.5) for two distinct time periods; 2036-2065 and 2070-2099, referred to as mid-century and late-century respectively. Climate projections indicate modest increases in average annual precipitation and higher increases in temperature relative to the baseline (1976-2005) period. Monthly variations of water yield and surface runoff demonstrate increasing trends in Spring and Fall, while winter months are projected as having decreasing trends. Evapotranspiration (ET) displayed a consistent increasing (decreasing) trend in winter (summer) under all the future scenarios. Spatial analysis indicated basin-wide increase in water yield with the north-central portions likely to experience the least increase resulting from the highest increases in ET. Meteorological and hydrological droughts were quantified using the Reconnaissance Drought Index (RDI) and Streamflow Drought Index (SDI). In general, maximum length of hydrological drought is expected to increase, while drought intensity might decrease under future conditions. Meteorological droughts,

however, are projected to be slightly less intense and of approximately the same persistence as for the baseline period. The overall findings suggest only modest changes in drought indices through the 21st century on a watershed basis, but changes (and thus the issue of future reliability) might be more significant on the subwatershed basis.

Keywords Climate Change. RCP. Kentucky River Basin. SWAT model. Reconnaissance Drought Index (RDI). Streamflow Drought Index (SDI).

5.1 Introduction

The current century is an era of ubiquitous climate change (Huntington, 2006; Green et al., 2011) and studies having a variety of provenances agree on the major role of anthropogenic global warming (Haddeland et al., 2014; Trenberth et al., 2014). Vijayavenkatraman et al. (2012) pointed out that there has always been variation in the earth's climate, but the recent and rapid changes on a global scale are of growing concern. In the U.S., for example, Diffenbaugh and Ashfaq (2010) have reported that exceptionally long heat waves and other hot events could become commonplace in the between 2010-2039. Higher future temperatures can increase rates of hydrologic system losses to evaporation and transpiration and, in turn, produce more rainfall. As a result, the Intergovernmental Panel on Climate Change (IPCC) have noted a widespread sense among climate scientists that extreme events (e.g., droughts and floods) will become increasingly frequent, intense and widespread in the future (IPCC, 2007).

Global climate models (GCMs) have been developed to predict characteristics of future in response to increased anthropogenic greenhouse gases. However, analyses based on GCM projections are constrained by mathematical representations of atmospheric dynamics at spatial resolutions finer than 2º of longitude and latitude. Accurate GCM

projections of precipitation, in particular, can be challenging due to the difficulties in applying the atmospheric dynamic equations to faithfully replicate the complex spatiotemporal behavior that this important variable exhibits (Emori et al., 2005; Khalil et al., 2010; Deser et al., 2012). However, relatively high-resolution projections can be important to reflect the known variation that can be present at the scales of practical management and political decision-making. Significant regional variation within larger-scale patterns, due to global circulation changes, has been demonstrated (Oki and Kanae, 2006; Giorgi et al., 2011; Kirtman et al., 2013). The U.S. state of Kentucky, for example, spans approximately 2.5^{o} of longitude and 7^{o} of latitude but demonstrated substantial north-south and east-west variation in historical temperature and precipitation trends (Chattopadhyay and Edwards, 2016). Downscaling GCM outputs is thus helpful in reproducing the underlying physics at finer spatial and temporal scales. When spatially downscaled (using either statistical or dynamical methods), GCM projections have been found useful for both long-term climate change projections as well as short term seasonal forecasts (Vitart and Stockdale, 2001; Robertson et al., 2004). Downscaled GCM projections are very commonly used in both assessments of future climate and follow-on studies to evaluate its impacts (droughts, floods, etc.).

Projected GCM outputs are often used as inputs for process-based hydrologic models to assess the influence of climate variables on availability and quality of water resources. Numerous studies of this nature have been recently reported, with examples including Chattopadhyay and Jha (2016) for Haw River Watershed in North Carolina, Stewart et al. (2015) for the mountainous river basins of the southwestern United States, Daggupati et al. (2016) for the Missouri River basin, Uniyal et al. (2015) for Upper Baitarani River

basin in India and Xu et al. (2015) for two climate regions in China. Reports of this type have generally emphasized the sensitivity of watershed hydrologic response to variations in atmospheric carbon dioxide concentrations, precipitation and temperature. As an example of a larger-scale study, Naz et al. (2016) analyzed hydrologic response of the conterminous US using high resolution hydroclimatic simulations. Using a suite of 10 GCMs, dynamically downscaled to 4 km resolution to provide inputs to the Variable Infiltration Capacity model, the authors found that most regions of the US are expected to experience an average 20% more winter precipitation, which can cause considerable increases in Spring and Winter runoff. As noted by Xu et al. (2013), hydroclimatic modelling study results can reflect uncertainties due to selection of hydrological model, specification of model parameters, greenhouse scenario selection and GCMs used for climate projections as duly noted in some of these studies. Even so, hydroclimatic modelling represents one of the few tools available to policy makers and water resource managers for proactively identifying acceptable climate change mitigation strategies.

Some of the consequences of climate change, such as more extreme floods and droughts, might be unavoidable. Some of the impacts, however, can be diminished with foreknowledge of the scope and magnitude of future events. Drought, for example, is an event that generally cannot be prevented but can be mitigated through policy and infrastructural measures. Quantified by a variety of indices applicable over a variety of spatio-temporal scales (Mitra and Srivastava, 2016), droughts are often classified as meteorological (low precipitation), hydrological (low stream flows, low groundwater availability and/or low reservoir storage), and agricultural (low crop yields) (Wang et al. 2011). The objective of this study was to evaluate the potential impacts of climate

change on droughts in the Kentucky River basin in the southeastern US. The focus was on meteorological and hydrological droughts, since agricultural production within the basin is relatively low. The findings can inform policy makers and resources managers on beneficial courses of action to ensure sustained water availability during changing climate.

5.2 Materials and methods

5.2.1 Description of study area

The Kentucky River Basin, encompassing 42 counties and a drainage area of roughly 18000 km^2, is centered at approximately 38°41´N 85°11´W in the north-central portion of Kentucky (Fig. 5.1). The river originates in the mountainous eastern region of the state and continues for almost 418 km northwest prior to its confluence with the Ohio River. Major tributaries of the Kentucky River include the Dix and Red Rivers as well as the North, South and Middle Forks of the Kentucky River. Elevations in the watershed range from 110 - 998 m with a decreasing gradient in the southeast-to-northwest direction. Average annual rainfall in the basin varies from 1107 in the south to 1308 mm in the north (Fig. 5.2). The average annual temperature across the basin is 13.1°C with highest temperatures tending to occur in the central portion of the basin (Fig 5.3). The major land uses in the watershed are forest (55%) and hay production (25%) with smaller proportions in urban (8%), rangeland (6%), agricultural (2%) and other (4%) land uses.

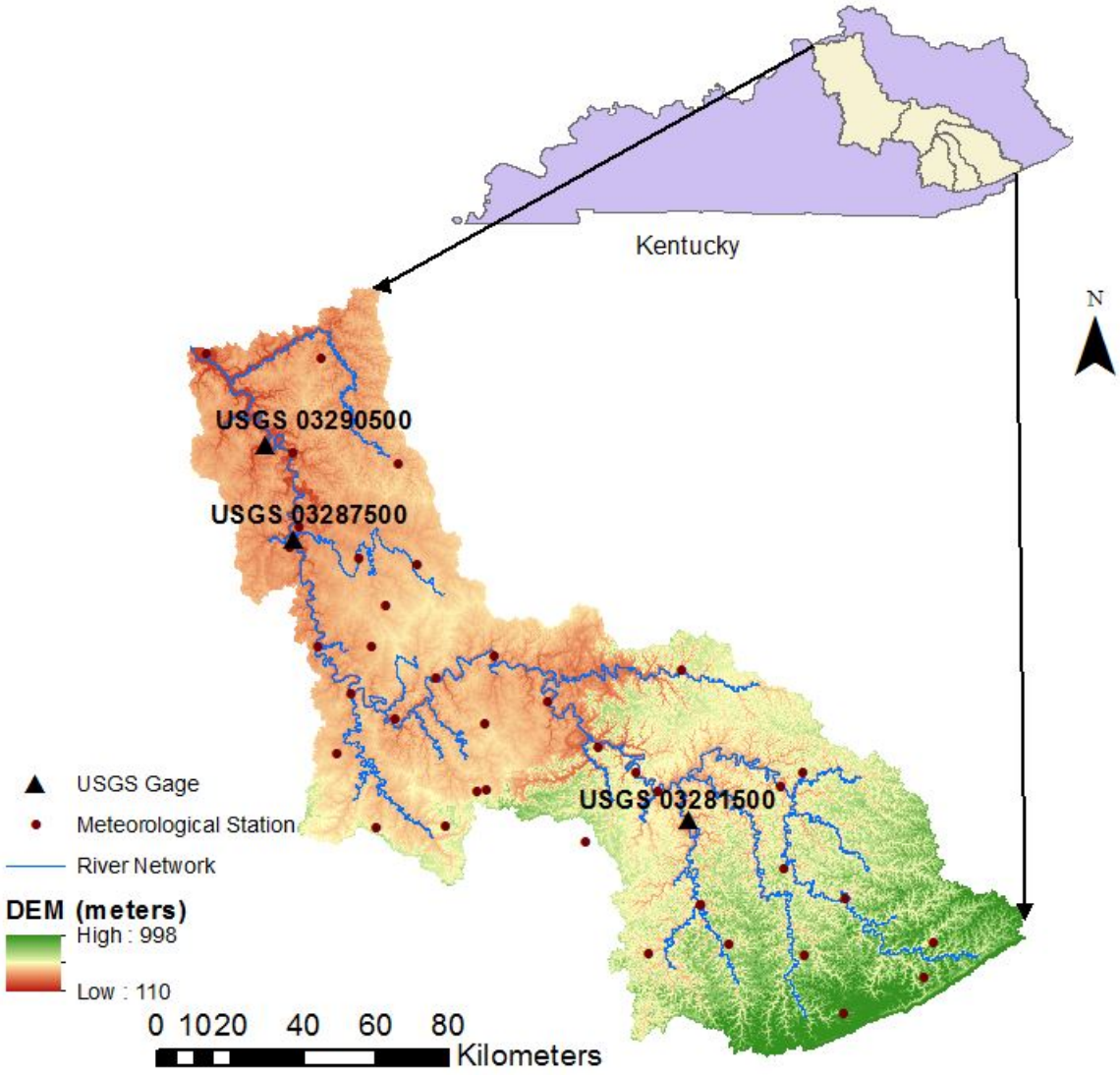

Figure 5.1 Location of the Kentucky River Basin in north-central Kentucky showing the USGS streamflow gages and weather stations.

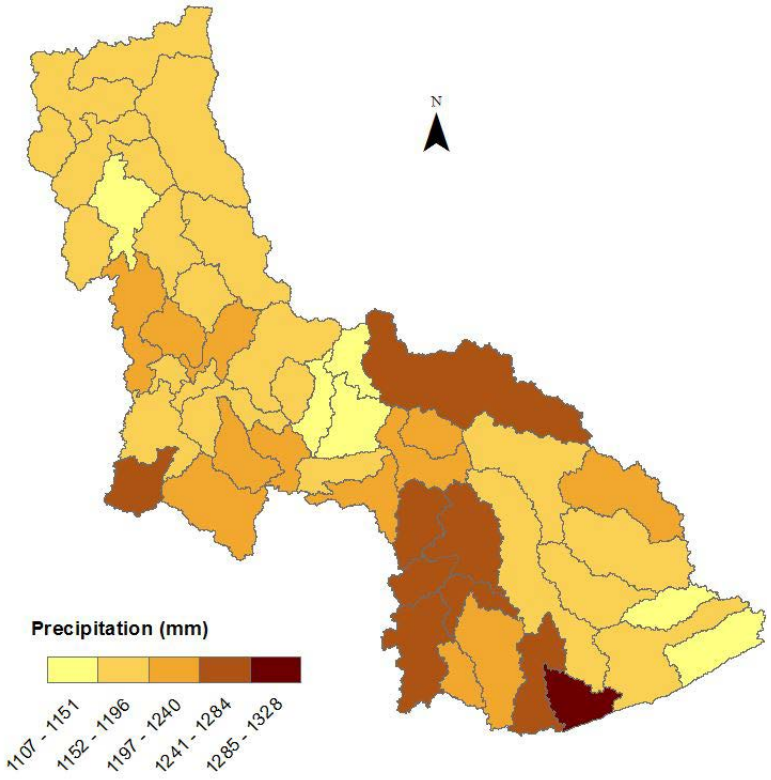

Figure 5.2 Spatial distribution of average annual rainfall in the Kentucky River Basin.

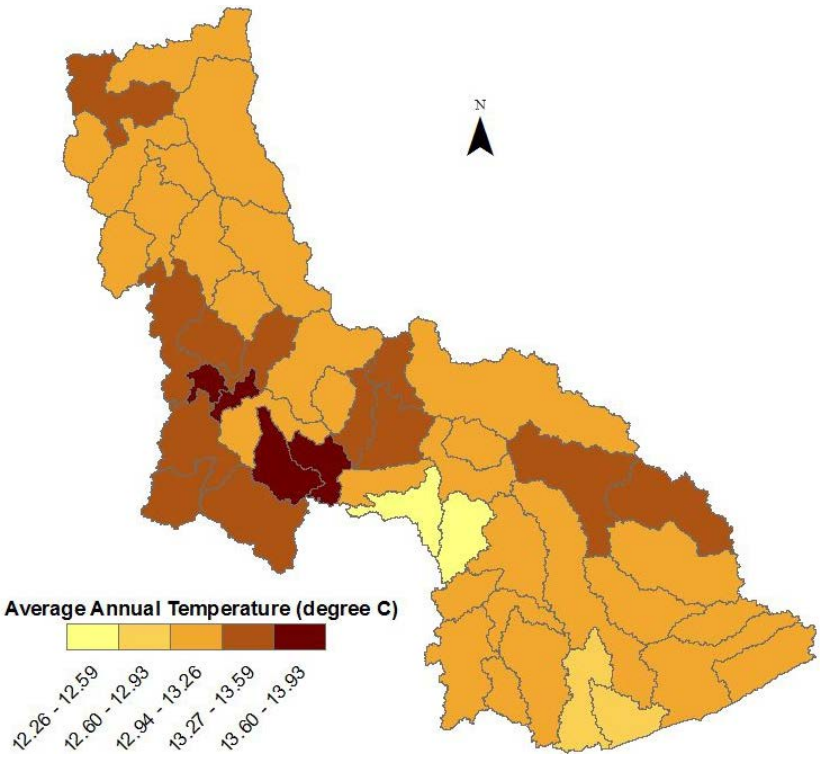

Figure 5.3 Spatial distribution of average annual temperature in the Kentucky River Basin.

5.2.2 SWAT model setup

SWAT is a long term, continuous, semi-distributed, process-based river basin or watershed scale model developed to analyze and predict the impacts of land-management practices on water, sediment and chemical yields (Arnold et al., 2012). Documentation of the SWAT model (Neitsch et al., 2005) provides details about the theoretical background of the model. The model has been used previously across a variety of scales, geomorphologic and climate conditions to evaluate the effect of management practices, climate change and other variables (Taylor et al., 2016; Yao et al., 2016; Chattopadhyay and Jha, 2016). The SWAT model was selected for use due to its widespread use and the compatibility between previously reported SWAT model applications and the objectives of this study.

Hydrologic simulation in SWAT involves data on topography, soils, land use and weather. Thirty-meter resolution raster Digital Elevation Model (DEM) data were obtained from the United States Geological Survey (USGS) Seamless Data Warehouse (http://viewer.nationalmap.gov/launch/) to represent the topography of the watershed. Subwatersheds were delineated on the basis of standard 12-digit hydrologic unit codes (Seaber et al., 1987). The stream network was created by processing the DEM using the ArcHydro algorithm (Maidment, 2002). Land use data were obtained from the National Land Cover Database (NLCD, 2006) of USGS, and the Soil Survey Geographic Database (https://websoilsurvey.sc.egov.usda.gov/App/HomePage.htm) was used to generate the soil map. This configuration resulted in 49 subwatersheds and 14,289 hydrologic response units (HRUs; the smallest unit defined with a unique combination of soil, landuse, slope). Model calculations of water balance are performed at the HRU level and then aggregated for each subbasin. Daily precipitation and air temperature for 38 weather stations within and near the basin were obtained from the United States Department of Agriculture (USDA ARS, http://www.ars.usda.gov/Research/docs.htm?docid=19390). Daily streamflow data were obtained from the USGS (http://waterdata.usgs.gov/nwis) for three gauging stations (Fig. 5.1).

5.2.3 Model calibration and validation process

The SWAT model was calibrated and validated for three gaging stations in the watershed, selected on the basis of data availability and quality: Lockport (USGS station 03290500), Frankfort (USGS station 03287500) and Booneville USGS (station 03281500). The Lockport station is closest to the basin outlet, with nearly 90% of the entire basin draining to that location. Data for time frames of 1991-2000 and 2002-2009

(http://waterdata.usgs.gov/nwis) were used in model calibration and validation, respectively. It is recommended to have few "warm-up" years so that the model approaches reasonable values initially (Kalogerophoulous and Chalkias, 2012). Consistent with these guidelines, the calibration period involved a three-year warm-up period, while the validation period included a one-year warm-up period.

Due to the very large number of parameters contained in the SWAT model, Sequential Uncertainty Fitting II (SUFI2) (Abbaspour et al., 2007) was used with the Nash-Sutcliffe Efficiency (NSE) as the objective function to identify the parameters to be calibrated on the basis of their respective sensitivities. The most sensitive model parameters were calibrated using the SWAT Calibration and Uncertainty Procedure (SWAT-CUP) software (Abbaspour et al., 2007). Calibrated values of SWAT model parameters are given in Table 5.1. Guidelines given by Moriasi et al. (2007) for model evaluation were followed in assessing model performance.

5.2.4 Climate data

Bias corrected (Multivariate Adopted Constructed Analogue or MACA; Abatzoglou and Brown, 2012; Records et al., 2014; Rana and Moradkhani, 2016) 4-km resolution daily data on precipitation and maximum and minimum temperature were obtained from the University of Idaho (http://maca.northwestknowledge.net/index.php) for 10 GCMs (Table 5.2). The MACA algorithm is a statistical downscaling method, capable of transferring GCM outputs to the spatial scales necessary for impact modelling while preserving meteorological patterns and spatiotemporal properties of the data. The GCM data reflect two RCP scenarios, RCP 4.5 and RCP 8.5, which are indicative of medium and high

Table 5.1 SWAT model initial and calibrated values.

Parameter	Initial value/range	Calibrated value
Curve Number (CN2)	Based on land use	Increased by 19%
Baseflow alpha factor (Alpha_BF)	[0-1]	0.14
Groundwater Delay (GW_DELAY)	[0-500]	8.75
Soil evaporation compensation factor (ESCO)	[0-1]	0.4
Plant uptake compensation factor (EPCO)	[0-1]	0.63
Groundwater revap coefficient (GW_REVAP)	[0-1]	0.15
Soil available water capacity (SOL_AWC)	[0.00-0.21]	Decreased by 5%
Deep aquifer percolation fraction (RCHRG_DP)	[0-1]	0.98
Groundwater REVAP minimum (REVAPMN)	[0-750]	369.37
Threshold depth of water in shallow aquifer (GWQMN)	[0-5000]	700
Surface Lag (SURLAG)	[0.05-24]	5.49

emission of carbon, respectively. Data were obtained for the periods 1976 – 2005 (defined as the *baseline period*), 2036 – 2065 (the *mid-century period*) and 2070-2099 (the *late-century period*).

Skill of the GCMs was evaluated by comparing GCM computations to observations for the baseline period. The metrics involved in the comparison were the commonly-used (Taye et al., 2011) mean absolute error (MAE) and normalized standard deviation (NSD) applied to basin-averaged annual mean temperature and annual total precipitation. Mid-

and late-century projections from only the top-three performing GCMs for each historical period variable/metric combination were used as SWAT model inputs for computation of drought indices as described in following paragraphs.

Table 5.2 Global Climate Models used in the study.

Model name	Institution	Spatial resolution	Reference
BCC-CSM 1.1	Beijing Climate Center, China Meteorological Administration, China	2.8° x 2.8°	Xin et al. (2013)
CCSM4	National Center for Atmospheric Research, United States	1.25° x 0.94°	Gent et al. (2011)
CNRM-CM5	National Center for Meteorological Research, France	1.4° x 1.4°	Voldoire et al. (2013)
GFDL-ESM2G	NOAA/Geophysical Fluid Dynamics Laboratory, United States	2.5° x 2.0°	Donner et al. (2011)
GFDL-ESM2M	NOAA/Geophysical Fluid Dynamics Laboratory, United States	2.5° x 2.0°	Donner et al. (2011)
HadGEM2-CC	Met Office Hadley Center, United Kingdom	1.9° x 1.2°	Jones et al. (2011)
IPSL-CM5A-MR	L'Institut Pierre-Simon Laplace, France	2.5° x 1.25°	Dufresne et al. (2013)
MIROC5	Japan Agency for Marine-Earth Sciences and Technology, Atmosphere and Ocean Research and National Institute for Environmental Studies, Japan	1.4° x 1.4°	Watanabe et al (2010)
MIROC-ESM	Japan Agency for Marine-Earth Sciences and Technology, Atmosphere and Ocean Research and National Institute for Environmental Studies, Japan	2.8° x 2.8°	Watanabe et al. (2010)
NorESM1-M	Norwegian Climate Center, Norway	2.5° x 1.8°	Bentsen et al. (2013)

5.2.5 Drought analysis

Two basic indices were used in defining drought events and in assessing their intensity: the reconnaissance drought index (RDI) and streamflow drought index (SDI).

The RDI is a relatively recently-developed meteorological index that accounts for both precipitation and potential evapotranspiration in calculating water deficits (Tsakiris and Vangelis, 2005; Tsakiris et al., 2007; Capetillo et al., 2016). The gamma probability density function was used to model the distribution of α_k, and monthly values of standardized RDI were computed in this study. Positive and negative values of RDI indicate wet and dry periods, respectively, while more negative values represent more severe droughts. Table 5.3 details the drought classification scheme used in this study.

Table 5.3 Drought classification scheme using RDI and SDI as indices (Tabari et al., 2013)

State	Drought Category	Criteria
0	Non-drought	$0 \leq$ RDI/SDI
1	Mild drought	-1.0 < RDI/SDI < 0
2	Moderate drought	-1.5 < RDI/SDI < -1.0
3	Severe drought	-2.0 < RDI/SDI<-1.5
4	Extreme Drought	RDI/SDI $\leq$ -2.0

The SDI (Nalbantis and Tsakiris. 2009; Tabari et al., 2013, Hong et al. 2015) is a hydrological drought index that is calculated on the basis of cumulative streamflow volumes $S_{i,k}$ for each reference period *k* of the *i*-th hydrological year. Monthly streamflow data from the SWAT model simulation were fitted using the gamma distribution function to calculate monthly SDI values. As with the RDI, positive values of SDI reflect

relatively wet conditions, while negative values indicate hydrological drought (Table 5.3).

A *drought event* was defined as a duration over which both the RDI and SDI were continuously negative. Drought onset was therefore determined as the month in which both RDI and SDI values first became negative, while the drought was considered as ending on the first month for which either RDI or SDI became positive. Additional indices were calculated to indicate drought magnitude for each identified drought event.

For a drought event of duration n months, drought severity (S) was calculated as the sum of absolute RDI/SDI values over that duration. Since S was calculated on the basis of both RDI and SDI values,

$$S_{RDI} = \sum_{j=1}^{n} \left| RDI_j \right| \quad (1)$$

and

$$S_{SDI} = \sum_{j=1}^{n} \left| SDI_j \right| \quad (2)$$

Drought intensity (I) was calculated as mean S over the drought event:

$$I_{RDI} = \frac{S_{RDI}}{n} \quad (3)$$

$$I_{SDI} = \frac{S_{SDI}}{n} \quad (4)$$

Maximum Drought Length (MDL) was calculated as the maximum drought event over each of the three timeframes investigated (historical, mid-century and late-century) for each of the subwatersheds.

5.3 Results and discussions

5.3.1 SWAT model performance

Monthly average observed and SWAT-simulated streamflow during the calibration and validation periods are given for the Lockport station in Fig. 5.4. As indicated, simulated and observed flows were, with the exception of some of the highest observed peaks, in generally good agreement. Comparisons for the Frankfort and Booneville stations are consistent with Fig. 5.4. Calculated values of coefficient of determination (R^2), NSE, percent bias (PBIAS), root mean squared error: standard deviation ratio (RSR) (Table 5.4) indicate acceptable model performance (Moriasi et al., 2007) for both the calibration and validation periods.

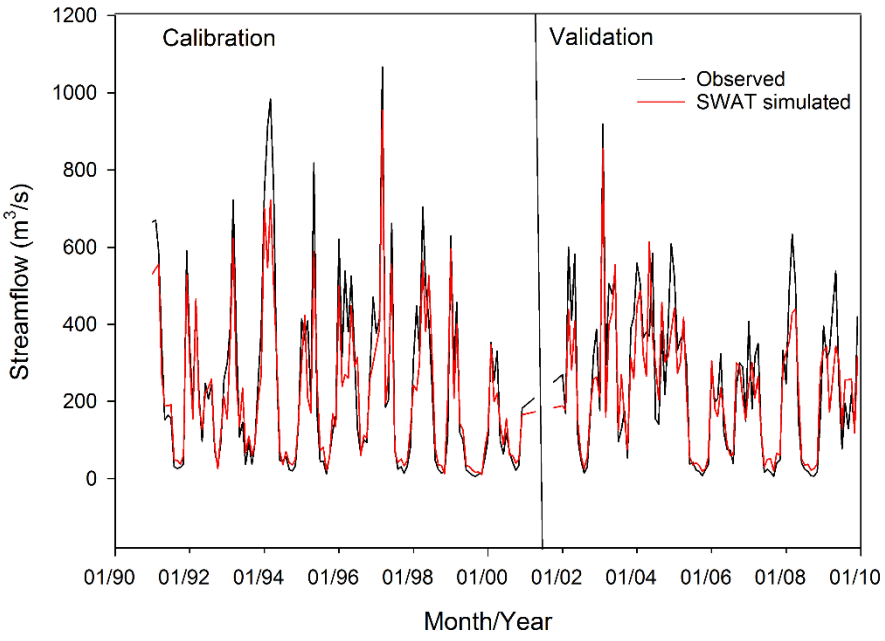

Figure 5.4 Monthly streamflow calibration (1991-2000) and validation (2002-2009) for the Lockport station.

Table 5.4 Summary of model performance for the calibration (1991 – 2000) and validation (2002 – 2009) periods.

Station	R^2	NSE	PBIAS	RSR
Lockport				
Calibration	0.91	0.87	9.9%	0.36
Validation	0.79	0.77	8.1%	0.46
Frankfort				
Calibration	0.89	0.87	3.7%	0.35
Validation	0.75	0.76	7.2%	0.52
Booneville				
Calibration	0.85	0.81	9.8%	0.43
Validation	0.84	0.78	10.8%	0.47

5.3.2 Evaluation of GCM performance

The performance of the GCMs in terms of simulating observed annual average temperature and annual total precipitation, as assessed using the MAE and NSD metrics, is indicated in Table 5.5. Though not used in subsequent SWAT model computations, the ensemble mean is also given for reference.

As indicated in Table 5.5, "best performance" varied both in terms of the simulated variable (annual average temperature vs. annual total precipitation) and metric (MAE vs. NSD). Thus, no single GCM was a clear and consistent top performer, and only two GCMs (CRNM-CM5 and HadGEM2-CC) were eliminated as subsequent sources of input to the SWAT model. In terms of the MAE, the ensemble mean is seen as performing better than any individual GCM (Table 5.5). In terms of NSD, however, the ensemble mean demonstrates a characteristically low NSD, reflecting less success in replicating observed variation as reported elsewhere (Chattopadhyay et al., 2017).

5.3.3 Projected climate in the Kentucky River Basin

5.3.3.1 Temperature

Projections from the GCMs indicate that the Kentucky River basin will experience increasing temperatures. The projected areal average increases (relative to baseline) for RCP 4.5 were 2.2 and 2.6 °C for the mid- and late-century, respectively, whereas RCP 8.5 led to projected increases of 2.7 and 4.9 °C for the mid- and late-century, respectively. Results with regard to daily minimum temperatures (data not shown) were similar though with somewhat smaller (10%) changes relative to baseline. As shown in Figure 5.5, mean daily maximum temperatures are projected to increase during all months, especially in late

Table 5.5 Mean Absolute Error (MAE) and Normalized Standard Deviation (NSD) for GCM simulation of historical (1976-2005) precipitation and temperature in the Kentucky River Basin. The three best-performing models for each variable/metric combination are highlighted in bold.

Model	Precipitation		Temperature	
	MAE (mm)	NSD	MAE (°C)	NSD
GFDL ESM2M	206.65	**0.96**	0.76	1.30
BCC-CSM 1.1	**161.78**	1.19	**0.67**	1.29
CCSM4	173.72	**0.89**	0.89	1.37
CNRM-CM5	199.17	1.19	0.90	1.59
GFDL-ESM2G	**153.56**	1.13	0.79	**1.24**
HadGEM2-CC	206.67	1.23	0.97	1.27
IPSL-CM5A-MR	284.18	1.32	**0.71**	1.35
MIROC5	190.77	1.17	0.78	**1.23**
MIROC-ESM	200.44	**1.12**	0.76	1.28
NorESM1-M	**157.48**	0.72	**0.65**	**1.22**
Ensemble Mean	137.88	0.33	0.60	0.68

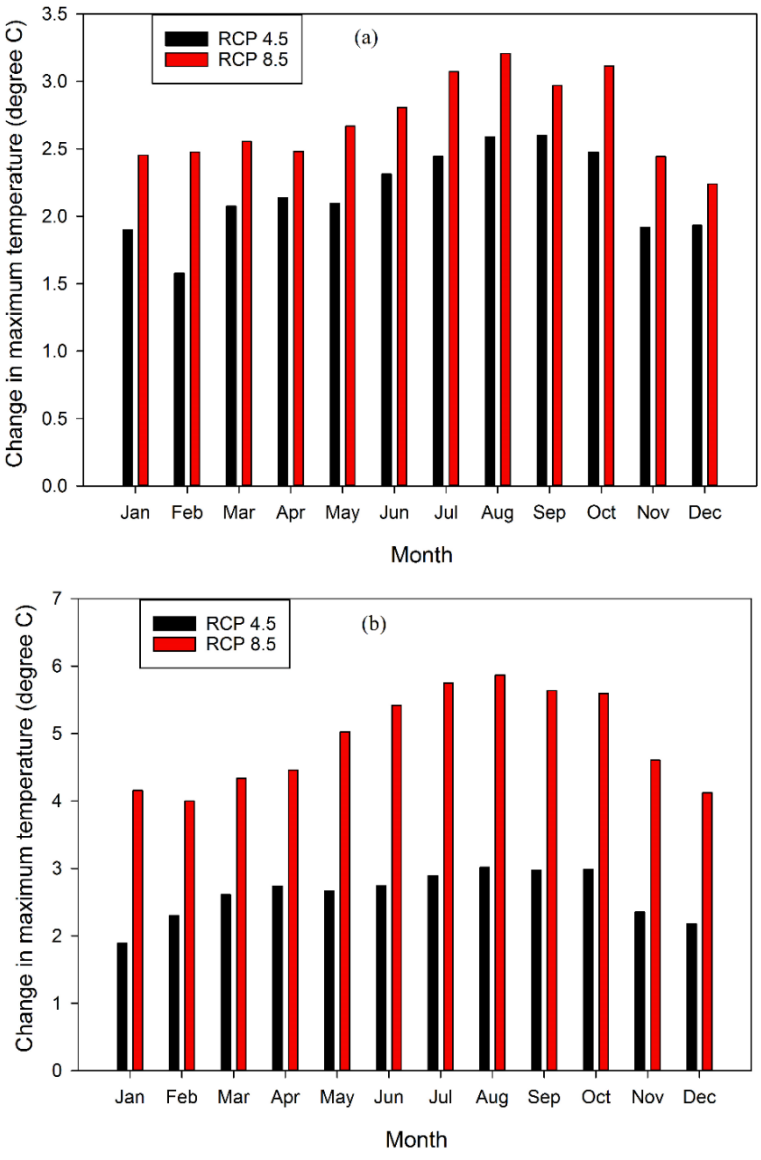

Figure 5.5 Basin-wide changes (relative to baseline) in mean maximum temperature in a) mid- and b) late-century.

summer and early fall. This finding suggests that, in the future, evaporation and transpiration will increase during the months in which it is already relatively high and, in the absence of offsetting factors, tend to promote hydrologic drought conditions in these months.

5.3.3.2 Precipitation

Projections from both RCP indicate modest (2.5 – 5%) increases in areal mean annual precipitation from the baseline. In contrast to the projected changes in temperature, however, changes in in areal mean annual precipitation do not differ substantially between the mid- and late-century periods. Precipitation projections also differ from temperature projections in that projected precipitation exhibited distinct monthly variations (Figure 5.6) with less consistency between the RCPs in terms of magnitude and direction of change. While both RCPs are relatively consistent in terms of projecting wetter winters and early springs (Figure 5.6), there is less agreement on precipitation changes during the warmer months. Figure 5.6 also indicates that, while the net change in areal mean annual precipitation between the mid-century and late-century might be negligible, the distribution of precipitation across months and seasons might change between those periods. The projected precipitation changes are thus relatively (to temperature) complex, which discourages straightforward translation to projected changes in droughts (particularly hydrologic droughts (e.g., 12% increase and 4% decrease in spring and summer in late-century).

5.3.4 Climate change impact analysis

5.3.4.1 Evapotranspiration

Projected changes in actual (as distinct from potential) evapotranspiration (ET), which plays a key role in hydrologic droughts, were based on SWAT model outputs, in which

ET is calculated as a function of crop/vegetation, soil water status and meteorological variables. Evapotranspiration outputs can thus be viewed as a modeled integration of

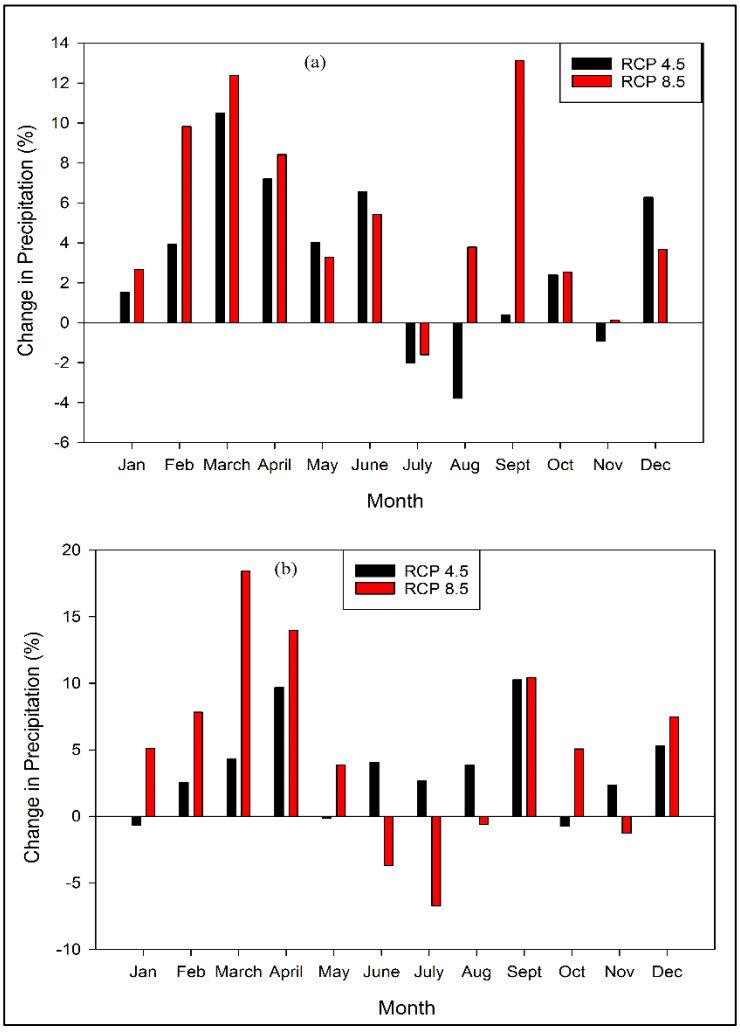

Figure 5.6 Basin-wide changes (relative to baseline) in mean precipitation in a) mid- and b) late-century.

previously-discussed projected temperatures, precipitation and other variables. Figure 5.7, in which projected ET is given as a function of RCP scenario and future timeframe, clearly indicates a consistent pattern of increasing ET during all months except for the summer season (for which ET is projected to decrease), with the greatest increases associated with the coldest months.

When considered on an areal mean annual basis, ET is projected to increase by 3% (RCP 4.5) to 5% (RCP 8.5) for the mid-century, with similar projections for the late-century (4% for RCP 4.5, 5% for RCP 8.5). While the changes are consistent with projected precipitation changes, the distributions of changes across months are amplified for ET relative to precipitation. For example, the maximum projected increase in precipitation was approximately 18% (late-century March for RCP 8.5), whereas the maximum projected increase in ET was roughly 42% (late-century January for RCP 8.5). It is also noteworthy that the overall pattern of Fig. 5.7 resembles that for precipitation (Fig. 5.6) more than temperature (Fig. 5.5), suggesting that ET projections demonstrate a controlling effect of relatively low soil moisture.

The spatial distribution of projected changes in ET is given in Fig. 5.8. As indicated, all of the 49 subwatersheds are projected as having increases in both the mid- and late-century periods, with spatial similarities between the RCPs in terms relative magnitudes of increase. The timeframes and RCPs are consistent in projecting the north-central portion of the basin as having the largest increases in ET. Coincidentally, this portion of the basin is in proximity to the Lexington-Fayette metropolitan statistical area, which has a population of nearly 500,000.

5.3.4.2 Water yield

Projected basin-wide temporal variations in water yield, which is directly associated with hydrologic drought, as based on SWAT model computations are shown in Fig. 5.9. Similar to findings for precipitation and ET, modest basin-wide increases in water yield are projected for both the mid-century (3% for RCP 4.5, 5% for RCP 8.5) and late-century (2% for RCP 4.5, 4% for RCP 8.5). Projected water yields are less-regularly

distributed across months than projected ET, which can be anticipated on the basis of water yield being

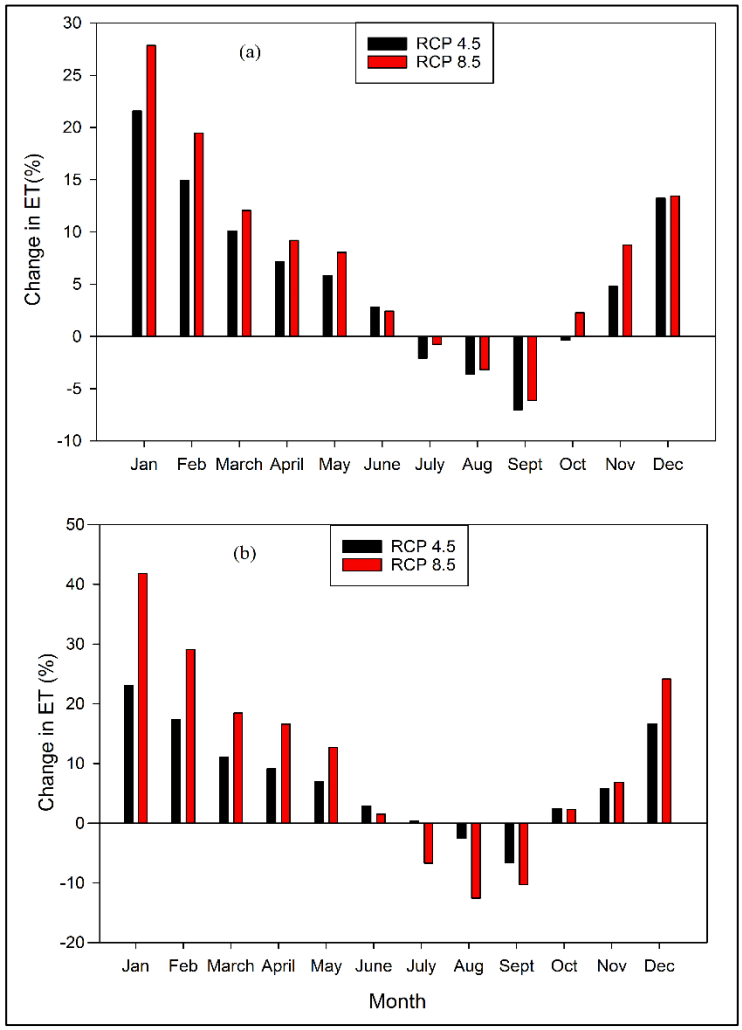

Figure 5.7 Basin-wide changes (relative to baseline) in ET in a) mid- and b) late-century.

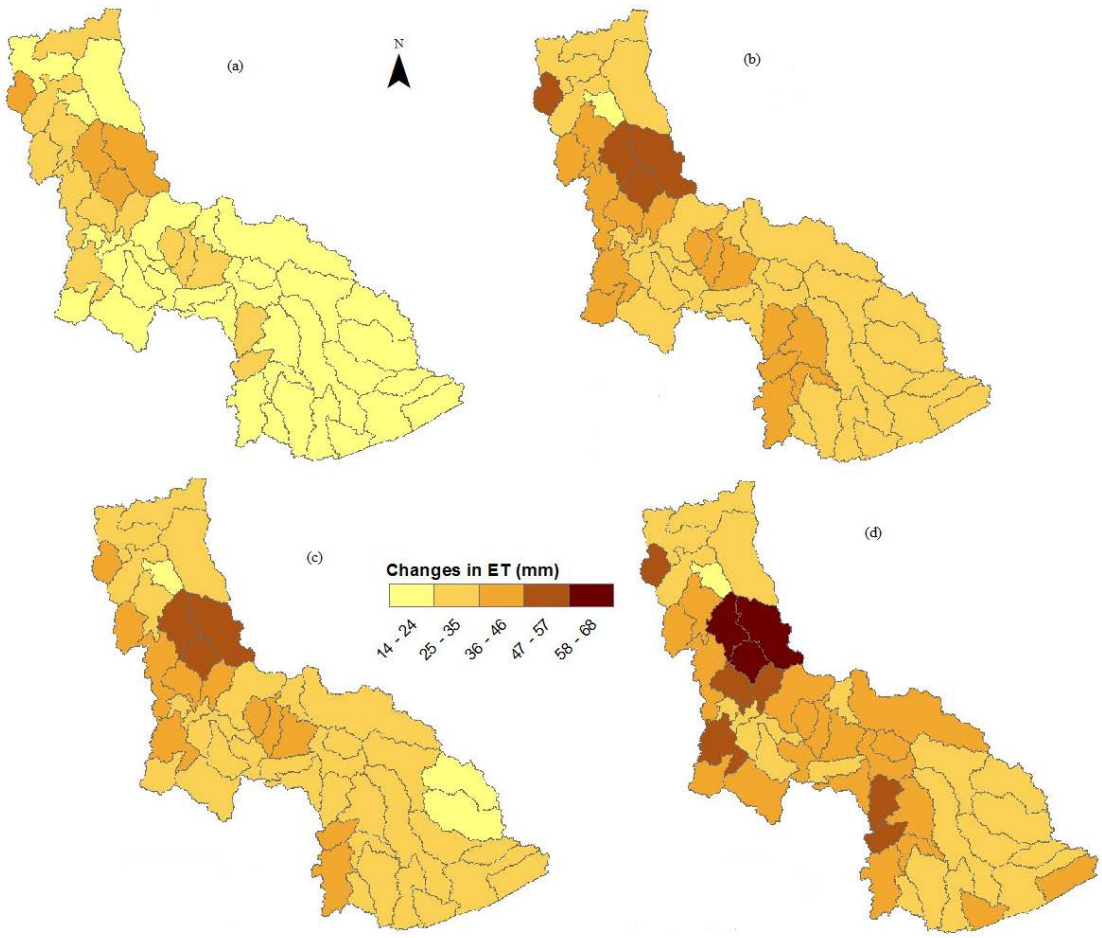

Figure 5.8 Change in mean annual ET (from baseline) (a-b) in the mid -century and late-century (c-d) under RCP 4.5 and RCP 8.5 respectively.

a higher-level hydrologic process (and described in SWAT as such) for which ET can be considered an input. However, the monthly distribution of projected water yields is highly similar to that for precipitation (Fig. 5.6), suggesting that future water yields and their temporal variation might be more dependent on precipitation than temperature and ET, at least in some regions. Both RCPs 4.5 and 8.5 are consistent in projecting mid-century increases in water yield for the spring (March through June) and fall months (October through December) months as well as decreases for January; i.e., there is

agreement on direction of change for eight of the 12 months. A similar result is apparent for late-century water yield projections, though with minor changes (February is more clearly projected as having decreased water yields, September with increased water yields, and May – August with RCP-dependent changes).

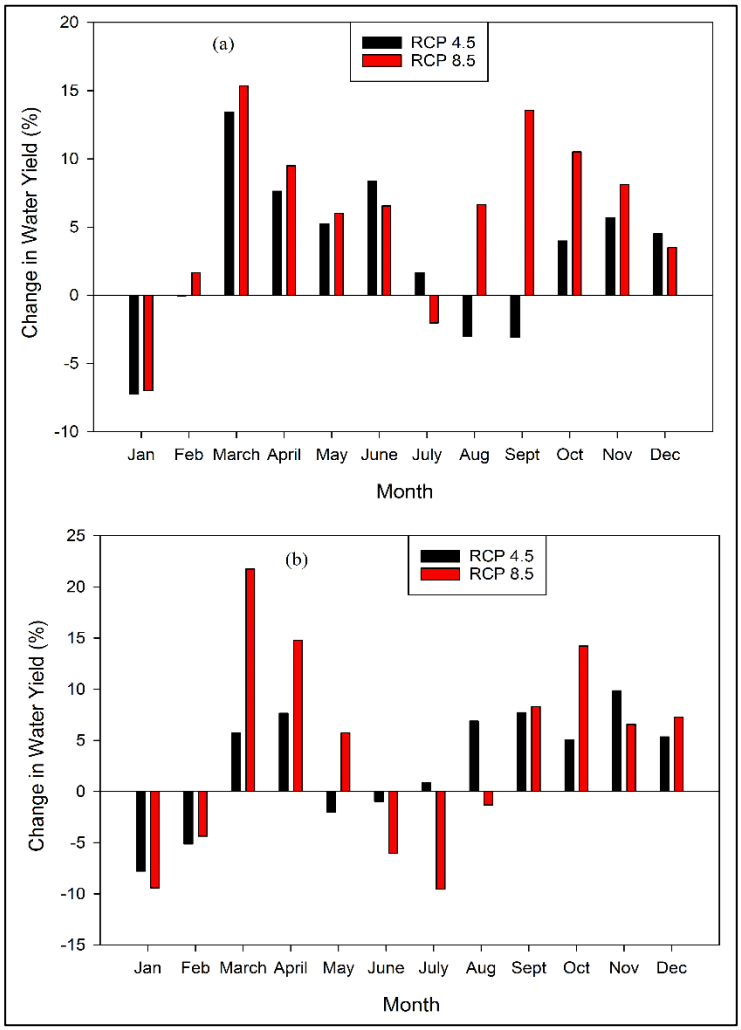

Figure 5.9 Basin-wide changes (relative to baseline) in water yield in a) mid- and b) late-century.

The spatial distribution of projected water yield changes is given in Fig. 5.10. For mid-century projections, all but one of the 49 subwatersheds are projected to experience

water yield increases. Late-century projections for RCP 8.5 indicate the same result (and involving the same subwatershed), while RCP 4.5 projections identify approximately 88% of the subwatersheds as experiencing water yield increases. The portion of the basin having decreasing projected water yields (north-central) is also associated with the highest projected ET values (Fig. 5.8), suggesting of the importance of ET in the context of water yield for this region.

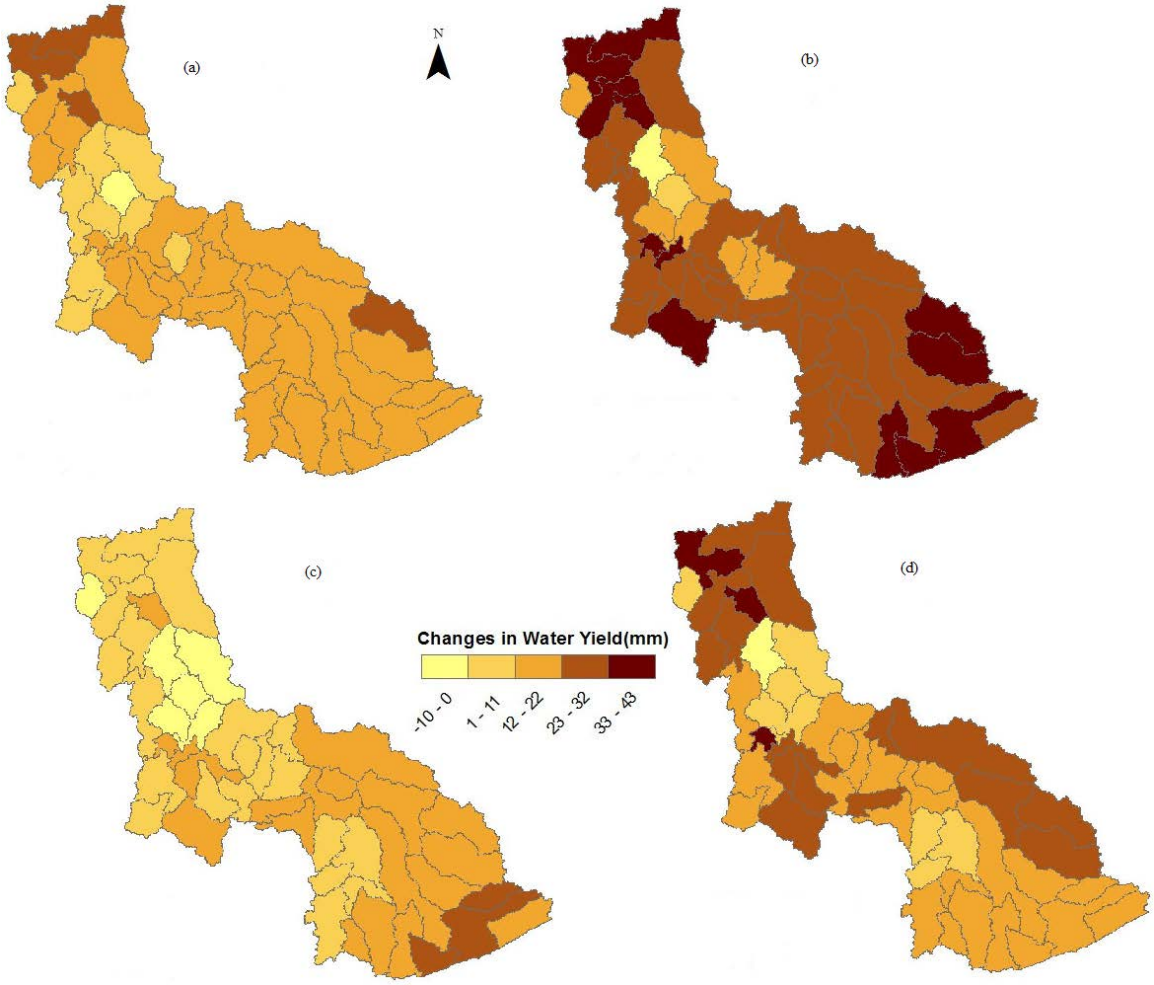

Figure 5.10 Change in mean annual water yield (from baseline) (a-b) in the mid -century and late-century (c-d) under RCP 4.5 and RCP 8.5 respectively.

5.3.5 Drought analysis

5.3.5.1 Overview

Computations of RDI and SDI for the baseline period produced the expected finding that the basin was in an overall state of drought (negative RDI/SDI) for basically half the time (Table 5.6). This proportion did not change appreciably for any projected timeframes/RCP scenarios, consistent with the previously-discussed results with respect to rainfall, ET and water yield. The results with respect to SDI-defined droughts are consistent with earlier work reported by Chattopadhyay et al. (2017), who suggested that, relative to the baseline period, the region might experience fewer drought years in the late 21st century.

Table 5.6 Proportions of total months (%) under basin-wide drought conditions.

	Index	
Scenario	RDI	SDI
Baseline	51.0	51.1
Mid-Century		
RCP 4.5	49.8	50.6
RCP 8.5	50.2	50.3
Late-Century		
RCP 4.5	47.3	50.9
RCP 8.5	50.0	50.2

Analysis of RDI drought durations for each of the 49 subwatersheds indicated average drought lengths of 1-4 months, with 80% in the 3-4 month range (Fig. 5.11(a)) for the baseline period. Projected average drought durations were similar for the mid-century timeframe but exhibited more differences for the late-century. The late-century RCP 4.5 scenario indicated subwatersheds shifting from the 1-2 month into the 3-4 month average

drought duration category, while the reverse was true for RCP 8.5. In comparison to the RDI findings, Fig. 5.11(b) indicates that droughts as defined the SDI are of a more chronic nature; for the baseline timeframe, roughly 45% of subwatersheds had average drought lengths of 4-5 months. Projected average drought (SDI) lengths were consistent for all timeframes and RCP scenarios except for late-century RCP 8.5 which, similar to RDI-defined drought lengths, demonstrated a shift of subwatersheds away from the 4-5 month and toward the 3-4 month average drought length category.

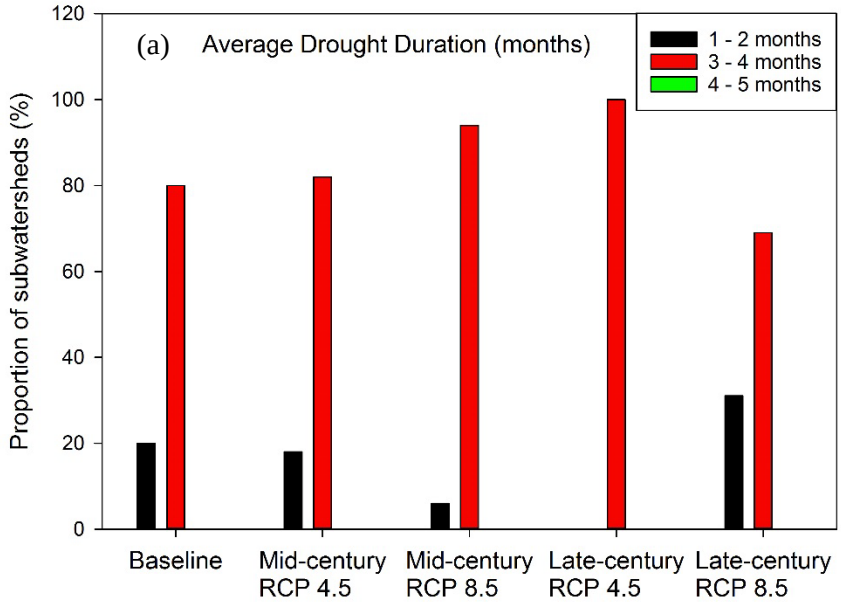

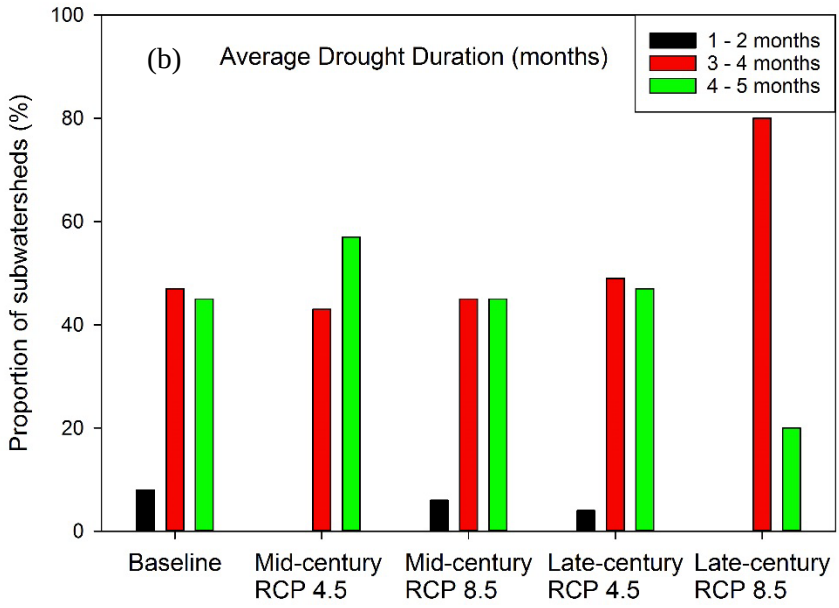

Figure 5.11 Proportion of subwatersheds in average drought length categories as defined by (a) RDI and (b) SDI.

5.3.5.2 Maximum drought length

Basin-wide MDLs are given in Table 5.7 for all timeframes/scenarios and for both RDI- and SDI-defined droughts. Consistent with previous discussion, Table 5.7 reflects the more persistent nature of hydrological droughts (SDI) relative to meteorological droughts (RDI), with MDLs for SDI-defined droughts being about 50% greater than those for RDI-defined droughts. Projected MDL deviations from the baseline timeframe tended to be relatively small except for the mid-century RCP 4.5 projections, which were associated with a 25% increase in SDI-defined MDL.

Table 5.7 Basin-wide duration and intensity of drought events calculated from RDI/SDI values for the Kentucky River Basin.

Scenario	Maximum Drought Length		Average Drought Intensity	
	RDI	SDI	RDI	SDI
	----- Months -----			
Baseline	8	12	1.38	1.20
Mid-century				
RCP 4.5	9	15	1.37	1.11
RCP 8.5	7	13	1.31	1.24
Late-century				
RCP 4.5	8	12	1.33	1.17
RCP 8.5	9	13	1.27	1.14

The spatial distribution of MDL for the baseline timeframe is given in Figure 5.12, which indicates that the southern portion of the basin experienced greater MDLs for both RDI- and SDI-defined droughts. Figure 5.12(b) also indicates that the region of greatest MDL is coincident with the previously-discussed Lexington-Fayette area, the most heavily developed region in the basin.

Differences in spatial MDL distribution due to type of drought and RCP scenario are apparent in Fig. 5.13 for projected mid-century MDL values. The RCP 4.5 projections indicate that the northern portion of the basin is generally associated with increasing MDL for both RDI- and SDI-defined droughts. In contrast, RCP 8.5 projections indicate near-uniform decreases in MDL for meteorological drought, with increasing MDL for hydrological drought associated primarily with the southern portion basin. More consistency is apparent in late-century MDL projections, as shown in Fig 5.14. For both RDI- and SDI-defined droughts, the highest MDL values are generally, though with some variation, associated with the northern and central portions of the basin.

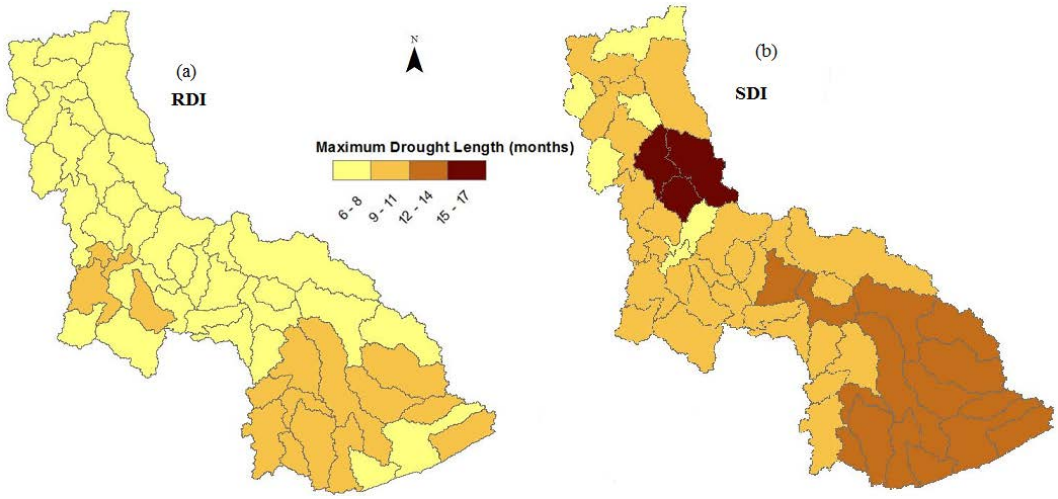

Figure 5.12 Spatial distribution of maximum drought length calculated from a) RDI b) SDI values in the baseline

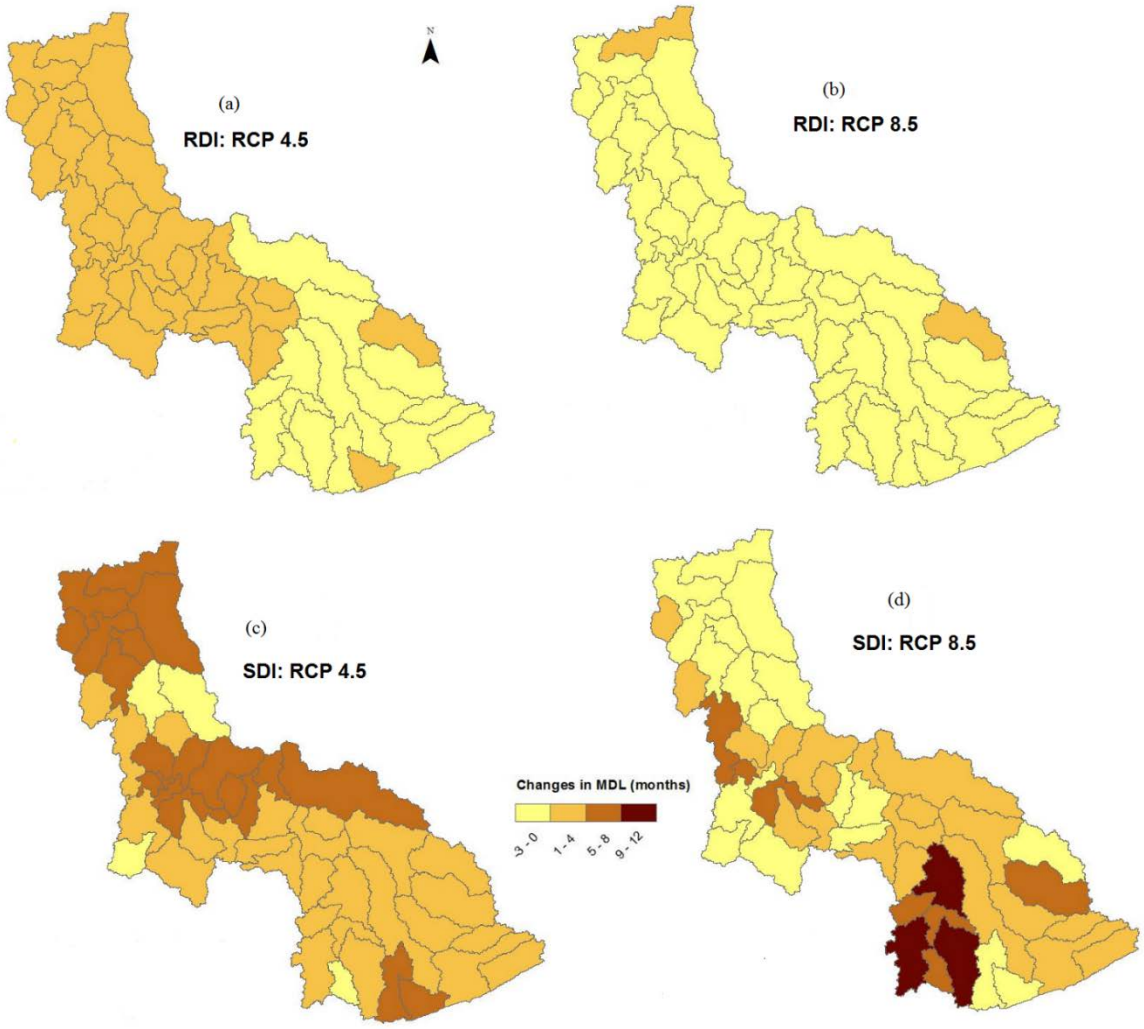

Figure 5.13 Spatial distribution of changes in maximum drought length in the mid-century calculated from RDI (a-b) and SDI (c-d) under RCP 4.5 and 8.5 respectively.

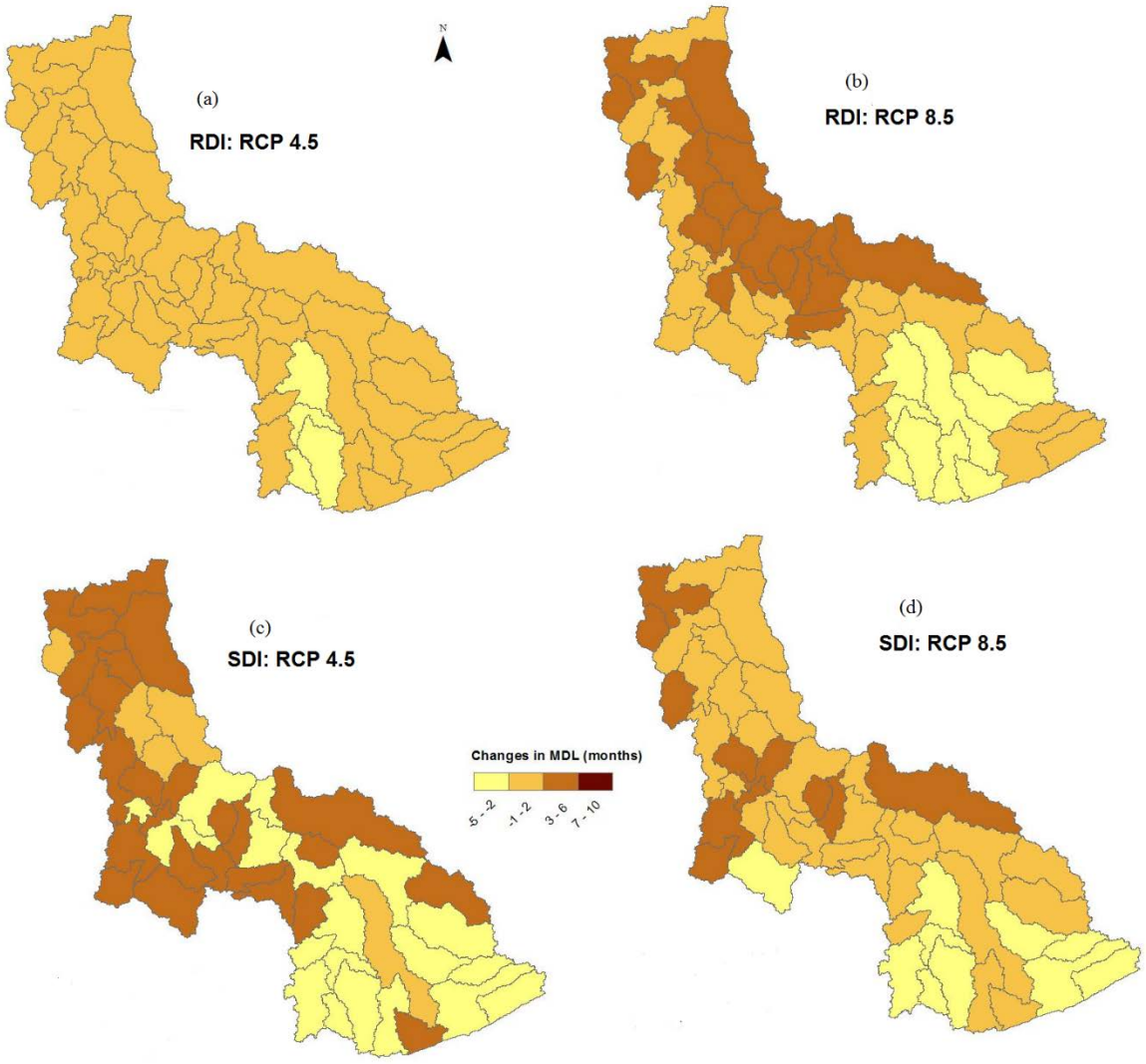

Figure 5.14 Spatial distribution of changes in maximum drought length in the late-century calculated from RDI (a-b) and SDI (c-d) under RCP 4.5 and 8.5 respectively.

5.3.5.3 Drought intensity

In contrast to the findings for MDL, basin-wide average intensities were lower for SDI-defined droughts (1.20) than for RDI-defined droughts (1.38) during the baseline period (Table 5.7). This result suggests that hydrologic droughts, insofar as regards their intensity, experienced a damping effect, perhaps as a result of the additional processes and storages involved. The same relationship was generally (with the exception of mid-

century, RCP 8.5) true for drought projections for all timeframes and scenarios. Additionally, with the same exception, intensities of both SDI- and RDI-defined basin-wide droughts decreased relative to the baseline period for all drought projections.

The spatial distribution of drought intensities for the baseline period is given in Figure 5.15. The figure reinforces the generally higher intensities of meteorological drought, but with some differences in spatial distribution. Both RDI- and SDI-defined droughts tend to be highest near the central and northern portions of the basin; however, intensities differ in the southern portion, being among the highest for meteorological droughts and lowest for hydrological droughts.

The spatial distribution of projected drought intensities (Figs. 5.16 and 5.17) is quite complex. Mid-century drought intensity projections (Fig. 5.16) demonstrate no clear pattern of behavior with the possible exception of a tendency toward more intense droughts (as defined by both indices) in the northern and eastern portions of the basin, with subwatersheds projected as having less intense droughts scattered throughout. Late-century drought projections (Fig. 5.17) are similarly complex in terms of spatial distribution, but possibly more RCP-dependent than mid-century projections. Projections for RCP 4.5 suggest that the highest increases in drought (both meteorological and hydrological) intensity are associated with the northern portion of the basin, whereas these increases are associated more with the southern portion for RCP 8.5.

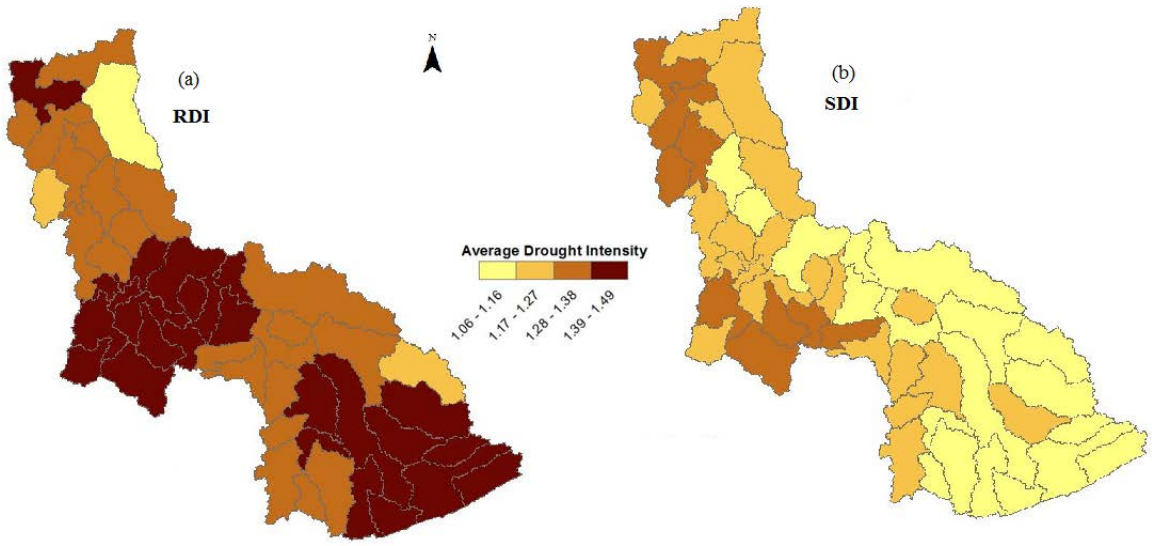

Figure 5.15 Spatial distribution of drought intensity calculated from a) RDI and b) SDI values for the baseline period.

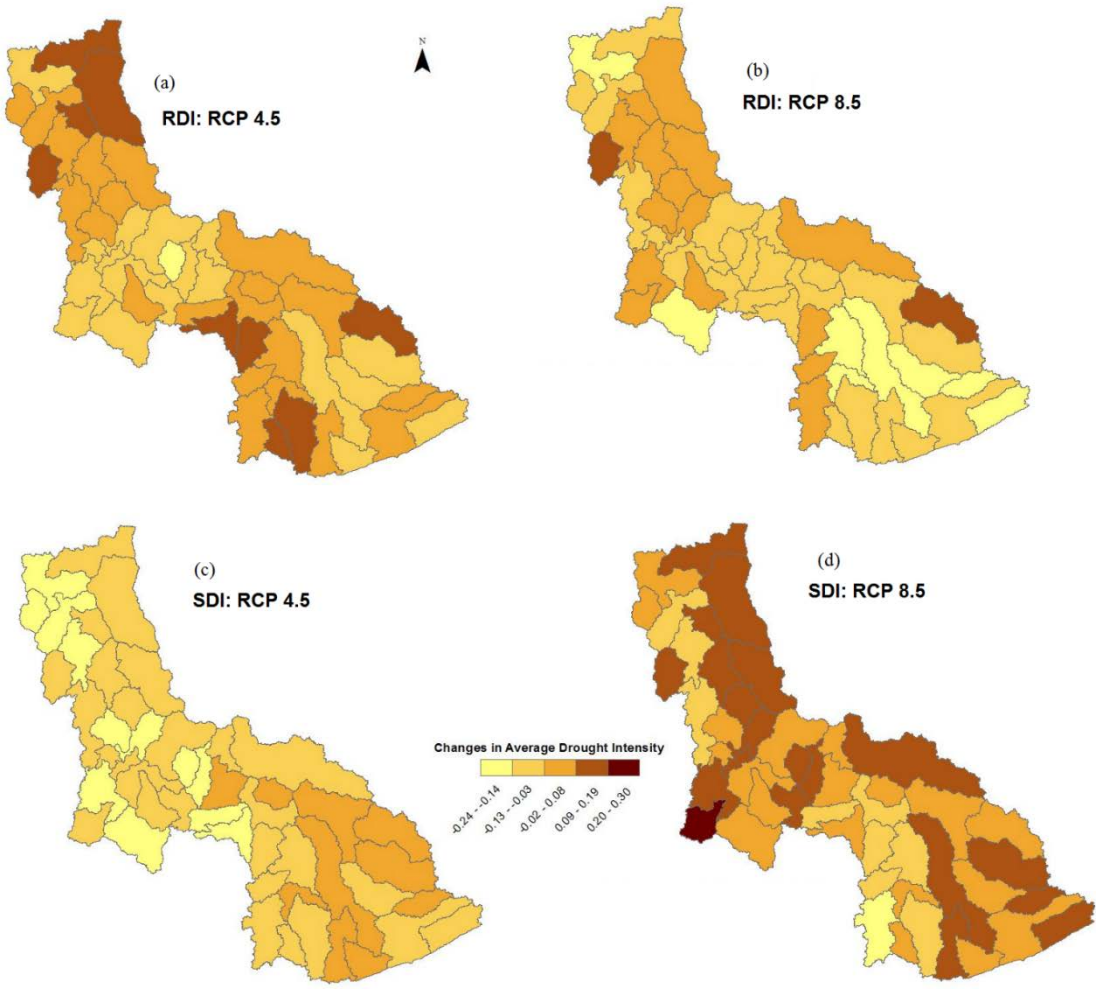

Figure 5.16 Spatial distribution of changes in average drought intensity in the mid-century calculated from RDI (a-b) and SDI (c-d) under RCP 4.5 and 8.5 respectively.

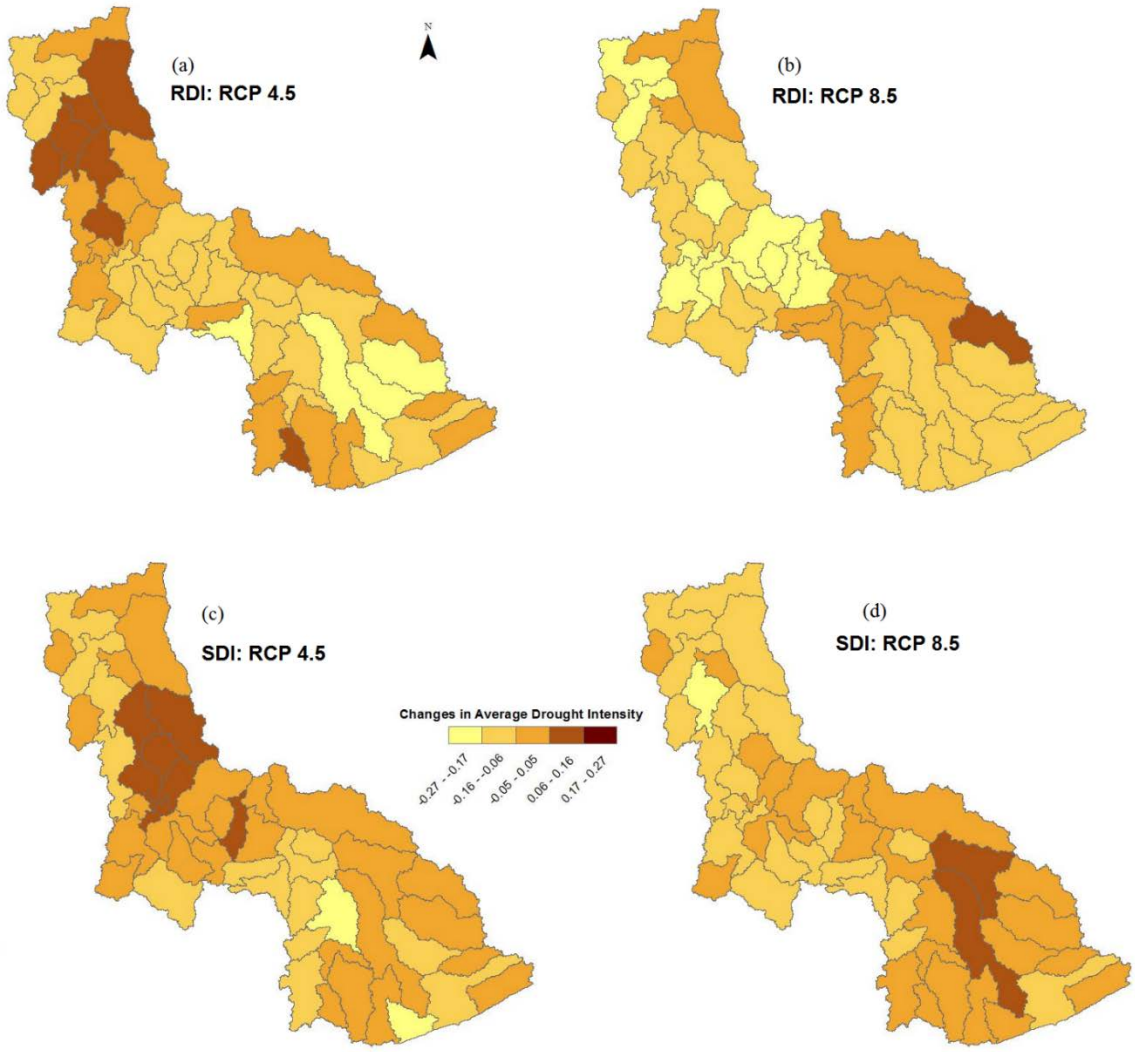

Figure 5.17 Spatial distribution of changes in average drought intensity in the mid-century calculated from RDI (a-b) and SDI (c-d) under RCP 4.5 and 8.5 respectively.

5.4 Conclusions

The objective of this study was to evaluate historical and projected droughts, both meteorological (RDI) and hydrological (SDI), for the Kentucky River Basin. The basic approach was to combine historical data and projections from a suite of GCMs with the calibrated SWAT model for computation of subwatershed-level and basin-wide

hydrological drought indices, whereas meteorological drought indices were calculated on the basis of meteorological data only.

Relative to the baseline period, GCM projections indicate modest basin-wide increases in precipitation (2.5 – 5%, with relatively consistent increases in the winter) with more substantial basin-wide increases in average annual temperature (2 – 4.7 ^{o}C, with greatest increases during the summer months), depending on timeframe (mid-century or late-century) and RCP scenario (4.5 or 8.5). Similar basin-wide increases (3-5% relative to baseline) are projected for ET, with greatest increases during the winter and decreases in the summer. Basin-wide water yield is projected to increase (2-5%), though the pattern of increasing and decreasing months appears more related to RCP scenario than for other variables.

Findings indicated that, basin-wide, there was very little projected change in the proportion of time in a drought condition or in the average length of drought conditions. Projections further indicated that maximum length of basin-wide hydrological droughts might increase slightly, but changes in maximum drought length for meteorological droughts were minimal. Drought projections additionally indicated that basin-wide drought severity is anticipated to generally decrease, even if slightly.

When drought indices were calculated on the subwatershed level, broad and consistent spatial patterns were usually difficult to identify. Whether for meteorological or hydrological droughts, the spatial distribution of changes was dependent on the timeframe (historical, mid-century and late-century) and RCP scenario.

The overall findings suggest that, as assessed using the methods of this study, changes in investigated hydrological and meteorological drought indices investigated will change only slightly (and perhaps in the direction of less severity) in the mid- to late-21st century on the basin level. However, smaller-scale (subwatershed level) changes may be significant, suggesting that water resources originating from smaller drainage areas might merit more scrutiny to evaluate their reliability in coming years.

CHAPTER 6: CONCLUSIONS

The present research focused on determining long-term natural climate variability for the Commonwealth of Kentucky, trends in extreme precipitation events, and climate change impacts on hydrological behavior and extreme hydrological events for a watershed in the southeastern United States. For the first objective, non-parametric statistical tests were conducted using long-term (61 years) precipitation and temperature datasets to evaluate the annual trends in the time series. The second objective of this work involved examining spatiotemporal variability in six extreme precipitation indices for the Kentucky River Basin, a major tributary of the Ohio River Basin. The last objective was focused on determining hydrological impacts caused by anticipated climate change on water balance components and droughts in both near- and long-term future time frames. Major findings from this research are summarized below:

6.1 Major conclusions

a) Kentucky's climate has generally become wetter and warmer over the last 60 years. Some stations on Kentucky's western and southern borders have demonstrated statistically significant increases in average annual rainfall and temperature.

b) The majority of the extreme precipitation indices evidenced increasing trends for the baseline period (1986-2015) in the Kentucky River Basin. Urban portions of Kentucky River Basin have experienced statistically significant trends in extreme precipitation indices such as total precipitation in wet days and number of days with more than 20mm of rainfall for the baseline period.

c) The research described in Chapter 4 identified inconsistencies between baseline period trends and late-century projections. These inconsistencies can be considered cautionary; at a minimum, they suggest limitations in reconciling analyses on relatively small temporal and spatial scales to GCM projections, even when those projections are bias-corrected and spatially downscaled. Findings with regard to baseline period conditions and trends might be reflective of relatively large influences of small-scale variables such as elevation and land cover, whose relative importance diminishes in the context of relatively low-resolution GCM projections. While scale- and timeframe-related anomalies need not be irreconcilable, their occurrence can represent challenges to those charged with applying low-resolution projections to smaller scales of decision-making and effective management.

d) Late-century (2070-2099) projections indicated that indices such as total wet day precipitation (PRCPTOT), lengths of dry and wet spells (CDD and CWD) that are related to the macroweather regime were consistent with the baseline trends, whereas indices that were closely linked with the weather regime such as simple daily precipitation index (SDII) indicated reversals of baseline trends. This finding might be due in part to GCMs having inherent weaknesses in simulating events on the weather scale of time. As defined on an annual basis, droughts are expected to be less frequent in the Kentucky River Basin compared to the baseline.

e) A successfully-calibrated SWAT model was executed with projected climate data from a suite of CMIP5 GCMs, corresponding to two different representative

concentration pathways (RCP 4.5 and 8.5) for two distinct time periods; 2036-2065 and 2070-2099 referred to as mid-century and late-century, respectively, to quantify the impact of future climate on surface water availability and droughts for the Kentucky River Basin. The climate models predicted slight increases in average annual precipitation and temperature in the future compared to the baseline period.

f) Spring and fall months were found to be associated with increasing trends in surface runoff and water yield, in contrast to decreasing trends in winter. Evapotranspiration evidenced a generally increasing trend in winter and a decreasing trend in summer, consistent across scenarios/time frames.

g) Hydrological and metrological aspects of drought were studied using two different indices: Streamflow Drought Index and Reconnaissance Drought Index (RDI). Results indicated that future would be characterized by longer but less intense drought events. Hydrological droughts, however, are projected to be less intense but more persistent than the meteorological droughts.

6.2 Recommendations for future research

a) In the first objective, absolute homogenization was performed on the time series data before assessing the linear trends using the Mann-Kendall test. It might be instructive to adopt a relative homogenization approach and subsequently use a parametric method to detect trends such as regression and finally compare the trend estimates. This address the issue of sensitivity of inferences to methods of analysis. Future research should also focus on subdividing the entire time series

data into shorter intervals (e.g., decades) for a more comprehensive evaluation of short term variability and change point detection.

b) This study only considered six extreme precipitation indices from the set of available ETCCDI indices. Future research should also investigate other precipitation indices as well as temperature indices to more fully characterize the range of plausible extreme climate scenarios. Furthermore, only daily data were considered in this study; future studies might explore trends at a finer time resolution (e.g., subdaily data). Notwithstanding the challenges in some of the GCMs to simulate finer temporal resolution data as noted from results of the second study, such an effort might be of interest to researchers. Research efforts should also focus on considering different downscaling methods and more RCP scenarios.

c) This study used 10 GCMs with two scenarios each. Statistical methods were adopted to downscale and bias-correct the GCM outputs. Future studies should explore dynamic downscaling methods from RCM outputs as well as apply different bias-correction techniques such as the delta change method to the forecasted climatic time series.

d) Changes in future land use were not explicitly accounted for in terms of model input specification. Land use changes can have significant influences on hydrologic processes, and future modelling efforts should consider land use change scenarios along with climate change scenarios in the Kentucky River Basin. Further studies are also needed to determine combined impacts of climate and land use changes in water quality of the Kentucky River Basin.

e) The implications of this study (Chapter 3, in particular) with respect to intensive crop production (e.g., western Kentucky) were not investigated in detail. It seems possible that parameters of future climate will be of mixed value in this context. Should the apparent broad trends of increasing temperatures and rainfall continue, then benefits in the forms of longer growing seasons, ground water recharge, and decreased irrigation requirements are possible. However, wetter field conditions could hinder agricultural operations, and increased evapotranspiration demand might more than offset the increased rainfall. A more detailed and focused study on questions of this nature could help to clarify probable future scenarios and enable producers to begin the process of helpful adjustments in practices and techniques.

6.3 Suggestions for water resource managers

a) The results from this study indicate that the north-central urbanized portion of the Basin might merit more scrutiny in terms of developing sustainable management plans, as some of the longest durations of droughts (corresponding to greatest decreases in future water yield) were noted for this area. In particular, the Lexington-Fayette Metropolitan Statistical Area (Lexington, Versailles, Georgetown, Nicholasville, Winchester and smaller cities) may require attention in the planning process to alleviate some of the climate change impacts by effectively utilizing available water resources.

b) At the same time, the future potential for increasing days of heavy (> 20 mm) rainfall in the Lexington-Fayette Metropolitan Statistical area could promote increased and more frequent flooding. This scenario could call into question the

effectiveness of existing flood mitigation measures (e.g., stormwater detention basins) and require revisions to the design process in order to achieve current levels of protection.

c) It was also noticed that in the future, flow in the Kentucky River will decrease in the winter months. Although peak water demand usually occurs in the summer season, further analysis might be helpful in terms of ensuring that relatively non-seasonal demands (e.g., household and industrial) will not be adversely affected by declining winter flows.

d) Projections of climate and its impacts are necessarily accompanied by appreciable uncertainty. Some of these sources of uncertainty have been mentioned in this dissertation using words such as "limitations" or "challenges." Whether this uncertainty is quantified, it is inherent in all projections and can make the already-challenging tasks of water resource planning and management even more difficult. The framework offered by adaptive management might be helpful in the context of resource planning, management and policy development, as it promotes flexible decisions that can be revised as newer and more precise information becomes available.

Appendix 1. List of weather stations in the initial dataset

Station Number	Station Code	Weather station	Longitude	Latitude
1	C150043	Allen1	-86.2500	36.6333
2	C150422	Allen2	-86.1333	36.9000
3	C157215	Allen3	-86.2167	36.7333
4	C154967	Ballard	-88.8333	36.9667
5	C150700	Bell1	-83.5167	36.7833
6	C151973	Bell2	-83.6833	36.6000
7	C153006	Bell3	-83.7500	36.7833
8	C156170	Bourbon	-82.6167	38.4500
9	C150254	Boyd1	-82.7000	38.4333
10	C150268	Boyd2	-84.7667	37.6667
11	C152040	Boyle	-86.5667	37.9167
12	C154196	Breathitt1	-86.4333	37.7833
13	W03889	Breathitt2	-86.2833	37.8833
14	C156624	Breathitt3	-86.5000	37.6167
15	C150031	Breckinridge1	-85.6500	37.9167
16	C153604	Breckinridge2	-85.7000	38.0000
17	C154165	Breckinridge3	-88.3000	36.6000
18	C156988	Breckinridge4	-89.0000	36.8333
19	C150630	Bullitt1	-88.9667	36.8833
20	C157334	Bullitt2	-88.8833	36.8000
21	C155694	Calloway	-85.1500	38.6667
22	C150214	Carlisle1	-87.5667	36.6667
23	C150402	Carlisle2	-87.5167	36.8500
24	C155415	Carlisle3	-85.1333	36.6833
25	C151345	Carroll	-88.1000	37.4667
26	C154755	Casey	-88.0667	37.3333
27	C153798	Christian1	-85.4000	36.7833
28	C153994	Christian2	-87.1500	37.7667
29	C150687	Clay1	-87.0667	37.8000
30	C155111	Clay2	-87.0833	37.7667
31	C150063	Clinton	-86.2667	37.2000
32	C152961	Crittenden1	-86.2667	37.2000
33	C155150	Crittenden2	-86.0833	37.1833
34	C151137	Cumberland	-84.6000	38.0333
35	C156091	Daviess1	-84.5000	38.1333
36	C156094	Daviess2	-89.1667	36.5667
37	C156096	Daviess3	-84.9667	38.7667
38	C151046	Edmonson1	-84.4333	37.4833
39	C155097	Edmonson2	-84.5667	37.6167
40	C155834	Edmonson3	-84.5833	38.7167

41	C154748	Fayette1	-84.7833	38.6500
42	W93820	Fayette2	-84.6167	38.6667
43	C153028	Franklin	-88.6500	36.7333
44	C153186	Fulton	-86.5167	37.4167
45	C158446	Gallatin	-86.5500	37.6000
46	C151890	Garrard1	-86.3000	37.5167
47	C154620	Garrard2	-85.5000	37.2500
48	C152250	Grant1	-85.5500	37.2333
49	C154309	Grant2	-86.9000	37.9000
50	C158714	Grant3	-87.7000	37.1667
51	C155230	Graves	-87.5167	37.3500
52	C151294	Grayson1	-85.5333	38.2667
53	C152770	Grayson2	-85.7667	38.2333
54	C155438	Grayson3	-83.8833	36.8833
55	C153430	Green1	-85.7333	37.5333
56	C153435	Green2	-84.3000	37.5667
57	C154732	Hancock	-84.8167	38.5167
58	C151998	Harrison1	-82.6000	37.2000
59	C152003	Harrison2	-84.3333	37.3500
60	C152072	Hopkins1	-86.5667	36.7167
61	C155067	Hopkins2	-87.9667	36.7667
62	C153382	Jackson	-87.9500	37.7667
63	C150155	Jefferson1	-84.1000	36.9500
64	C154949	Jefferson2	-84.3167	36.8333
65	C153837	Jessamine	-84.2333	38.2000
66	C150381	Knox	-83.3833	37.5500
67	C153929	Larue	-83.3167	37.5833
68	C154893	Laurel	-83.3667	37.5333
69	C153741	Lee	-84.9333	37.3167
70	C150619	Madison	-83.5667	37.1667
71	C157129	Magoffin	-83.8167	37.1500
72	C156104	Owen	-84.8667	38.2333
73	C151080	Perry1	-84.3000	38.3833
74	C152131	Perry2	-84.2833	38.3833
75	C151119	Pike	-83.9500	37.4000
76	C151576	Powell	-84.7167	37.8167
77	C155648	Rockcastle	-84.0667	37.1167
78	C157324	Shelby	-83.7667	37.5500
79	C153036	Simpson	-83.0833	37.7500
80	C151206	Trigg	-83.3833	37.3500
81	C158197	Union	-83.0667	37.0333
82	C151806	Whitley1	-83.9333	37.8667
83	C151969	Whitley2	-85.2000	38.2000
84	C153716	Wolfe	-83.4500	37.7833

References

Abatzoglou, J. T. and T. J. Brown, 2012. A comparison of statistical downscaling methods suited for wildfire applications. *International Journal of Climatology* **32**:772-780.

Abbaspour, K. C., J. Yang, I. Maximov, R. Siber, K. Bogner, J. Mieleitner, J. Zobrist and R. Srinivasan, 2007. Modelling hydrology and water quality in the pre-alpine/alpine Thur watershed using SWAT. *Journal of Hydrology* **333**:413-430.

Abbaspour, K. C., M. Faramarzi, S. S. Ghasemi and H. Yang, 2009. Assessing the impact of climate change on water resources in Iran. *Water Resources Research* **45**:n/a-n/a.

Abdo, K. S., B. M. Fiseha, T. H. M. Rientjes, A. S. M. Gieske and A. T. Haile, 2009. Assessment of climate change impacts on the hydrology of Gilgel Abay catchment in Lake Tana basin, Ethiopia. *Hydrological Processes* **23**:3661-3669.

Aguilar, E., I. Auer, M. Brunet, T. C Peterson and J. Wieringa, 2003. Guidelines on Climate Metadata and Homogenization; *World Meteorological Organization*, Geneva, Switzerland.

Aguilar, E., T. C. Peterson, P. R. Obando, R. Frutos, J. A. Retana, M. Solera, J. Soley, I. G. García, R. M. Araujo, A. R. Santos, V. E. Valle, M. Brunet, L. Aguilar, L. Álvarez, M. Bautista, C. Castañón, L. Herrera, E. Ruano, J. J. Sinay, E. Sánchez, G. I. H. Oviedo, F. Obed, J. E. Salgado, J. L. Vázquez, M. Baca, M. Gutiérrez, C. Centella, J. Espinosa, D. Martínez, B. Olmedo, C. E. O. Espinoza, R. Núñez, M. Haylock, H. Benavides and R. Mayorga, 2005. Changes in precipitation and temperature extremes in Central America and northern South America, 1961–2003. *Journal of Geophysical Research: Atmospheres* **110**:n/a-n/a.

Alamgir, M., S. Shahid, M. K. Hazarika, S. Nashrrullah, S. B. Harun and S. Shamsudin, 2015. Analysis of Meteorological Drought Pattern During Different Climatic and Cropping Seasons in Bangladesh. *JAWRA Journal of the American Water Resources Association* **51**:794-806.

Al-Faraj, F., M. Scholz and D. Tigkas, 2014. Sensitivity of Surface Runoff to Drought and Climate Change: Application for Shared River Basins. *Water* **6**:3033.

AlSarmi, S. H. and R. Washington, 2014. Changes in climate extremes in the Arabian Peninsula: analysis of daily data. *International Journal of Climatology* **34**:1329-1345.

Argüeso, D., J. P. Evans and L. Fita, 2013. Precipitation bias correction of very high resolution regional climate models. *Hydrol. Earth Syst. Sci.* **17**:4379-4388.

Arnell, N. and C. Liu 2001, Hydrology and water resources. In: Climate Change 2001, Impacts, Adaptation, and Vulnerability. Intergovernmental Panel on Climate Change. Cambridge University Press, Cambridge, UK.

Arnold, J. G., D. N. Moriasi, P. W. Gassman, K. C. Abbaspour, M. J. White, R. Srinivasan, C. Santhi, R. D. Harmel, A. v. Griensven, M. W. V. Liew, N. Kannan and M. K. Jha, 2012. SWAT: Model Use, Calibration, and Validation. **55**.

Asadi Zarch, M. A., B. Sivakumar and A. Sharma, 2015. Droughts in a warming climate: A global assessment of Standardized precipitation index (SPI) and Reconnaissance drought index (RDI). *Journal of Hydrology* **526**:183-195.

Ashraf Vaghefi, S., S. J. Mousavi, K. C. Abbaspour, R. Srinivasan and H. Yang, 2014. Analyses of the impact of climate change on water resources components, drought and wheat yield in semiarid regions: Karkheh River Basin in Iran. *Hydrological Processes* **28**:2018-2032.

Basheer, A. K., H. Lu, A. Omer, A. B. Ali and A. M. S. Abdelgader, 2016. Impacts of climate change under CMIP5 RCP scenarios on the streamflow in the Dinder River and ecosystem habitats in Dinder National Park, Sudan. *Hydrol. Earth Syst. Sci.* **20**:1331-1353.

Bautista-Capetillo, C., B. Carrillo, G. Picazo and H. Júnez-Ferreira, 2016. Drought Assessment in Zacatecas, Mexico. *Water* **8**:416.

Bennett, K. E., A. T. Werner and M. Schnorbus, 2012. Uncertainties in Hydrologic and Climate Change Impact Analyses in Headwater Basins of British Columbia. *Journal of Climate* **25**:5711-5730.

Bentsen, M., I. Bethke, J. B. Debernard, T. Iversen, A. Kirkevåg, Ø. Seland, H. Drange, C. Roelandt, I. A. Seierstad, C. Hoose and J. E. Kristjánsson, 2013. The Norwegian Earth System Model, NorESM1-M – Part 1: Description and basic evaluation of the physical climate. *Geosci. Model Dev.* **6**:687-720.

Bocheva, L., T. Marinova, P. Simeonov and I. Gospodinov, 2009. Variability and trends of extreme precipitation events over Bulgaria (1961–2005). *Atmospheric Research* **93**:490-497.

Bonsal, B. R., R. Aider, P. Gachon and S. Lapp, 2013. An assessment of Canadian prairie drought: past, present, and future. *Climate Dynamics* **41**:501-516.

Boyles, R. P. and S. Raman, 2003. Analysis of climate trends in North Carolina (1949–1998). *Environment International* **29**:263-275.

Brath, A., A. Montanari and G. Moretti, 2006. Assessing the effect on flood frequency of land use change via hydrological simulation (with uncertainty). *Journal of Hydrology* **324**:141-153.

Brianna, R. P., A. Moetasim, R. Deeksha, R. K. Donald, K. Shih-Chieh, S. N. Bibi, M. Rui and S. P. Jeremy, 2016. Extreme hydrological changes in the southwestern US drive reductions in water supply to Southern California by mid century. *Environmental Research Letters* **11**:094026.

Bronaugh, D. Package 'climdex.pcic'. 2014. Available online: https://cran.r-project.org/web/packages/climdex.pcic/climdex.pcic.pdf

Brutsaert, W. and M. B. Parlange, 1998. Hydrologic cycle explains the evaporation paradox. *Nature* **396**:30-30.

Burn, D. H. and P. H. Whitfield, 2016. Changes in floods and flood regimes in Canada. *Canadian Water Resources Journal / Revue canadienne des ressources hydriques* **41**:139-150.

Ceppi, P., S. C. Scherrer, A. M. Fischer and C. Appenzeller, 2012. Revisiting Swiss temperature trends 1959–2008. *International Journal of Climatology* **32**:203-213.

Chandniha, S. K., S. G. Meshram, J. F. Adamowski and C. Meshram, 2016. Trend analysis of precipitation in Jharkhand State, India. *Theoretical and Applied Climatology* 10.1007/s00704-016-1875-x:1-14.

Chattopadhyay, S. and D. Edwards, 2016. Long-Term Trend Analysis of Precipitation and Air Temperature for Kentucky, United States. *Climate* **4**:10.

Chattopadhyay, S., D. Edwards and Y. Yu, 2017. Contemporary and Future Characteristics of Precipitation Indices in the Kentucky River Basin. *Water* **9**:109.

Chattopadhyay, S. and M. K. Jha, 2016. Hydrological response due to projected climate variability in Haw River watershed, North Carolina, USA. *Hydrological Sciences Journal* **61**:495-506.

Chen, T., G. R. Werf, R. A. M. Jeu, G. Wang and A. J. Dolman, 2013. A global analysis of the impact of drought on net primary productivity. *Hydrol. Earth Syst. Sci.* **17**:3885-3894.

Chien, H., P. J. F. Yeh and J. H. Knouft, 2013. Modeling the potential impacts of climate change on streamflow in agricultural watersheds of the Midwestern United States. *Journal of Hydrology* **491**:73-88.

Coats, R., M. Costa-Cabral, J. Riverson, J. Reuter, G. Sahoo, G. Schladow and B. Wolfe, 2013. Projected 21st century trends in hydroclimatology of the Tahoe basin. *Climatic Change* **116**:51-69.

Costa, A. C. and A. Soares, 2008. Homogenization of Climate Data: Review and New Perspectives Using Geostatistics. *Mathematical Geosciences* **41**:291-305.

Coumou, D. and S. Rahmstorf, 2012. A decade of weather extremes. *Nature Clim. Change* **2**:491-496.

Daggupati, P., D. Deb, R. Srinivasan, D. Yeganantham, V. M. Mehta and N. J. Rosenberg, 2016. Large-Scale Fine-Resolution Hydrological Modeling Using Parameter Regionalization in the Missouri River Basin. *JAWRA Journal of the American Water Resources Association* **52**:648-666.

Dahal, V., N. M. Shakya and R. Bhattarai, 2016. Estimating the Impact of Climate Change on Water Availability in Bagmati Basin, Nepal. *Environmental Processes* **3**:1-17.

Dai, A., I. Y. Fung and A. D. D. Genio, 1997. Surface Observed Global Land Precipitation Variations during 1900–88. *Journal of Climate* **10**:2943-2962.

Dai, S., M. D. Shulski, K. G. Hubbard and E. S. Takle, 2016. A spatiotemporal analysis of Midwest US temperature and precipitation trends during the growing season from 1980 to 2013. *International Journal of Climatology* **36**:517-525.

DeAngelis, A., F. Dominguez, Y. Fan, A. Robock, M. D. Kustu and D. Robinson, 2010. Evidence of enhanced precipitation due to irrigation over the Great Plains of the United States. *Journal of Geophysical Research: Atmospheres* **115**:n/a-n/a.DeGaetano, A. T. and R. J. Allen, 2002. Trends in Twentieth-Century Temperature Extremes across the United States. *Journal of Climate* **15**:3188-3205.

de Lima, M. I. P., F. E. Santo, A. M. Ramos and R. M. Trigo, 2015. Trends and correlations in annual extreme precipitation indices for mainland Portugal, 1941–2007. *Theoretical and Applied Climatology* **119**:55-75.

del Río, S., L. Herrero, C. Pinto-Gomes and A. Penas, 2011. Spatial analysis of mean temperature trends in Spain over the period 1961–2006. *Global and Planetary Change* **78**:65-75.

Deser, C., A. Phillips, V. Bourdette and H. Teng, 2012. Uncertainty in climate change projections: the role of internal variability. *Climate Dynamics* **38**:527-546.

Diaz-Nieto, J. and R. L. Wilby, 2005. A comparison of statistical downscaling and climate change factor methods: impacts on low flows in the River Thames, United Kingdom. *Climatic Change* **69**:245-268.

Diffenbaugh, N. S. and M. Ashfaq, 2010. Intensification of hot extremes in the United States. *Geophysical Research Letters* **37**:n/a-n/a.

Donat, M. G., L. V. Alexander, H. Yang, I. Durre, R. Vose, R. J. H. Dunn, K. M. Willett, E. Aguilar, M. Brunet, J. Caesar, B. Hewitson, C. Jack, A. M. G. Klein Tank, A. C. Kruger, J. Marengo, T. C. Peterson, M. Renom, C. Oria Rojas, M. Rusticucci, J. Salinger, A. S. Elrayah, S. S. Sekele, A. K. Srivastava, B. Trewin, C. Villarroel, L. A. Vincent, P. Zhai, X. Zhang and S. Kitching, 2013. Updated analyses of temperature and precipitation extreme indices since the beginning of the twentieth century: The HadEX2 dataset. *Journal of Geophysical Research: Atmospheres* **118**:2098-2118.

Donner, L. J., B. L. Wyman, R. S. Hemler, L. W. Horowitz, Y. Ming, M. Zhao, J.-C. Golaz, P. Ginoux, S.-J. Lin, M. D. Schwarzkopf, J. Austin, G. Alaka, W. F. Cooke, T. L. Delworth, S. M. Freidenreich, C. T. Gordon, S. M. Griffies, I. M. Held, W. J. Hurlin, S. A. Klein, T. R. Knutson, A. R. Langenhorst, H.-C. Lee, Y. Lin, B. I. Magi, S. L. Malyshev, P. C. D. Milly, V. Naik, M. J. Nath, R. Pincus, J. J. Ploshay, V. Ramaswamy, C. J. Seman, E. Shevliakova, J. J. Sirutis, W. F. Stern, R. J. Stouffer, R. J. Wilson, M. Winton, A. T. Wittenberg and F. Zeng, 2011. The Dynamical Core, Physical Parameterizations, and Basic Simulation Characteristics of the Atmospheric Component AM3 of the GFDL Global Coupled Model CM3. *Journal of Climate* **24**:3484-3519.

Douglas, E. B., R. M. Vogel and C. N. Knoll, 2000. Trends in floods and low flows in the United States: Impact of serial correlation. *Journal of Hydrolgy* **240**, 90–105.

Duan, W., B. He, K. Takara, P. Luo, M. Hu, N. E. Alias and D. Nover, 2015. Changes of precipitation amounts and extremes over Japan between 1901 and 2012 and their connection to climate indices. *Climate Dynamics* **45**:2273-2292.

Dufresne, J.-L., M.-A. Foujols, S. Denvil, A. Caubel, O. Marti, O. Aumont, Y. Balkanski, S. Bekki, H. Bellenger, R. Benshila, S. Bony, L. Bopp, P. Braconnot, P. Brockmann, P. Cadule, F. Cheruy, F. Codron, A. Cozic, D. Cugnet, N. de Noblet, J.-P. Duvel, C. Ethé, L. Fairhead, T. Fichefet, S. Flavoni, P. Friedlingstein, J.-Y. Grandpeix, L. Guez, E. Guilyardi, D. Hauglustaine, F. Hourdin, A. Idelkadi, J. Ghattas, S. Joussaume, M. Kageyama, G. Krinner, S. Labetoulle, A. Lahellec, M.-P. Lefebvre, F. Lefevre, C. Levy, Z. X. Li, J. Lloyd, F. Lott, G. Madec, M. Mancip, M. Marchand, S. Masson, Y. Meurdesoif, J. Mignot, I. Musat, S. Parouty, J. Polcher, C. Rio, M. Schulz, D. Swingedouw, S. Szopa, C. Talandier, P. Terray, N. Viovy and N. Vuichard, 2013. Climate change projections using the IPSL-CM5 Earth System Model: from CMIP3 to CMIP5. *Climate Dynamics* **40**:2123-2165.

Easterling, D., R., J. L. Evans, P. Ya. Groisman, T. R. Karl, K. E. Kunkel, and P.Ambenje, 2000. Observed variability and trends in extreme climate events: A brief review. *Bulletin of American Meteorological Society* **81**:417–425.

Edossa, D. C., M. S. Babel and A. Das Gupta, 2010. Drought Analysis in the Awash River Basin, Ethiopia. *Water Resources Management* **24**:1441-1460.

El Kenawy, A., J. I. López-Moreno and S. M. Vicente-Serrano, 2012. Trend and variability of surface air temperature in northeastern Spain (1920–2006): Linkage to atmospheric circulation. *Atmospheric Research* **106**:159-180.

Emori, S., A. Hasegawa, T. Suzuki and K. Dairaku, 2005. Validation, parameterization dependence, and future projection of daily precipitation simulated with a high-resolution atmospheric GCM. *Geophysical Research Letters* **32**:n/a-n/a.

Ertürk, A., A. Ekdal, M. Gürel, N. Karakaya, C. Guzel and E. Gönenç, 2014. Evaluating the impact of climate change on groundwater resources in a small Mediterranean watershed. *Science of The Total Environment* **499**:437-447.

Ficklin, D. L., S. L. Letsinger, I. T. Stewart and E. P. Maurer, 2016. Assessing differences in snowmelt-dependent hydrologic projections using CMIP3 and CMIP5 climate forcing data for the western United States. *Hydrology Research* **47**:483-500.

Ficklin, D. L. and B. L. Barnhart, 2014. SWAT hydrologic model parameter uncertainty and its implications for hydroclimatic projections in snowmelt-dependent watersheds. *Journal of Hydrology* **519, Part B**:2081-2090.

Fu, G., Z. Liu, S. P. Charles, Z. Xu and Z. Yao, 2013. A score-based method for assessing the performance of GCMs: A case study of southeastern Australia. *Journal of Geophysical Research: Atmospheres* **118**:4154-4167.

Gajbhiye, S., C. Meshram, R. Mirabbasi and S. K. Sharma, 2016. Trend analysis of rainfall time series for Sindh river basin in India. *Theoretical and Applied Climatology* **125**:593-608.

Gao, Y., J. S. Fu, J. B. Drake, Y. Liu and J. F. Lamarque, 2012. Projected changes of extreme weather events in the eastern United States based on a high resolution climate modeling system. *Environmental Research Letters* **7**:044025.

Gent, P. R., G. Danabasoglu, L. J. Donner, M. M. Holland, E. C. Hunke, S. R. Jayne, D. M. Lawrence, R. B. Neale, P. J. Rasch, M. Vertenstein, P. H. Worley, Z.-L. Yang and M. Zhang, 2011. The Community Climate System Model Version 4. *Journal of Climate* **24**:4973-4991.

Giorgi, F., E.-S. Im, E. Coppola, N. S. Diffenbaugh, X. J. Gao, L. Mariotti and Y. Shi, 2011. Higher Hydroclimatic Intensity with Global Warming. *Journal of Climate* **24**:5309-5324.

Gocic, M. and S. Trajkovic, 2014. Spatiotemporal characteristics of drought in Serbia. *Journal of Hydrology* **510**:110-123.

Gocic, M. and S. Trajkovic, 2013. Analysis of changes in meteorological variables using Mann-Kendall and Sen's slope estimator statistical tests in Serbia. *Global and Planetary Change* **100**:172-182.

Green, T. R., M. Taniguchi, H. Kooi, J. J. Gurdak, D. M. Allen, K. M. Hiscock, H. Treidel and A. Aureli, 2011. Beneath the surface of global change: Impacts of climate change on groundwater. *Journal of Hydrology* **405**:532-560.

Guijarro, J.A. User’s Guide to Climatol. 2013. Available online: http://www.climatol.eu/climatol-guide.pdf

Guilbert, J., A. K. Betts, D. M. Rizzo, B. Beckage and A. Bomblies, 2015. Characterization of increased persistence and intensity of precipitation in the northeastern United States. *Geophysical Research Letters* **42**:1888-1893.

Haddeland, I., J. Heinke, H. Biemans, S. Eisner, M. Flörke, N. Hanasaki, M. Konzmann, F. Ludwig, Y. Masaki, J. Schewe, T. Stacke, Z. D. Tessler, Y. Wada and D. Wisser, 2014. Global water resources affected by human interventions and climate change. *Proceedings of the National Academy of Sciences* **111**:3251-3256.

Hanssen-Bauer, I. and E. Førland, 2000. Temperature and precipitation variations in Norway 1900–1994 and their links to atmospheric circulation. *International Journal of Climatology* **20**: 1693–1708.

Hartmann, D. L., A. M. G. K. Tank, M. Rusticucci, L. V. Alexander, S. Bronnimann, Y. Charabi, F. J. Dentener, E. J. Dlugokencky, D. R. Easterling and A. Kaplan; *et al*. Observations: Atmosphere and Surface. In *Climate Change 2013: The Physical Science Basis*; Contribution of Working Group I to the Fifth Assessment Report of the Intergovernmental Panel on Climate Change; Stocker, T.F., Qin, D., Plattner, G.-K., Tignor, M., Allen, S.K., Boschung, J., Nauels, A., Xia, Y., Bex, V., Midgley, P.M., Eds.; Cambridge University Press: Cambridge, UK; New York, NY, USA, 2013; pp. 159–255

Hayes, M., M. Svoboda, N. Wall and M. Widhalm, 2011. The Lincoln Declaration on drought indices: Universal meteorological drought index recommended. *Bull. American Meteorological Society* **92**:485-488.

Hirabayashi, Y., R. Mahendran, S. Koirala, L. Konoshima, D. Yamazaki, S. Watanabe, H. Kim and S. Kanae, 2013. Global flood risk under climate change. *Nature Clim. Change* **3**:816-821.

Hirsch, R. M., J. R. Slack and R. A. Smith, 1982. Techniques of trend analysis for monthly water quality data. *Water Resources Research* **18**:107-121.

Hong, X., S. Guo, Y. Zhou and L. Xiong, 2015. Uncertainties in assessing hydrological drought using streamflow drought index for the upper Yangtze River basin. *Stochastic Environmental Research and Risk Assessment* **29**:1235-1247.

Hosseinzadeh Talaee, P., H. Tabari and S. Sobhan Ardakani, 2014. Hydrological drought in the west of Iran and possible association with large-scale atmospheric circulation patterns. *Hydrological Processes* **28**:764-773.

Huang, J., S. Sun and J. Zhang, 2013. Detection of trends in precipitation during 1960–2008 in Jiangxi province, southeast China. *Theoretical and Applied Climatology* **114**:237-251.

Hulme, M., T. J. Osborn and T. C. Johns, 1998. Precipitation sensitivity to global warming: Comparison of observations with HadCM2 simulations. *Geophysical Research Letters* **25**:3379-3382.

Huntington, T. G., 2006. Evidence for intensification of the global water cycle: Review and synthesis. *Journal of Hydrology* **319**:83-95.

Ines, A. V. M. and J. W. Hansen, 2006. Bias correction of daily GCM rainfall for crop simulation studies. *Agricultural and Forest Meteorology* **138**:44-53.

IPCC. Climate Change 2001: The Scientific Basis; Contribution of Working Group I to the Third Assessment Report of the Intergovernmental Panel on Climate Change; .Houghton, J.T.; Ding, Y.; Griggs, D.J.; Noguer, M.; van der Linden, P.J.; Dai, X.; Maskell, K.; Johnson, C.A. Cambridge University Press: Cambridge, UK; New York, NY, USA, 2001.

Irannezhad, M., H. Marttila and B. Kløve, 2014. Long-term variations and trends in precipitation in Finland. *International Journal of Climatology* **34**:3139-3153.

Jain, S. K., V. Kumar and M. Saharia, 2013. Analysis of rainfall and temperature trends in northeast India. *International Journal of Climatology* **33**:968-978.

Jenkins, K. and R. Warren, 2015. Quantifying the impact of climate change on drought regimes using the Standardised Precipitation Index. *Theoretical and Applied Climatology* **120**:41-54.

Jha, M. K. and A. K. Singh, 2013. Trend analysis of extreme runoff events in major river basins of Peninsular Malaysia. *International Journal of Water* **7**, 142–158.

Jha, M. K. and P. W. Gassman, 2014. Changes in hydrology and streamflow as predicted by a modelling experiment forced with climate models. *Hydrological Processes* **28**:2772-2781.

Jhajharia, D. and V. P. Singh, 2011. Trends in temperature, diurnal temperature range and sunshine duration in Northeast India. *International Journal of Climatology* **31**:1353-1367.

Jiang, P., Z. Yu, M. R. Gautam and K. Acharya, 2016. The Spatiotemporal Characteristics of Extreme Precipitation Events in the Western United States. *Water Resources Management* **30**:4807-4821.

Jin, X. and V. Sridhar, 2012. Impacts of Climate Change on Hydrology and Water Resources in the Boise and Spokane River Basins1. *JAWRA Journal of the American Water Resources Association* **48**:197-220.

Johnson, F. and A. Sharma, 2009. Measurement of GCM Skill in Predicting Variables Relevant for Hydroclimatological Assessments. *Journal of Climate* **22**:4373-4382.

Jones, C. D., J. K. Hughes, N. Bellouin, S. C. Hardiman, G. S. Jones, J. Knight, S. Liddicoat, F. M. O'Connor, R. J. Andres, C. Bell, K. O. Boo, A. Bozzo, N. Butchart, P. Cadule, K. D. Corbin, M. Doutriaux-Boucher, P. Friedlingstein, J. Gornall, L. Gray, P. R. Halloran, G. Hurtt, W. J. Ingram, J. F. Lamarque, R. M. Law, M. Meinshausen, S. Osprey, E. J. Palin, L. Parsons Chini, T. Raddatz, M. G. Sanderson, A. A. Sellar, A. Schurer, P. Valdes, N. Wood, S. Woodward, M. Yoshioka and M. Zerroukat, 2011. The HadGEM2-ES implementation of CMIP5 centennial simulations. *Geosci. Model Dev.* **4**:543-570.

Jones, J. R., J. S. Schwartz, K. N. Ellis, J. M. Hathaway and C. M. Jawdy, 2015. Temporal variability of precipitation in the Upper Tennessee Valley. *Journal of Hydrology: Regional Studies* **3**:125-138.

Jung, I.-W., D.-H. Bae and G. Kim, 2011. Recent trends of mean and extreme precipitation in Korea. *International Journal of Climatology* **31**:359-370.

Jung, I. W., D. H. Bae and B. J. Lee, 2013. Possible change in Korean streamflow seasonality based on multi-model climate projections. *Hydrological Processes* **27**:1033-1045.

Kalkstein, L. S., G. Tan and J. A. Skindlov, 1987. An Evaluation of Three Clustering Procedures for Use in Synoptic Climatological Classification. *Journal of Climate and Applied Meteorology* **26**:717-730.

Kalogeropoulos, K. and C. Chalkias, 2013. Modelling the impacts of climate change on surface runoff in small Mediterranean catchments: empirical evidence from Greece. *Water and Environment Journal* **27**:505-513.

Kamruzzaman, M., S. Beecham and A. V. Metcalfe, 2016. Estimation of trends in rainfall extremes with mixed effects models. *Atmospheric Research* **168**:24-32.

Kao, S.-C. and R. S. Govindaraju, 2010. A copula-based joint deficit index for droughts. *Journal of Hydrology* **380**:121-134.

Karl, T. R. and R. W. Knight, 1998. Secular Trends of Precipitation Amount, Frequency, and Intensity in the United States. *Bulletin of the American Meteorological Society* **79**:231-241.

Karmeshu, N. Trend Detection in Annual Temperature & Precipitation Using the Mann Kendall Test—A Case Study to Assess Climate Change on Select States in the Northeastern United States. Master's Thesis, University of Pennsylvania, Philadelphia, PA, USA, August 2012.

Kendall, M. G, 1975. *Rank Correlation Measures*; Charles Griffin: London, UK.

Kentucky Climate Center. 2014—Kentucky Weather Year in Review. Available online: http://kyclimate.org/

Khalil, A. F., H.-H. Kwon, U. Lall and Y. H. Kaheil, 2010. Predictive downscaling based on non-homogeneous hidden Markov models. *Hydrological Sciences Journal* **55**:333-350.

Khalili, D., T. Farnoud, H. Jamshidi, A. A. Kamgar-Haghighi and S. Zand-Parsa, 2011. Comparability Analyses of the SPI and RDI Meteorological Drought Indices in Different Climatic Zones. *Water Resources Management* **25**:1737-1757.

Kousari, M. R., M. T. Dastorani, Y. Niazi, E. Soheili, M. Hayatzadeh and J. Chezgi, 2014. Trend Detection of Drought in Arid and Semi-Arid Regions of Iran Based on Implementation of Reconnaissance Drought Index (RDI) and Application of Non-Parametrical Statistical Method. *Water Resources Management* **28**:1857-1872.

Kunkel, K. E. 2003. North American trends in extreme precipitation. *Natural. Hazards*, **29**: 291–305.

Lafon, T., S. Dadson, G. Buys and C. Prudhomme, 2013. Bias correction of daily precipitation simulated by a regional climate model: a comparison of methods. *International Journal of Climatology* **33**:1367-1381.

Lee, J. H. and C. J. Kim, 2013. A multimodel assessment of the climate change effect on the drought severity–duration–frequency relationship. *Hydrological Processes* **27**:2800-2813.

Lejiang, Y., Z. Shiyuan, P. Lisi, B. Xindi and E. H. Warren, 2016. Contribution of large-scale circulation anomalies to changes in extreme precipitation frequency in the United States. *Environmental Research Letters* **11**:044003.

Li, H., J. Sheffield and E. F. Wood, 2010. Bias correction of monthly precipitation and temperature fields from Intergovernmental Panel on Climate Change AR4 models using equidistant quantile matching. *Journal of Geophysical Research: Atmospheres* **115**:n/a-n/a.

Li, Y.-G., D. He, J.-M. Hu and J. Cao, 2015. Variability of extreme precipitation over Yunnan Province, China 1960–2012. *International Journal of Climatology* **35**:245-258.

Li, F., G. Zhang and Y. Xu, 2016. Assessing Climate Change Impacts on Water Resources in the Songhua River Basin. *Water* **8**:420.

Li, X., Z.-Z. Hu, X. Jiang, Y. Li, Z. Gao, S. Yang, J. Zhu and B. Jha, 2016. Trend and seasonality of land precipitation in observations and CMIP5 model simulations. *International Journal of Climatology* **36**:3781-3793.

Liuzzo, L., E. Bono, V. Sammartano and G. Freni, 2016. Analysis of spatial and temporal rainfall trends in Sicily during the 1921–2012 period. *Theoretical and Applied Climatology* **126**:113-129.

Longobardi, A. and P. Villani, 2010. Trend analysis of annual and seasonal rainfall time series in the Mediterranean area. *International Journal of Climatology* **30**:1538-1546.

Lovejoy, S., 2013. What Is Climate? *Eos, Transactions American Geophysical Union* **94**:1-2.

Lupikasza, E., 2010. Spatial and temporal variability of extreme precipitation in Poland in the period 1951–2006. *International Journal of Climatology* **30**:991-1007.

Mahoney, K., M. Alexander, J. D. Scott and J. Barsugli, 2013. High-Resolution Downscaled Simulations of Warm-Season Extreme Precipitation Events in the Colorado Front Range under Past and Future Climates. *Journal of Climate* **26**:8671-8689.

Maidment, D. 2002. ArcHydro GIS for Water Resources. ESRI Press, Redlands, CA

Mallakpour, I. and G. Villarini, 2016. Analysis of changes in the magnitude, frequency, and seasonality of heavy precipitation over the contiguous USA. *Theoretical and Applied Climatology* 10.1007/s00704-016-1881-z:1-19.

Manabe, S. and R. T. Wetherald, 1975. The Effects of Doubling the CO2 Concentration on the climate of a General Circulation Model. *Journal of the Atmospheric Sciences* **32**:3-15.

Mann, H. B, 1945. Non-parametric tests against trend. *Econometrica, 13*, 245–259.

Markonis, Y., S. C. Batelis, Y. Dimakos, E. Moschou and D. Koutsoyiannis, 2016. Temporal and spatial variability of rainfall over Greece. *Theoretical and Applied Climatology* 10.1007/s00704-016-1878-7:1-16.

Martinez, C. J., J. J. Maleski and M. F. Miller, 2012. Trends in precipitation and temperature in Florida, USA. *Journal of Hydrology* **452–453**:259-281.

Matalas, N. C. and A. Sankarasubramanian, 2003. Effect of persistence on trend detection via regression. *Water Resources Research* **39**:n/a-n/a.

Maurer, E. P., J. C. Adam and A. W. Wood, 2009. Climate model based consensus on the hydrologic impacts of climate change to the Rio Lempa basin of Central America. *Hydrol. Earth Syst. Sci.* **13**:183-194.

McKee, T., N. Doesken and J. Kleist, 1993. The relationship of drought frequency and duration to time scales. In Proceedings of the 8th Conference on Applied Climatology, Anaheim, California.

McVicar, T. R., T. G. Van Niel, L. Li, M. F. Hutchinson, X. Mu and Z. Liu, 2007. Spatially distributing monthly reference evapotranspiration and pan evaporation considering topographic influences. *Journal of Hydrology* **338**:196-220.

Mearns, L. O., D. P. Lettenmaier and S. McGinnis, 2015. Uses of Results of Regional Climate Model Experiments for Impacts and Adaptation Studies: the Example of NARCCAP. *Current Climate Change Reports* **1**:1-9.

Mehan, S., N. Kannan, R. Neupane, R. McDaniel and S. Kumar, 2016. Climate Change Impacts on the Hydrological Processes of a Small Agricultural Watershed. *Climate* **4**:56.

Miao, C., Q. Duan, L. Yang and A. G. L. Borthwick, 2012. On the Applicability of Temperature and Precipitation Data from CMIP3 for China. *PLoS ONE* **7**:e44659.

Middelkoop, H., K. Daamen, D. Gellens, W. Grabs, J. C. J. Kwadijk, H. Lang, B. W. A. H. Parmet, B. Schädler, J. Schulla and K. Wilke, 2001. Impact of Climate Change on Hydrological Regimes and Water Resources Management in the Rhine Basin. *Climatic Change* **49**:105-128.

Mikkonen, S., M. Laine, H. M. Mäkelä, H. Gregow, H. Tuomenvirta, M. Lahtinen and A. Laaksonen, 2015. Trends in the average temperature in Finland, 1847–2013. *Stochastic Environmental Research and Risk Assessment* **29**:1521-1529.

Millett, B., W. C. Johnson and G. Guntenspergen, 2009. Climate trends of the North American prairie pothole region 1906–2000. *Climatic Change* **93**:243-267.

Milly, P. C. D., R. T. Wetherald, K. A. Dunne, and T. L. Delworth, 2002. Increasing risk of great floods in a changing climate. *Nature,* **415,** 514–517.

Minville, M., F. Brissette and R. Leconte, 2008. Uncertainty of the impact of climate change on the hydrology of a nordic watershed. *Journal of Hydrology* **358**:70-83.

Mishra, A. K. and V. P. Singh, 2010. A review of drought concepts. *Journal of Hydrology* **391**:202-216.

Mishra, V. and D. P. Lettenmaier, 2011. Climatic trends in major U.S. urban areas, 1950–2009. *Geophysical Research Letters* **38**:n/a-n/a.

Mishra, V. and R. Lilhare, 2016. Hydrologic sensitivity of Indian sub-continental river basins to climate change. *Global and Planetary Change* **139**:78-96.

Misra, V., J.-P. Michael, R. Boyles, E. P. Chassignet, M. Griffin and J. J. O'Brien, 2012. Reconciling the Spatial Distribution of the Surface Temperature Trends in the Southeastern United States. *Journal of Climate* **25**:3610-3618.

Mitra, S. and P. Srivastava, 2016. Spatiotemporal variability of meteorological droughts in southeastern USA. *Natural Hazards* 10.1007/s11069-016-2728-8:1-32.

Modala, R. Assessing the Impact of Climate Change on Cotton Production in the Texas High Plains and Rolling Plains. Ph.D. Thesis, Texas A & M University, College Station, TX, USA, December 2014.

Modarres, R. and V. de Paulo Rodrigues da Silva, 2007. Rainfall trends in arid and semi-arid regions of Iran. *Journal of Arid Environments* **70**:344-355.

Modarres, R. and A. Sarhadi, 2009. Rainfall trends analysis of Iran in the last half of the twentieth century. *Journal of Geophysical Research: Atmospheres* **114**:n/a-n/a.

Mohsin, T. and W. A. Gough, 2010. Trend analysis of long-term temperature time series in the Greater Toronto Area (GTA). *Theoretical and Applied Climatology* **101**:311-327.

Mondal, A. and P. P. Mujumdar, 2015. On the detection of human influence in extreme precipitation over India. *Journal of Hydrology* **529, Part 3**:1161-1172.

Moral, F. J., 2010. Comparison of different geostatistical approaches to map climate variables: application to precipitation. *International Journal of Climatology* **30**:620-631.

Moriasi, D. N., J. G. Arnold, M. W. V. Liew, R. L. Bingner, R. D. Harmel and T. L. Veith, 2007. Model Evaluation Guidelines for Systematic Quantification of Accuracy in Watershed Simulations. **50**.

Muslih, K. D. and K. Błażejczyk, 2016. The inter-annual variations and the long-term trends of monthly air temperatures in Iraq over the period 1941–2013. *Theoretical and Applied Climatology* 10.1007/s00704-016-1915-6:1-14.

Nalbantis, I. and G. Tsakiris, 2009. Assessment of Hydrological Drought Revisited. *Water Resources Management* **23**:881-897.

Narsimlu, B., A. K. Gosain and B. R. Chahar, 2013. Assessment of Future Climate Change Impacts on Water Resources of Upper Sind River Basin, India Using SWAT Model. *Water Resources Management* **27**:3647-3662.

National Center for Environmental Information Database. Available online: http://www.ncdc.noaa.gov/cag/

Naz, B. S., S.-C. Kao, M. Ashfaq, D. Rastogi, R. Mei and L. C. Bowling, 2016. Regional hydrologic response to climate change in the conterminous United States using high-resolution hydroclimate simulations. *Global and Planetary Change* **143**:100-117.

Nazrul Islam, M., M. Almazroui, R. Dambul, P. D. Jones and A. O. Alamoudi, 2015. Long-term changes in seasonal temperature extremes over Saudi Arabia during 1981–2010. *International Journal of Climatology* **35**:1579-1592.

Neitsch, S.L., J.G. Arnold, J.R Kiniry and J.R. Williams, 2005. Soil and water assessment tool, theoretical documentation: version. Agricultural Research Service and Texas A&M Blackland Research Center, Temple

Neupane, R. P., J. Yao and J. D. White, 2014. Estimating the effects of climate change on the intensification of monsoonal-driven stream discharge in a Himalayan watershed. *Hydrological Processes* **28**:6236-6250.

New, M., M. Todd, M. Hulme and P. Jones, 2001. Precipitation measurements and trends in the twentieth century. *International Journal of Climatology* **21**:1889-1922.

Ning, L., E. E. Riddle and R. S. Bradley, 2015. Projected Changes in Climate Extremes over the Northeastern United States. *Journal of Climate* **28**:3289-3310.

Novotny, E. V. and H. G. Stefan, 2007. Stream flow in Minnesota: Indicator of climate change. *Journal of Hydrology* **334**:319-333.

Oki, T. and S. Kanae, 2006. Global Hydrological Cycles and World Water Resources. *Science* **313**:1068-1072.

Oliveira, P. T., C. M. Santos e Silva and K. C. Lima, 2016. Climatology and trend analysis of extreme precipitation in subregions of Northeast Brazil. *Theoretical and Applied Climatology* 10.1007/s00704-016-1865-z:1-14.

Omondi, P. A. o., J. L. Awange, E. Forootan, L. A. Ogallo, R. Barakiza, G. B. Girmaw, I. Fesseha, V. Kululetera, C. Kilembe, M. M. Mbati, M. Kilavi, S. M. King'uyu, P. A. Omeny, A. Njogu, E. M. Badr, T. A. Musa, P. Muchiri, D. Bamanya and E. Komutunga, 2014. Changes in temperature and precipitation extremes over the Greater Horn of Africa region from 1961 to 2010. *International Journal of Climatology* **34**:1262-1277.

Palmer, W.C., 1965. Meteorological drought. Research Paper No. 45, U.S. Department of Commerce Weather Bureau, Washington, D.C

Panofsky, H.A. and G.W Brier, 1968. Some Applications of Statistics to Meteorology; Pennsylvania State University, University Park: State College, PA, USA, p. 224

Peterson, T. C., R. R. H. Jr., R. Hirsch, D. P. Kaiser, H. Brooks, N. S. Diffenbaugh, R. M. Dole, J. P. Giovannettone, K. Guirguis, T. R. Karl, R. W. Katz, K. Kunkel, D. Lettenmaier, G. J. McCabe, C. J. Paciorek, K. R. Ryberg, S. Schubert, V. B. S. Silva, B. C. Stewart, A. V. Vecchia, G. Villarini, R. S. Vose, J. Walsh, M. Wehner, D. Wolock, K. Wolter, C. A. Woodhouse and D. Wuebbles, 2013. Monitoring and Understanding Changes in Heat Waves, Cold Waves, Floods, and Droughts in the United States: State of Knowledge. *Bulletin of the American Meteorological Society* **94**:821-834.

Philandras, C. M., P. T. Nastos, J. Kapsomenakis, K. C. Douvis, G. Tselioudis and C. S. Zerefos, 2011. Long term precipitation trends and variability within the Mediterranean region. *Nat. Hazards Earth Syst. Sci.* **11**:3235-3250.

Phillips, N. A., 1956. The general circulation of the atmosphere: A numerical experiment. *Quarterly Journal of the Royal Meteorological Society* **82**:123-164.

Pierce, D. W., D. R. Cayan, E. P. Maurer, J. T. Abatzoglou and K. C. Hegewisch, 2015. Improved Bias Correction Techniques for Hydrological Simulations of Climate Change. *Journal of Hydrometeorology* **16**:2421-2442.

Portmann, R. W., S. Solomon and G. C. Hegerl, 2009. Spatial and seasonal patterns in climate change, temperatures, and precipitation across the United States. *Proceedings of the National Academy of Sciences* **106**:7324-7329.

Powell, E. J. and B. D. Keim, 2015. Trends in Daily Temperature and Precipitation Extremes for the Southeastern United States: 1948–2012. *Journal of Climate* **28**:1592-1612.

Pradhanang, S. M., R. Mukundan, E. M. Schneiderman, M. S. Zion, A. Anandhi, D. C. Pierson, A. Frei, Z. M. Easton, D. Fuka and T. S. Steenhuis, 2013. Streamflow Responses to Climate Change: Analysis of Hydrologic Indicators in a New York City Water Supply Watershed. *JAWRA Journal of the American Water Resources Association* **49**:1308-1326.

Prat, O. P. and B. R. Nelson, 2014. Characteristics of annual, seasonal, and diurnal precipitation in the Southeastern United States derived from long-term remotely sensed data. *Atmospheric Research* **144**:4-20.

Prudhomme, C., D. Jakob and C. Svensson, 2003. Uncertainty and climate change impact on the flood regime of small UK catchments. *Journal of Hydrology* **277**:1-23.

Qiao, L., Z. Pan, R. B. Herrmann and Y. Hong, 2014. Hydrological Variability and Uncertainty of Lower Missouri River Basin Under Changing Climate. *JAWRA Journal of the American Water Resources Association* **50**:246-260.

Radić, V. and G. K. C. Clarke, 2011. Evaluation of IPCC Models' Performance in Simulating Late-Twentieth-Century Climatologies and Weather Patterns over North America. *Journal of Climate* **24**:5257-5274.

Rahmani, V., S. L. Hutchinson, J. A. Harrington Jr, J. M. S. Hutchinson and A. Anandhi, 2015. Analysis of temporal and spatial distribution and change-points for annual precipitation in Kansas, USA. *International Journal of Climatology* **35**:3879-3887.

RÄIsÄNen, J. and H. Alexandersson, 2003. A probabilistic view on recent and near future climate change in Sweden. *Tellus A* **55**:113-125.

Rana, A. and H. Moradkhani, 2016. Spatial, temporal and frequency based climate change assessment in Columbia River Basin using multi downscaled-scenarios. *Climate Dynamics* **47**:579-600.

Raziei, T., I. Bordi and L. S. Pereira, 2013. Regional Drought Modes in Iran Using the SPI: The Effect of Time Scale and Spatial Resolution. *Water Resources Management* **27**:1661-1674.

Records, R. M., M. Arabi, S. R. Fassnacht, W. G. Duffy, M. Ahmadi and K. C. Hegewisch, 2014. Climate change and wetland loss impacts on a western river's water quality. *Hydrol. Earth Syst. Sci.* **18**:4509-4527.

Ren, Z., M. Zhang, S. Wang, F. Qiang, X. Zhu and L. Dong, 2015. Changes in daily extreme precipitation events in South China from 1961 to 2011. *Journal of Geographical Sciences* **25**:58-68.

Ribeiro, S., J. Caineta and A. C. Costa, Review and discussion of homogenisation methods for climate data. *Physics and Chemistry of the Earth, Parts A/B/C* http://dx.doi.org/10.1016/j.pce.2015.08.007.

Robertson, A. W., S. Kirshner and P. Smyth, 2004. Downscaling of Daily Rainfall Occurrence over Northeast Brazil Using a Hidden Markov Model. *Journal of Climate* **17**:4407-4424.

Rocheta, E., M. Sugiyanto, F. Johnson, J. Evans and A. Sharma, 2014. How well do general circulation models represent low-frequency rainfall variability? *Water Resources Research* **50**:2108-2123.

Rosenzweig, C., A. Iglesias, X. B. Yang, P. R. Epstein and E. Chivian, 2001. Climate Change and Extreme Weather Events; Implications for Food Production, Plant Diseases, and Pests. *Global Change and Human Health* **2**:90-104.

Roth, M., T. A. Buishand and G. Jongbloed, 2015. Trends in Moderate Rainfall Extremes: A Regional Monotone Regression Approach. *Journal of Climate* **28**:8760-8769.

Saboohi, R., S. Soltani and M. Khodagholi, 2012. Trend analysis of temperature parameters in Iran. *Theoretical and Applied Climatology* **109**:529-547.

Salmi, T., A. Maatta, P. Anttila, T. Ruoho-Airola and T. Amnell, 2002. Detecting Trends of Annual Values of Atmospheric Pollutants by the Mann-Kendall Test and Sen's Slope Estimates—The Excel Template Application MAKESENS. Finnish Meteorological Institute: Helsinki, Finland.

Santos, M. and M. Fragoso, 2013. Precipitation variability in Northern Portugal: Data homogeneity assessment and trends in extreme precipitation indices. *Atmospheric Research* **131**:34-45.

Sayemuzzaman, M. and M. K. Jha, 2014. Seasonal and annual precipitation time series trend analysis in North Carolina, United States. *Atmospheric Research* **137**:183-194.

Sayemuzzaman, M., M. K. Jha and A. Mekonnen, 2015. Spatio-temporal long-term (1950–2009) temperature trend analysis in North Carolina, United States. *Theoretical and Applied Climatology* **120**:159-171.

Sayemuzzaman, M., M. K. Jha, A. Mekonnen and K. A. Schimmel, 2014. Subseasonal climate variability for North Carolina, United States. *Atmospheric Research* **145–146**:69-79.

Sayemuzzaman, M., A. Mekonnen and M. K. Jha, 2015. Diurnal temperature range trend over North Carolina and the associated mechanisms. *Atmospheric Research* **160**:99-108.

Schoof, J. T., 2015. High-resolution projections of 21st century daily precipitation for the contiguous U.S. *Journal of Geophysical Research: Atmospheres* **120**:3029-3042.

Schoof, J. T. and S. M. Robeson, 2016. Projecting changes in regional temperature and precipitation extremes in the United States. *Weather and Climate Extremes* **11**:28-40.

Sellers, P. J., Y. Mintz, Y. C. Sud and A. Dalcher, 1986. A Simple Biosphere Model (SIB) for Use within General Circulation Models. *Journal of the Atmospheric Sciences* **43**:505-531.

Setegn, S. G., D. Rayner, A. M. Melesse, B. Dargahi and R. Srinivasan, 2011. Impact of climate change on the hydroclimatology of Lake Tana Basin, Ethiopia. *Water Resources Research* **47**:n/a-n/a.

Shafer, B.A. and L.E. Dezman, 1982. Development of a surface water supply index to assess the severity of drought conditions in snowpack runoff areas. *Proceedings of the 50th Annual Western Snow Conference*, Nevada.

Shahid, S., 2008. Spatial and temporal characteristics of droughts in the western part of Bangladesh. *Hydrological Processes* **22**:2235-2247.

Shen, Z., L. Chen, Q. Liao, R. Liu and Q. Hong, 2012. Impact of spatial rainfall variability on hydrology and nonpoint source pollution modeling. *Journal of Hydrology* **472–473**:205-215.

Shi, X. and X. Xu, 2008. Interdecadal trend turning of global terrestrial temperature and precipitation during 1951–2002. *Progress in Natural Science* **18**:1383-1393.

Shi, Z., N. Shan, L. Xu, X. Yang, J. Gao, H. Guo, X. Zhang, A. Song and L. Dong, 2016. Spatiotemporal variation of temperature, precipitation and wind trends in a desertification prone region of China from 1960 to 2013. *International Journal of Climatology* **36**:4327-4337.

Shine, K. P. and A. Henderson-Sellers, 1983. Modelling climate and the nature of climate models: A review. *Journal of Climatology* **3**:81-94.

Shrestha, S. and A. Y. Htut, 2016. Modelling the potential impacts of climate change on hydrology of the Bago River Basin, Myanmar. *International Journal of River Basin Management* **14**:287-297.

Shukla, S. and A. W. Wood, 2008. Use of a standardized runoff index for characterizing hydrologic drought. *Geophysical Research Letters* **35**:n/a-n/a.

Sillmann, J., V. V. Kharin, F. W. Zwiers, X. Zhang and D. Bronaugh, 2013. Climate extremes indices in the CMIP5 multimodel ensemble: Part 2. Future climate projections. *Journal of Geophysical Research: Atmospheres* **118**:2473-2493.

Small, D., S. Islam and R. M. Vogel, 2006. Trends in precipitation and streamflow in the eastern U.S.: Paradox or perception? *Geophysical Research Letters* **33**:n/a-n/a.

Solomon, S., D. Qin, M. Manning, M. Marquis, K. Averyt, M.M.B. Tignor, H.L., Miller Jr and Z. Chen, Climate Change 2007: The Physical Science Basis; Cambridge University Press: Cambridge, UK, 2007; p. 996.

Sonali, P. and D. Nagesh Kumar, 2013. Review of trend detection methods and their application to detect temperature changes in India. *Journal of Hydrology* **476**:212-227.

Song, X., S. Song, W. Sun, X. Mu, S. Wang, J. Li and Y. Li, 2015. Recent changes in extreme precipitation and drought over the Songhua River Basin, China, during 1960–2013. *Atmospheric Research* **157**:137-152.

Spinoni, J., G. Naumann, H. Carrao, P. Barbosa and J. Vogt, 2014. World drought frequency, duration, and severity for 1951–2010. *International Journal of Climatology* **34**:2792-2804.

Steve, L., M. Richard and P. William, 2007. Recent California climate variability: spatial and temporal patterns in temperature trends. *Climate Research* **33**:159-169.

Stewart, I. T., D. L. Ficklin, C. A. Carrillo and R. McIntosh, 2015. 21st century increases in the likelihood of extreme hydrologic conditions for the mountainous basins of the Southwestern United States. *Journal of Hydrology* **529, Part 1**:340-353.

Stone, B., 2007. Urban and rural temperature trends in proximity to large US cities: 1951–2000. *International Journal of Climatology* **27**:1801-1807.

Sunyer, M. A., Y. Hundecha, D. Lawrence, H. Madsen, P. Willems, M. Martinkova, K. Vormoor, G. Bürger, M. Hanel, J. Kriaučiūnienė, A. Loukas, M. Osuch and I. Yücel, 2015. Inter-comparison of statistical downscaling methods for projection of extreme precipitation in Europe. *Hydrol. Earth Syst. Sci.* **19**:1827-1847.

Svoboda, M. D., B. A. Fuchs, C. C. Poulsen and J. R. Nothwehr, 2015. The drought risk atlas: Enhancing decision support for drought risk management in the United States. *Journal of Hydrology* **526**:274-286.

Tabari, H., B. S. Somee and M. R. Zadeh, 2011. Testing for long-term trends in climatic variables in Iran. *Atmospheric Research* **100**:132-140.

Tabari, H., J. Nikbakht and P. Hosseinzadeh Talaee, 2013. Hydrological Drought Assessment in Northwestern Iran Based on Streamflow Drought Index (SDI). *Water Resources Management* **27**:137-151.

Tallaksen, L. M. and H. A. J. van Lanen, 2004. Hydrological Drought – Processes and Estimation Methods for Streamflow and Groundwater, *Developments in Water Sciences* **48**, Elsevier B.V., Amsterdam.

Tan, C., J. Yang and M. Li, 2015. Temporal-Spatial Variation of Drought Indicated by SPI and SPEI in Ningxia Hui Autonomous Region, China. *Atmosphere* **6**:1399.

Tank, A. M. G. K. and G. P. Können, 2003. Trends in Indices of Daily Temperature and Precipitation Extremes in Europe, 1946–99. *Journal of Climate* **16**:3665-3680.

Taylor, K. E., 2001. Summarizing multiple aspects of model performance in a single diagram. *Journal of Geophysical Research: Atmospheres* **106**:7183-7192.

Taylor, S. D., Y. He and K. M. Hiscock, 2016. Modelling the impacts of agricultural management practices on river water quality in Eastern England. *Journal of Environmental Management* **180**:147-163.

Tebaldi, C., D. Adams-Smith and N. Heller, 2012. The Heat is On: US Temperature Trends; Climate Central: Princeton, NJ, USA.

Thomson, A. M., R. A. Brown, N. J. Rosenberg, R. C. Izaurralde, D. M. Legler and R. Srinivasan, 2003. Simulated impacts of el nino/southern oscillation on united states water resources. *JAWRA Journal of the American Water Resources Association* **39**:137-148.

Thrasher, B., E. P. Maurer, C. McKellar and P. B. Duffy, 2012. Technical Note: Bias correcting climate model simulated daily temperature extremes with quantile mapping. *Hydrol. Earth Syst. Sci.* **16**:3309-3314.

Towler, E., B. Rajagopalan, E. Gilleland, R. S. Summers, D. Yates and R. W. Katz, 2010. Modeling hydrologic and water quality extremes in a changing climate: A statistical approach based on extreme value theory. *Water Resources Research* **46**:n/a-n/a.

Tramblay, Y., S. El Adlouni and E. Servat, 2013. Trends and variability in extreme precipitation indices over Maghreb countries. *Nat. Hazards Earth Syst. Sci.* **13**:3235-3248.

Trenberth, K. E., A. Dai, G. van der Schrier, P. D. Jones, J. Barichivich, K. R. Briffa and J. Sheffield, 2014. Global warming and changes in drought. *Nature Clim. Change* **4**:17-22.

Tsakiris, G. and H. Vangelis, 2005. Establishing a drought index incorporating evapotranspiration. *European Water* **9**/10:3–11

Tsakiris, G., D. Pangalou and H. Vangelis, 2007. Regional Drought Assessment Based on the Reconnaissance Drought Index (RDI). *Water Resources Management* **21**:821-833.

Unal, Y., T. Kindap and M. Karaca, 2003. Redefining the climate zones of Turkey using cluster analysis. *International Journal of Climatology* **23**:1045-1055.

Uniyal, B., M. K. Jha and A. K. Verma, 2015. Assessing Climate Change Impact on Water Balance Components of a River Basin Using SWAT Model. *Water Resources Management* **29**:4767-4785.

United States Department of Agriculture, Agricultural Research Service. Available online: http://www.ars.usda.gov/Research/docs.htm?docid=19440

van Vuuren, D. P., J. Edmonds, M. Kainuma, K. Riahi, A. Thomson, K. Hibbard, G. C. Hurtt, T. Kram, V. Krey, J.-F. Lamarque, T. Masui, M. Meinshausen, N. Nakicenovic, S. J. Smith and S. K. Rose, 2011. The representative concentration pathways: an overview. *Climatic Change* **109**:5.

Venkataraman, K., S. Tummuri, A. Medina and J. Perry, 2016. 21st century drought outlook for major climate divisions of Texas based on CMIP5 multimodel ensemble: Implications for water resource management. *Journal of Hydrology* **534**:300-316.

Vicente-Serrano, S. M., S. Beguería and J. I. López-Moreno, 2010. A Multiscalar Drought Index Sensitive to Global Warming: The Standardized Precipitation Evapotranspiration Index. *Journal of Climate* **23**:1696-1718.

Vidal, J.-P. and S. D. Wade, 2008. Multimodel projections of catchment-scale precipitation regime. *Journal of Hydrology* **353**:143-158.

VijayaVenkataRaman, S., S. Iniyan and R. Goic, 2012. A review of climate change, mitigation and adaptation. *Renewable and Sustainable Energy Reviews* **16**:878-897.

Villarini, G., J. A. Smith, M. L. Baeck and W. F. Krajewski, 2011. Examining Flood Frequency Distributions in the Midwest U.S. *JAWRA Journal of the American Water Resources Association* **47**:447-463.

Vitart, F. and T. N. Stockdale, 2001. Seasonal Forecasting of Tropical Storms Using Coupled GCM Integrations. *Monthly Weather Review* **129**:2521-2537.

Voldoire, A., E. Sanchez-Gomez, D. Salas y Mélia, B. Decharme, C. Cassou, S. Sénési, S. Valcke, I. Beau, A. Alias, M. Chevallier, M. Déqué, J. Deshayes, H. Douville, E. Fernandez, G. Madec, E. Maisonnave, M.-P. Moine, S. Planton, D. Saint-

Martin, S. Szopa, S. Tyteca, R. Alkama, S. Belamari, A. Braun, L. Coquart and F. Chauvin, 2013. The CNRM-CM5.1 global climate model: description and basic evaluation. *Climate Dynamics* **40**:2091-2121.

Wachter, J. A, 2013. 10-Year Perspective of the Merger of Louisville and Jefferson County, KY: Louisville Metro Vaults from 65th to 18th Largest City in the Nation; The Abell Foundation: Baltimore, MD, USA.

Wang, D., M. Hejazi, X. Cai and A. J. Valocchi, 2011. Climate change impact on meteorological, agricultural, and hydrological drought in central Illinois. *Water Resources Research* **47**:n/a-n/a.

Wang, Q.-x., X.-h. Fan, Z.-d. Qin and M.-b. Wang, 2012. Change trends of temperature and precipitation in the Loess Plateau Region of China, 1961–2010. *Global and Planetary Change* **92–93**:138-147.

Wang, Q., J. Wu, T. Lei, B. He, Z. Wu, M. Liu, X. Mo, G. Geng, X. Li, H. Zhou and D. Liu, 2014. Temporal-spatial characteristics of severe drought events and their impact on agriculture on a global scale. *Quaternary International* **349**:10-21.

Watanabe, M., T. Suzuki, R. O'ishi, Y. Komuro, S. Watanabe, S. Emori, T. Takemura, M. Chikira, T. Ogura, M. Sekiguchi, K. Takata, D. Yamazaki, T. Yokohata, T. Nozawa, H. Hasumi, H. Tatebe and M. Kimoto, 2010. Improved Climate Simulation by MIROC5: Mean States, Variability, and Climate Sensitivity. *Journal of Climate* **23**:6312-6335.

Wood, A. W., L. R. Leung, V. Sridhar and D. P. Lettenmaier, 2004. Hydrologic Implications of Dynamical and Statistical Approaches to Downscaling Climate Model Outputs. *Climatic Change* **62**:189-216.

Wuebbles, D., G. Meehl, K. Hayhoe, T. R. Karl, K. Kunkel, B. Santer, M. Wehner, B. Colle, E. M. Fischer, R. Fu, A. Goodman, E. Janssen, V. Kharin, H. Lee, W. Li, L. N. Long, S. C. Olsen, Z. Pan, A. Seth, J. Sheffield and L. Sun, 2014. CMIP5 Climate Model Analyses: Climate Extremes in the United States. *Bulletin of the American Meteorological Society* **95**:571-583.

Xiao-Ge, X., W. Tong-Wen and Z. Jie, 2013. Introduction of CMIP5 Experiments Carried out with the Climate System Models of Beijing Climate Center. *Advances in Climate Change Research* **4**:41-49.

Xu, H. and Y. Luo, 2015. Climate change and its impacts on river discharge in two climate regions in China. *Hydrol. Earth Syst. Sci.* **19**:4609-4618.

Xu, K., D. Yang, H. Yang, Z. Li, Y. Qin and Y. Shen, 2015. Spatio-temporal variation of drought in China during 1961–2012: A climatic perspective. *Journal of Hydrology* **526**:253-264.

Xu, W., Y. Zou, G. Zhang and M. Linderman, 2015. A comparison among spatial interpolation techniques for daily rainfall data in Sichuan Province, China. *International Journal of Climatology* **35**:2898-2907.

Xu, Y.-P., X. Zhang, Q. Ran and Y. Tian, 2013. Impact of climate change on hydrology of upper reaches of Qiantang River Basin, East China. *Journal of Hydrology* **483**:51-60.

Xu, Z. X., K. Takeuchi, H. Ishidaira and J. Y. Li, 2005. Long-term trend analysis for precipitation in Asian Pacific FRIEND river basins. *Hydrological Processes* **19**:3517-3532.

Yao, X., J. Yu, H. Jiang, W. Sun and Z. Li, 2016. Roles of soil erodibility, rainfall erosivity and land use in affecting soil erosion at the basin scale. *Agricultural Water Management* **174**:82-92.

Ye, L. and N. B. Grimm, 2013. Modelling potential impacts of climate change on water and nitrate export from a mid-sized, semiarid watershed in the US Southwest. *Climatic Change* **120**:419-431.

Yuan, X., E. F. Wood, L. Luo and M. Pan, 2011. A first look at Climate Forecast System version 2 (CFSv2) for hydrological seasonal prediction. *Geophysical Research Letters* **38**:L13402.

Yue, S., P. Pilon, B. Phinney and G. Cavadias, 2002. The influence of autocorrelation on the ability to detect trend in hydrological series. *Hydrological Processes* **16**:1807-1829.

Zabaleta, A., M. Meaurio, E. Ruiz and I. Antigüedad, 2014. Simulation Climate Change Impact on Runoff and Sediment Yield in a Small Watershed in the Basque Country, Northern Spain. *Journal of Environmental Quality* **43**:235-245.

Zhai, J., B. Su, V. Krysanova, T. Vetter, C. Gao and T. Jiang, 2010. Spatial Variation and Trends in PDSI and SPI Indices and Their Relation to Streamflow in 10 Large Regions of China. *Journal of Climate* **23**:649-663.

Zhao, P., P. Jones, L. Cao, Z. Yan, S. Zha, Y. Zhu, Y. Yu and G. Tang, 2014. Trend of Surface Air Temperature in Eastern China and Associated Large-Scale Climate Variability over the Last 100 Years. *Journal of Climate* **27**:4693-4703.

Zhang, L., Z. Nan, W. Yu and Y. Ge, 2016. Hydrological Responses to Land-Use Change Scenarios under Constant and Changed Climatic Conditions. *Environmental Management* **57**:412-431.

Zhang, X., K.D. Harvey, W.D. Hogg and T.R Yuzyk. 2001. Trends in Canadian streamflow. *Water Resources Research*. **37**, 987–998.

Zhang, Q., J. Li, V. P. Singh and C.-Y. Xu, 2013. Copula-based spatio-temporal patterns of precipitation extremes in China. *International Journal of Climatology* **33**:1140-1152.

Zhang, Y., F. Su, Z. Hao, C. Xu, Z. Yu, L. Wang and K. Tong, 2015. Impact of projected climate change on the hydrology in the headwaters of the Yellow River basin. *Hydrological Processes* **29**:4379-4397.

Zhou, H. and Y. Liu, 2016. SPI Based Meteorological Drought Assessment over a Humid Basin: Effects of Processing Schemes. *Water* **8**:373.

Zilli, M. T., L. M. V. Carvalho, B. Liebmann and M. A. Silva Dias, 2016. A comprehensive analysis of trends in extreme precipitation over southeastern coast of Brazil. *International Journal of Climatology* 10.1002/joc.4840:n/a-n/a.

Wang, H.S., M.S. Schubert, C. Junye, H. Martin, K. Arun and P. Pegion, 2009. Attribution of the seasonality and regionality in climate trends over the United States during 1950–2000. *Journal of Climate*., **22**, 2571–2590.

Vita
Somsubhra Chattopadhyay

Education:

August 2014 – May 2017: Ph.D. in Biosystems and Agricultural Engineering, Department of Biosystems and Agricultural Engineering, University of Kentucky, Lexington, KY, USA

Dissertation title: Impact of climate change on extreme hydrological events in the Kentucky River Basin

August 2011 – December 2012: M.S in Civil and Environmental Engineering, Department of Civil, Architectural and Environmental Engineering , North Carolina Agricultural and Technical State University, Greensboro, NC, USA

Thesis title: Quantifying hydrological response for predicted Mid-Century climate variability and extremes in Haw River Watershed, North Carolina

August 2005 – July 2009: **B.Tech in Agricultural Engineering**, Faculty of Technology, North Bengal Agricultural University, Coochbehar, West Bengal, India

Thesis title: Delineation of Teesta and Torsa River Basins from remotely sensed digital elevation data

Research Grant Awarded:

Edwards, DR. (P.I), **Chattopadhyay, S**. (Co-PI) 2015. Impact of climate change on extreme hydrological events in the Kentucky River Basin. KWRI- Kentucky Water Resources Institute. $5000 for one year 03/2016- 04/2017

Publications:

Refereed Journal Articles:

1. Edwards, DR., **Chattopadhyay, S**. (2017) Evaluation of global climate model suitability for hydrologic and water quality analysis. *Transactions of ASABE (In review)*
2. **Chattopadhyay, S**., Edwards, DR., Yu, Y., Hamidisepehr, A. (2017) An assessment of climate change impacts on future water availability and droughts in the Kentucky River Basin. *Environmental Processes* (In review)
3. **Chattopadhyay, S**., Edwards, DR., Yu, Y. (2017) Contemporary and future characteristics of precipitation indices in the Kentucky River Basin. *Water*, 9, 109 DOI: 10.3390/w9020109
4. **Chattopadhyay, S**., Edwards, DR. (2016). Long term trend analysis of precipitation and air temperature for Kentucky, United States. *Climate*, 4(10) DOI: 10.3390/cli4010010
5. **Chattopadhyay, S**., Jha, MK. (2016). Hydrological response due to projected climate variability in Haw River Watershed, North Carolina, USA. *Hydrological Sciences* DOI: 10.1080/02626667.2014.934823

6. **Chattopadhyay, S**., Jha, MK. (2014) Climate change impact assessment on watershed hydrology: a comparison of three approaches. *American Journal of Engineering and Applied Sciences*, Vol 7 Issue 1 (122-128), DOI: 10.3844/ajeassp.2014.122.128
7. **Chattopadhyay, S**., Jha, MK. (2012) Watershed modeling of Haw River Basin for hydrology, water quality and climate change study. Paper No: 121337896, *Proceeding of the ASABE Annual International Meeting, 2012*

Conference/Meeting Presentations:

- ***Oral***

- **Chattopadhyay,** S., Edwards, DR. Assessing climate change impacts on future water availability and droughts in the Kentucky River Basin. March 20, 2017. Kentucky Water Resources Institute, Annual Symposium, Lexington, KY, USA
- **Chattopadhyay, S**., Jha, MK. Assessment of climate change impact on watershed hydrology. September 17-19, 2013 , National Conference on Advancement of Environmental Science and Technology, Greensboro, NC, USA
- **Chattopadhyay, S**., Jha, MK. Watershed Modeling of Haw River Basin using SWAT for Hydrology, Water Quality and Climate Change Study. July 29 – August 1, 2012, American Society of Agricultural and Biological Engineers, Annual International Meeting, Dallas, Texas, USA
- **Chattopadhyay, S**., Jha, MK. Watershed Modeling of Haw River Basin using SWAT for Hydrology, Water Quality and Climate Change Study. July 16 -20, 2012, International SWAT conference, New Delhi, India
- **Chattopadhyay, S**., Jha, MK. Effects of climate variability and change on water availability in the Haw River Basin, North Carolina. March 24 – 25, 2012, Water Resource Research Institute (WRRI) Annual Conference, NC State University, Raleigh, NC, USA

- ***Poster***

- **Chattopadhyay, S**., Edwards, DR. Spatiotemporal variability of historical extreme precipitation events in the Kentucky River Basin. July 17- 20, 2016, American Society of Agricultural and Biological Engineers, Annual International Meeting, Orlando, FL, USA
- **Chattopadhyay, S**., Jha, MK. Watershed Modeling of Haw River Basin using SWAT for Hydrology, Water Quality and Climate Change Study. April 24, 2012, Graduate Research Symposium, College of Engineering, NC A&T State University, Greensboro, NC, USA
- **Chattopadhyay, S**., Jha, MK. Hydrological response due to predicted climatic variability in Haw River Watershed, North Carolina. November 15, 2012, 3rd Annual International Conference in Green and Sustainable Technology, Greensboro, NC, USA

Extension Publications:

1. **Chattopadhyay, S**., Agouridis, C., Fox, J. (2016) Sediment fingerprinting. Cooperative Extension Service, University of Kentucky, College of Agriculture, Food and Environment

2. **Chattopadhyay, S**., Agouridis, C., Warner, R. (2016) Modelling Best Management Practices. Cooperative Extension Service, University of Kentucky, College of Agriculture, Food and Environment

Scholarships, Awards and Achievements:

- 1st position in the poster competition at 3rd Annual International Conference in Green and Sustainable Technology, 2012
- Junior Research Fellowship exam (JRF) PG 2009 conducted by Indian Council of Agricultural Research (ICAR) with all India rank 77
- Regular recipient of University Merit Scholarship (2005-2009)
- Certificate of Academic Achievement, 2005

Professional Affiliations:

- Student member, American Society of Agricultural and Biological Engineers (ASABE)
- Student member, American Geophysical Union (AGU)

Responsibilities:

- Vice President, Alpha Epsilon of University of Kentucky, April 2016- April 2017
- Treasurer, Alpha Epsilon of University of Kentucky, April 2015- April 2016